

PIK Report

No. 94

URBANISED TERRITORIES
AS A SPECIFIC COMPONENT
OF THE GLOBAL CARBON CYCLE

Anastasia Svirejeva-Hopkins and Hans-Joachim Schellnhuber



POTSDAM INSTITUTE
FOR
CLIMATE IMPACT RESEARCH (PIK)

Authors:

Dr. Anastasia Svirejeva-Hopkins
Potsdam Institute for Climate Impact Research
P.O. Box 60 12 03, D-14412 Potsdam, Germany
Phone: +49-331-288-2623
Fax: +49-331-288-2600
E-mail: svirejev@pik-potsdam.de

Prof. Dr. Hans-Joachim Schellnhuber
Potsdam Institute for Climate Impact Research and
Tyndall Centre (HQ),
Zuckerman Institute for Connective Environmental Research
School of Environmental Sciences,
University of East Anglia,
Norwich, NR4 7TJ, UK
Phone: +49-331-288-2501
Fax: +44-160-359-12-27
E-mail: H.J.Schellnhuber@uea.ac.uk

Herausgeber:

Prof. Dr. F.-W. Gerstengarbe

Technische Ausführung:

U. Werner

POTSDAM-INSTITUT
FÜR KLIMAFOLGENFORSCHUNG
Telegrafenberg
Postfach 60 12 03, 14412 Potsdam
GERMANY

Tel.: +49 (331) 288-2500
Fax: +49 (331) 288-2600
E-mail-Adresse: pik@pik-potsdam.de

Abstract:

Although Urbanised Territories (UT) produce most part of the anthropogenic emissions, we will only consider the following impacts on the Global Carbon Cycle (GCC):

- a) the additional carbon emissions that result from the conversion of natural, surrounding a city land, caused by urbanisation and
- b) the change of carbon flows by “urbanised” ecosystems, when the atmospheric carbon is “pumping” through “urbanised” ecosystems into neighboring natural ecosystems along the chain: atmosphere → vegetation → dead organic matter, i.e. export flow.

The main task is to estimate the annual regional dynamics of the total carbon balance in UT with respect to the atmosphere from 1980 till 2050.

As a scenario, we use the prognoses of regional urban populations produced by the “hybrid” model (multiregional demographic model + UN regional prognoses). All the estimations of carbon flows are based on two models. In the first model (minimal estimates), a regression equation relating the city area and population, is used, as well as an assumption about a random spatial distribution of cities. In the second model (maximal estimates), the so-called Γ -model is used, based on the assumption that the distribution of populated areas with respect to population density is a Γ -distribution with a non-random spatial distribution of cities. The urbanised area is sub-divided into „green“ (parks, etc.), built-up and informal settlements (*favelas*) areas.

The regional and world dynamics of carbon emission and export, and the annual total carbon balance are calculated. Qualitatively, both models give similar results, but there are some quantitative differences. In the first model, the world annual emissions as a result of land conversion will attain a maximum of 205 MtC between ca. 2020-2030. Emissions will then slowly decrease, so that by the year 2050, they will equal ca. 150 MtC. The maximum contributions to world emissions are given by China and the Asia and Pacific regions. In the second model, the world annual emissions increase from 1.12 GtC per year in 1980 up to 1.25 GtC per year in 2005, after which it will begin to decrease, such that by the year 2050, emissions will have decreased to 623 MtC. If we compare the emission maximum, 1.25 GtC per year, with the annual emission caused by the process of deforestation, 1.36GtC per year in 1980, then we can say that the role of UT is of a comparable magnitude to the role of deforestation.

Regarding the world dynamics of the annual export of carbon by UT, we observe its monotonous, almost linear growth by almost three times, from 24 MtC in 1980 up to

66 MtC in 2050 in the first model, and from 249 MtC up to 505 MtC in the second one. In the latter case, the transport power of UT is therefore comparable to the amount of carbon transported by rivers into the Ocean (196-537 MtC per year).

By estimating the total balance we find that “urbanistic” land conversion shifts the total balance towards a “sink” state. This is most distinctly seen in the Asia and Pacific, China and Africa regions at the initial stage of their “urbanistic” evolution, while UT of the Economies in Transition, and all Highly Industrialised regions play the role of carbon sink (because of the dominance of export flows). The Arabian and Latin America and the Caribbean regions are carbon sources.

According to the first model, the world UT are functioning as a source with power increasing up to its maximal value, 160 MtC, in the year 2020. Fortunately, urbanisation is inhibited in the interval 2020-2030, and by the middle of this century, the growth of urbanised areas would almost stop. Hence, the total emission of natural carbon at that stage will stabilise at the level of the 1980s (80MtC per year).

As estimated by the second model, the total balance, being almost constant until 2000, then starts to decrease at an almost constant rate. If its maximal value in 2000 was 905 MtC, then by 2050 this value has fallen to 118 MtC. By extrapolating this dynamics into the future, we can say that by the end of the XXI century, the total carbon balance will be equal to zero, and may even become negative. This means that the world UT are evolving from a “source” state, when at the beginning of this century they emit annually about 1 GtC, to a “neutralistic” state, when the exchange flows are fully balanced and therefore can be excluded from consideration in the GCC. In the second model, when the balance becomes negative, the system begins to take up carbon from the atmosphere, i.e., to become a “sink”. However, it is necessary to note that the formation of “sink” in urbanised territory is accompanied by the appearance of “sources” in other locations.

Table of contents:

1 INTRODUCTION	5
2 OVERVIEW AND MAIN ASPECT OF A PROBLEM	8
2.1. Global Carbon Cycle and the phenomenon of urbanisation	8
2.2. Spatial aspect of urbanisation. Distribution of population density and landscape approach.....	14
2.3. Urbanised territory from the ecologist's point of view	17
2.4. The city as a specific heterotrophic ecosystem. Carbon balance in urbanised territories.....	21
2.5. Carbon balance in urbanised territories and the role of human metabolism: global scale.....	26
2.6. Maps of population density and areas of urbanised territories.....	30
2.7. Urbanised territories: different definitions and a concept of the threshold density	34
2.8. Correlation between urban population and urban area: models	38
2.9. Other city models: a short overview.....	43
2.10. Setting of a problem	47
3 MODELS DESCRIBING THE AREA OF URBANISED TERRITORIES AS A FUNCTION OF THEIR POPULATIONS	49
3.1. Demographic prognoses.....	49
3.2. Regression model: "cleaning" of original information.....	53
3.3. Regression models for the eight regions	57
3.4. Regional urbanised area as a function of its population	59
3.5. Construction of a statistical predictor	61

3.6. Construction of a predictor based on the Γ -distribution	70
3.7. Summary and conclusions on the dynamics of UT	76
4 CARBON CYCLE IN URBANISED TERRITORIES.	
THEIR ROLE IN THE GLOBAL CARBON CYCLE.....	78
4.1. Introduction.....	78
4.2. Estimation of the city's green area.....	78
4.3. Losses of organic carbon as a result of urbanisation: a land use model.....	82
4.4. Redistribution of carbon flows by "urbanised" ecosystem The total balance of carbon flows.	82
4.5. Estimation of the NPP, living biomass and humus for different regions	85
4.6. Losses of carbon as a result of urbanisation, export of carbon into neighbouring territories, and the total carbon balance in urbanised areas. I. Regression model.....	91
4.7. Effect of non-random cities' distribution on components of the total carbon balance.....	99
4.8. Losses of carbon as a result of urbanisation, export of carbon into neighbouring territories, and the total carbon balance in urbanised areas. II. Γ -model.....	103
5 CONCLUSIONS.....	113
References.....	118

Appendix I. Demography of Urbanisation 127

- A1.1. Introduction..... 127
- A1.2. UN, 2001. World of cities..... 127
- A1.3. Multiregional demographic model (Svirezhev et al. 1997)..... 130
- A1.4. Data of the national demographic statistics and the modelling results 132

Appendix II. The Global City Database 137

- A2.1. Description 137
- A2.2. Data..... 140
- A2.3. Statistical references 180

1 INTRODUCTION

In this investigation, we will consider the following question: does the urbanisation process influence the Global Carbon Cycle (GCC)?

We will not consider the clear influence of urbanisation associated with anthropogenic emissions of CO₂, since the related processes are strongly affected by the political and economic decisions made at national and international levels. We are, however, interested in more delicate, and, up until the present time, weaker processes, linked to the land conversion of natural ecosystems and landscapes. Such conversion inevitably takes place when cities are sprawling, with additional “natural” lands becoming “urbanised”.

Certainly, the expression “urbanised territory” does not automatically imply that the entire green surface of a natural territory is transformed into one covered totally by buildings, roads etc; some part remains “green” and continues to function as an ecosystem. Its characteristics and types of functioning, however, become very different, i.e. it is now an “urbanised” ecosystem. In particular, in this ecosystem not only the quantities but also the qualities of the carbon fluxes change significantly.

Naturally, the quantitative estimation of the “green” area depends to a large extent on the type of urbanisation, that has occurred, for example, the plan (or lack of) for city growth, regulations and laws, the attractiveness of a city for a rural population and “*favelisation*”, i.e. the growth of informal settlements.

We could, in principle, describe our studied processes quantitatively. However, their role may be very small and their impact on the GCC negligible. One particular reason may be that the area of urbanised territories is relatively insignificant compared to the total territory participating in the GCC, and in support of this point of view, some authors have estimated the total area of urbanised territories in the 1980s as 1% of the total land area. On the other hand, the paradoxes of exponential growth are well known, so that the factor being negligibly small these days could become significantly important in the near future. It is clear, therefore, that we should consider the dynamics of urbanisation in order to assess its influence on the GCC.

This report consists of five parts (including this one) and two appendices.

The second part is devoted to an overview of the numerous works whose authors have attempted to analyse the history of the phenomenon of urbanisation, as well as its present and future state. Several urban growth models are also described, providing city growth and areas' estimations based on the total density of the population of a region. One of the models, further implemented in our work, is based on the postulation that the distribution of the areas of populated territories with respect to population density is a Γ -distribution. Another important point of our overview is to analyse different concepts of "urbanised" ecosystems, and how it is possible to estimate its carbon productivity, sequestration, flows and storages. At the end of the second part, we briefly formulate the problems to be solved in the following two chapters.

In the third part, two models, connecting the values of city area and its population, are developed. The first model is based on the linear regression of the urban area on urban population. In order to construct this model, a database, including the statistical data at national level for 1248 cities, is collected for the time horizon of 1990. Next, the regression model is generalised for a dynamic case that allows us to predict the dynamics of urban areas into the future (until 2050). Hence, if we know the dynamics of urban population for a given region, it becomes possible to anticipate the corresponding urban area. The second model is based on the concept of a two-parametric Γ -distribution. By applying both models, we construct the dynamics of urban territories from 1980 till 2050. Note that the estimations of the regional urbanised areas, although qualitatively coinciding in dynamics, differ in their values from each other. In particular, the "regression" estimations are significantly lower than the gamma ones.

In the fourth part, using the real and prognostic dynamics of urban areas calculated previously in the third part, we calculate the dynamics of carbon flows that determines the exchange of carbon between the atmosphere and urbanised territories. Since an urbanised territory "reconstructs" the make-up of flows by exporting a part of it (in the form of dead organic matter) into the neighbouring territories, it therefore significantly

influences the total balance of carbon flows between the atmosphere and the urbanised territory. It is clear that this should also be taken into account.

All these estimations depend, on the one hand, upon the values of the specific Net Primary Production (NPP), and storages of living biomass and dead organic matter (humus), that are typical for the surrounding natural ecosystems, and, on the other hand, on the model of the distribution of cities within a considered region. Regarding the first aspect, we use the well known Bazilevich's database (biome's NPP, living biomass and humus contents), while in the second, we use two models of city distribution: random and non-random. Regarding the second aspect, we take into account the fact that human settlements are attracted to certain types of biomes.

The main results of this chapter are the calculations of the past, current and future (from 1980 till 2050) dynamics of carbon flows for urbanised territories. We present two types of estimations: minimal (the regression model and the random distribution of cities), and maximal (the Γ -model and a non-random distribution of cities).

The fifth part is devoted to the main conclusions of the work.

Appendix I contains the demographic database at the national level. For forecasting, we use the multi-regional demographic model. To estimate the percentage of urban population, we use UN data. Appendix II contains the database dealing with urban population and city areas collected from the UN and different national sources.

2 OVERVIEW AND MAIN ASPECT OF A PROBLEM.

2.1. Global Carbon Cycle and the phenomenon of urbanisation.

It is obvious today that the Global Carbon Cycle (GCC) is a leading actor in the performance known as "global warming". The ocean, terrestrial vegetation, represented by different species of plants, and various types of soils are all components of this "*biosphera machina*". All of these systems, occupying different parts of the Earth's surface (continents and oceans, biomes of the terrestrial vegetation, etc.) and forming a spatial mosaic of elementary units of the GCC – bio-geocoenoses, determine the structure and function of the GCC. But recently (since approximately one century ago), a new actor has entered the stage, one who has changed and continues to change both the magnitude of carbon flow (anthropogenic emission) and the "technical characteristics" of the "*biosphera machina*". These changes are the consequences of processes such as deforestation, agriculture, urbanisation - all that are generally called "land use". As a result, new spatial elementary units of the GCC are created, namely agricultural lands and *urbanised* (or, *urban*) *territories*, the latter being the subject of our investigation.

Let us first consider the phenomenon of urbanisation in some detail. We believe it is necessary to begin with a definition of what "urbanisation" means. In accordance with G. Heinke (1997), "Urbanisation is an increase of the ratio of urban population to rural population." J. Cohen (1995) in his book "How many people can the Earth support?" provides another definition: "the increasingly uneven distribution of people in space, with immense concentrations of people in cities". Unfortunately, the definition of urban territories varies between countries. In fact, the UN, compelled in its own generalised reports to use each individual country's definition, states that national statistics are "blurry in meaning".

Apparently, the phenomenon of urbanisation is coupled to a large degree with the *Homo sapiens*' total population growth (see Fig. 2.1.).

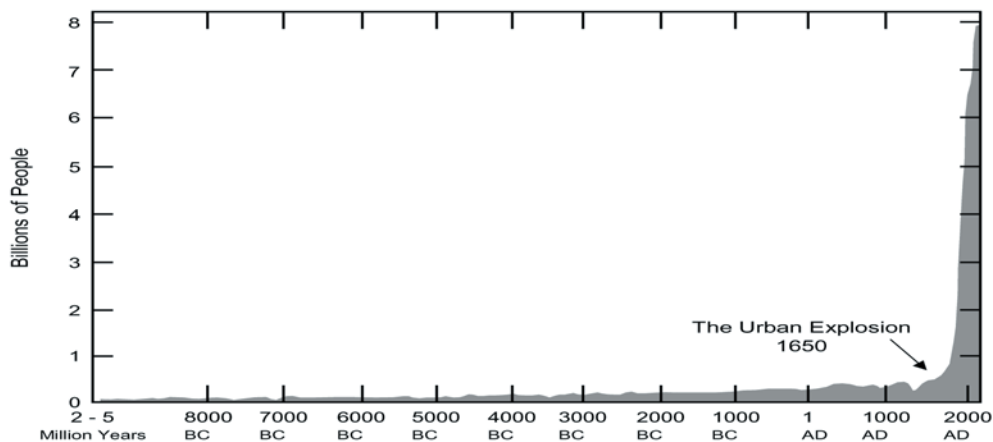


Fig. 2.1. Dynamics of the world population (from Heinke (1997)).

Two thousand years ago, there were a quarter of a billion people living on the planet. This doubled to about half a billion by the XVI-XVII centuries. The next doubling required two centuries (from the middle of the XVII century to 1800), the following doubling occurred only over 100 years, while the last one took only 39 years. Heinke (1997) names the year 1650 as the start of “the Urban Explosion”. Generally speaking, beginning from this date, the enormous population growth started.

Nevertheless, it is common practice to take the beginning of urbanisation to coincide with the start of the agricultural revolution (7000 - 5000 B.C.E.). It was at this time that nomadic hunters settled down and began to grow their food. A food surplus was created, and the division of labour made it possible to evolve gradually into the complex, interrelated social structures we know now as cities. The first cities were located along the Tigris and Euphrates Rivers (4000-3000 B.C.E.) in contemporary Iraq, with urbanisation then occurring in Egypt, North Africa, India, China, Japan and Europe, with Americas being the regions of most recent urbanization. Environmental factors were the major ones in the development of earlier cities. Fertile soils and easy access to water bodies, as well as adequate water supply were essential. The first environmental disaster was triggered by

the deforestation of the Middle East that led to soil degradation in the area, and, as a consequence, famine. This manifested in the extreme dependence of ancient cities on the surrounding ecosystems, in particular, on agricultural lands. For example, at the end of the Third Punic war in 146 B.C.E., each soldier of two Roman legions was ordered to pour out one sack of salt onto the fields surrounding Carthage, which was sufficient for it to be said that “Carthage is destroyed”.

In Europe since the XIth century, there has been a historical continuing flow of people from the countryside to the cities, although the “Black Death” in the XIVth century has very strongly defeated the process of urbanisation. Europe recovered from this only by the middle of the XVIIth century, when the “Urban Explosion” occurred. Urbanisation had also been occurring worldwide for at least two centuries. During the XVIIIth century we have seen modern urbanisation due to technologic development, while earlier – the process was driven by the migration of people from rural areas, since they were not needed in farming anymore.

However, namely in the last decades of the last century we observed the unprecedented global population growth and the accompanying process of urbanisation (see Fig. 2.2.). Generally speaking, this enormous population growth was accompanied by other significant changes:

1. The rise of each person’s ability to affect the natural environment through energy sources manipulation.
2. The rise of the unevenness of the spatial distribution of people through development of *cities*.
3. Migration and travels’ increase, while contacts between cultures also rise.

Although only 12% of the world’s population lived in urban centres in 1940, this percentage had risen to 33% by 1980 (Brundtland’s World Commission on Environment and Development, 1987). The estimation for the time horizon 1985 gives us the following: 43% of the World’s population lives in cities while urban settlements cover just over 1% of the Earth’s surface (G. Miller, 1988). After WW II, a 2% urbanisation rate was observed in the developed world, while it was almost 4% in the developing countries.

However, urban growth rates were double that of the total population. And while the total population growth rate in the developed world has been

decreasing, the urban population's proportion has increased from 55% to 70% of the total population. The major reason is the decline in rural population, as well as the arrival of new immigrants to the cities of some countries.

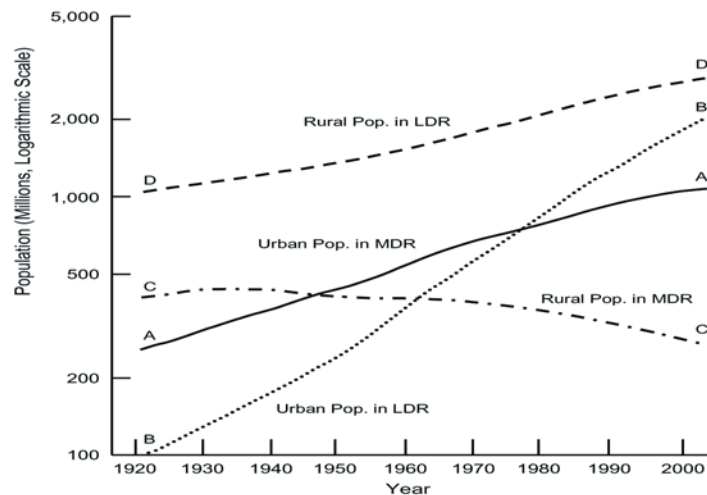


Fig. 2.2. Urban and rural population in more developed (MDR) and less developed regions (LDR). *Source:* UN, World Urbanisation Prospects, 1990, 1991. Here, urban population is defined as settlements of 20,000 people and above.

Since the middle of the last century, the following trend is observed in the percentages of urban population: 1950 - 29%, 1960 - 34%, 1970 - 37%, 1980 - 40%, 1990 - 43,5% and 45% in 1995. However, the definition of what is urban varies greatly, that is why the estimations differ as well, for example, another source (Hauser, 1992) estimates 20 % in 1950.

Urbanisation growth rate has significantly left total population growth behind. From the year 1800 to 1990, the absolute number of city dwellers increased from 18 million to 2.3 billion, a 128 fold increase, while the total population has increased by only 6 times (from 0.9 billion to 5.3 billion). Furthermore, more than 1.4 billion city dwellers live in the less-developed world. If we look at the rates of urban area growth and compare them with urban population growth, we find that the first grows faster than the population, which in turn grows at a faster rate than the total country population, and this is a common phenomenon (Stempell, 1985).

In 1990-95, the world's urban population grew by 2-4 % per year, while rural population only grew by 0.7% per year. Urban population increased by

2.1% during 1995-2000's period, while rural population only by 0.7%. Today, 75% of the world's population lives in the low developed countries, and 58% in Asia. In 1999, nineteen urban settlements had 10 million or more inhabitants, and 47% of all people lived in cities. (UN, 2001). This means that *megacities*, i.e., giant urban agglomerations with a densely settled urban core of the original city, appear. Around this core, the satellite-cities have grown, either planned or unplanned, linked to the central core by transport, communication, economic interdependence and political-administrative structures. This tendency is confirmed by the following statistics: from 1950 until 1975, many cities with population of 5 million people have doubled in total urban population, while at the same time, cities with less than 100,000 people declined in their relative importance. In 1992, there were 23 megacities with populations greater than 8 million: 6 in the developed world (Tokyo, New York, Los Angeles, Osaka, Paris and Moscow), and 17 in the developing world (11 were in Asia). For most Asian cities, the shortage of water will be the most critical issue and is the limiting factor for the further growth of Beijing, Manila, Bangkok, Jakarta and others cities (UN, 1999).

If the past and current demographic situations have been estimated more or less accurately, then future dynamics are forecasted with a very high uncertainty. The UN dramatically illustrates that if current exponential and hyperbolic growth continues in each major region and at the current rates, then the population will increase by more than 130-fold in 160 years, from 5,3 billion in 1990 to 694 billion in 2150. However, sooner or later, the problem will be how to feed these people, since food and water limitations will certainly arise. The UN also shows that future global population size is very sensitive to the future level of average fertility.

Projections of global population dynamics are also uncertain, because external factors such as climate may change unexpectedly. Furthermore, even if external factors change as expected, the relationship between those factors and demographic rates may change.

We have the following hypothetical picture for the next half of century: The global population will grow by 2-4 billion people, mostly in poor, but not rich, countries. It will also increase less rapidly than before and will become more urban than now. Hence, "from here on it is an urban world". Most of all,

the additional people will be living in cities in poor countries, which can become an epidemiological danger. Population of the more developed countries will decline slightly, but increase substantially in less developed countries.

In this century, almost all population growth will be associated with cities in the developing countries. By the year 2030, the world urban population will reach in total 4.9 billion (1 billion in developed countries and 3.9 in developing countries). The rural population will remain constant at 3.2 or 3.3 billion (UN 2001, p.2), although in the developed countries, rural population will decline. The trend in the developing countries is that rural population will slowly rise for the next couple of decades, reach 3.1 billion and then slowly decline. It is interesting that currently the growth rate of urban population in the developing countries has decreased faster than predicted.

The rise of urbanization and mixing trends illustrates the increase of mixing and merging across city administrative and national borders, for example, Los Angeles, San Diego, Tijuana, and Ensenada (USA and Mexico); El Paso and Ciudad Juarez, Laredo and Nuevo Laredo, San Cristobal and Cucuta (the latter in Venezuela and Colombia). In Asia, there are also such international city systems, as Hong Kong and Guangzhou (China), Singapore and Johor Bahru (South Malaysia), while in Africa, there are Kinshasa (Zaire) and Brazzaville (Congo).

By the year 2006, half of the World's population will be living in towns and cities, while the total population is projected to reach more than 6.5 billion (UN, 1999). In the same UN Report, it is projected that almost the whole global population growth over in the next 30 years is expected to be concentrated in urban areas and that most of this growth will occur in urban areas in less-developed regions. The UN Report "The State of the World's Cities 2001" (UN, 2001) forecasts an increase of global urban population by 1.8 times by 2020 (relative to 1990), while the total population will grow by only 1.4 times. Naturally, the situation differs from one country to another, but the general tendency remains the same, with the total number of very large cities increasing. The 1999 revision of the "UN World Urbanisation Prospects" (UN, 1999) points to the fact that the largest rates of population growth, expected in developing countries over the next 30 years, will not be in what

are presently the largest cities, but will take place in a larger number of what are currently smaller or medium-sized cities.

2.2. Spatial aspect of urbanisation. Distribution of population density and landscape approach.

The process of urbanisation is characterised by dense settlement over a relatively small land area. It is interesting that if we look at the global population density map, shown in Fig. 2.3. (Tobler et al., 1997), we can see that, contrary to popular opinion, most of the continental landmass is sparsely populated by humans. In 1990, 50% of the global population of *Homo sapiens* inhabited less than 3% of the Earth's ice-free land area (Small and Cohen, 1999).

If we now examine the spatial distribution of human settlements retrospectively, we can see that most humans have lived in small settlements dispersed within larger ecosystems. In these “patches”, the modification of energy and matter flows, typical for a given ecosystem, was insignificant; as well as the total area of all settlements was small in comparison with the ecosystem's area.

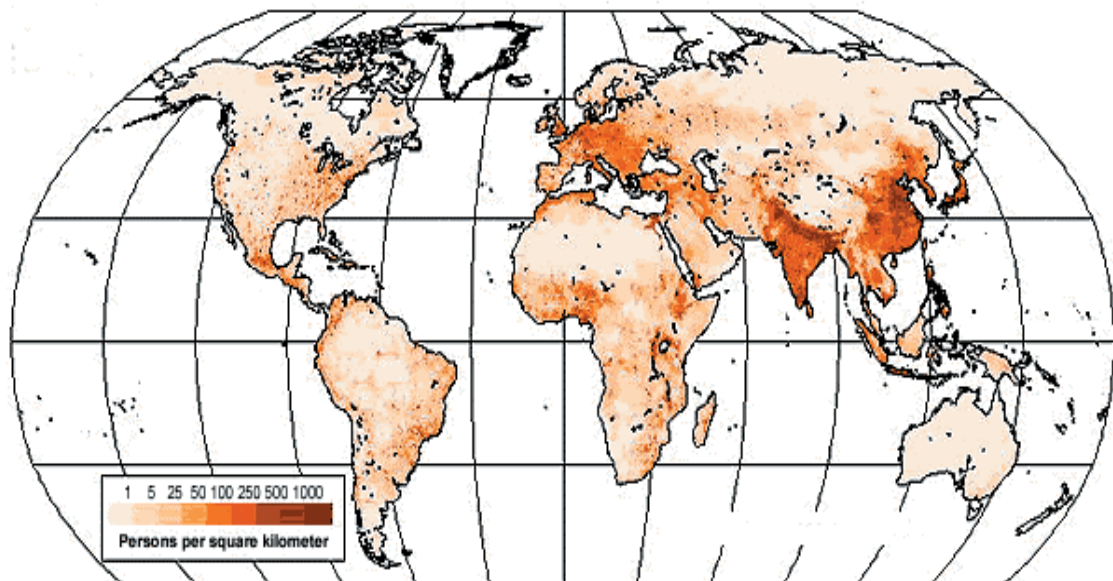


Fig. 2.3. The global population density map (Tobler et al., 1997).

However, today we observe the transition from the above mentioned global settlement pattern of dispersed settlements across large agricultural areas to another pattern that is dominated by dense urban settlement, which will therefore have significant environmental ramifications, both globally and within nations (Miller and Small, 2003).

The following three general aspects of the emerging urban environment can be defined:

1. An urbanised territory constitutes a unique, densely populated habitat that environmentally differs from a non-urbanised setting and, by virtue of its scale, differs from urban settings in the past.
2. This territory exerts a significant environmental impact on its immediate surroundings, its hinterland and on the region within which it is situated.
3. The largest urbanised territories are often linked by transportation, trade, and population migration in an interacting system of global cities. Within this system, economic, demographic and political decisions influence not only the local environment, but also the environments of distant regions.

The Bruntland World Commission on Environment and Development (1987) identified a number of serious environmental problems caused by rapid urban growth. Modern cities and their suburbs endure more contaminated atmosphere and water-body systems, less sunshine, and different microclimates from non-urbanised territories (the so-called “urban heat island effect”).

Considering the urbanisation of the countryside of Western Europe, Antrop (2000) uses the landscape ecology approach. It is clear that urbanisation causes many changes in the ecology and functioning of the landscape, resulting in the changing of spatial structures and patterns. Individual cities that are linked to each other by electricity lines, transportation and energy flows form a network of cities that affects increasingly larger areas of the countryside, and this area is greater than the sum of the individual city areas. We can say that urbanisation creates new landscapes that are highly dynamic.

The landscape ecology approach generates naturally some new definitions of urbanisation. For instance, "Urbanisation is a complex process that is characterised by the transformation of landscapes formed by rural life styles into urban ones. Urbanisation is a process of spatial diffusion caused by the interaction of very different factors that gradually results in the changing of spatial structure, i.e. creates new landscape patterns."

The processes behind diffusion urbanisation are the extension of a market economy and trade. Urbanisation also imposes a new way of living and of environment functioning. The general trend is towards an increased fragmentation of large rural areas, natural zones, agricultural land and cultural ensembles, and uniformity (possessing similar international characteristics) of landscapes and cities.

An advantage of urban form and the associated agglomeration economies is the creation of a surplus in goods and the freeing of labor. This promotes trade that develops communication networks. Site specialisation (such as administration, defense, culture, production, communication, trade and recreation) is reflected in the names of cities and is an important factor of urban growth (or decline). Climate, geology and relief created the complex environment for the development of different regions, however the diversity is also reinforced by cultural values. The process of urbanisation is not entirely based on local conditions, but tends towards a uniformity of landscapes and the loss of natural diversity, since it does not necessarily respect local conditions and aims to improve functionality.

Since urbanization is a dynamic process involving not only the city but also its environment, the following zones of urbanisation may be defined (using a central place of the city hierarchical model with a hexagonal structure): (1) urban core, (2) inner urban fringe, (3) outer urban fringe, (4) rural commuting zone and (5) depopulating countryside with relicts of old landscapes. This is common for large cities, while in the smaller ones geography has a stronger influence on the general urban pattern (for example, the inner urban fringe is missing and the outer fringe is smaller). In Europe, on the other hand, another explanation for the hexagonal pattern is possible, in that towns are located one coach day distance apart from the national roads, with smaller centers being traditional "resting" stops.

Finally, we can say that the urbanisation process acts more like a real diffusion process and is influenced by communication, accessibility and mobility. Disadvantages of growing urbanisation are in the expansion of urban areas that, eventually, leads to a loss of the advantages of agglomeration economies, meaning longer communication times and traffic congestion, crowding, crime and health problems resulting in the loss of quality of life.

2.3. Urbanised territory from the ecologist's point of view.

The role of cities (primary human habitat) is in the expanding human ecological niche that leads to their ecological footprint on these territories (Rees, 1997). The footprint concept is based on the quantitative conversion of the material and energy flows required to support human population in cities into the land area required to produce these flows. Although cities occupy a relatively small area on the planet, they are the dominant human ecosystem and the *ecological* space taken up by humans as a species is much higher. Every city depends (for its existence and growth) on a globally diffused productive hinterland up to 200 times the size of a city itself. This fact defines a major vulnerability of a city to ecological change and geopolitical instability. Most studies these days focus on economic values, however these are too removed from the physical reality, and reveal not the true structures ruling the city. The focus on money wealth and economic surpluses is misleading in relation to ecological health and long-term stability.

Rees (1997) suggested the concept of the "human carrying capacity", i.e. the maximum population of a given species that can be supported indefinitely in a defined habitat without permanently impairing the productivity of the habitat. Humans can increase their own carrying capacity by eliminating competing species, importing resources and with the help of technological innovations make this concept irrelevant to humans in general. Rees argues that, in his opinion, shrinking carrying capacity may soon become the single most important issue for humanity to deal with!

It is perhaps better to define the human carrying capacity as not the maximum population, but rather the maximum load, safely imposed on the environment by people. People are consuming more energy per capita, thus becoming 'larger' from an ecological point of view. For example, in 1970, the

average daily energy consumption by Americans was 11 000 kcal, while in 1980 this had increased 20 fold to 210 000 kcal. We should not only take into account the size of a population, but also the increased consumption when estimating carrying capacity for human ecosystems. The major material difference between humans and other species is that our metabolism includes not only biological metabolism, but also the industrial one.

It would make sense to redefine (although perhaps slightly too broadly and resource focused) human carrying capacity as the maximum rates of resource harvesting and waste generation that can be sustained indefinitely without progressively impairing the environment. To illustrate this, let us examine the following case studies. Firstly, the city of Vancouver (Canada) had in the year 1991 a population of 472 000 living in an area of 11400 hectares. If we assume that the per capita land consumption rate is 4.3 hectares, then the people in this city would require 2.03 million hectares of land. Hence, the inhabitants would require a land area of 180 times larger than their habitat. Furthermore, adding a marine footprint of 0.7 ha per person, the total area of Earth needed to support the city becomes 2.36 million hectares, or 200 times larger than the geographic area of the city. For London (UK) the equivalent footprint is calculated to be 120 times the area of the city itself.

Rees also defines and emphasizes such an important issue as a sustainable city as “*sheer more dispersed settlement patterns, dealing with many of ecological problems associated with them*”.

Bearing in mind that the energy approach is one of the most important elements in Lindemann’s description of ecological systems (Lindemann, 1942), we have estimated some energy values for urbanised territories. Note that one of the main human needs will always be food, and the concentration of people was always accompanied by the intensification of food provision. This statement is illustrated by Table 2.1. We see that even areas with traditional farming, with respect to the population density criterion, can be considered as totally urbanised areas (here we are no longer speaking about the lands of modern agriculture).

Table 2.1. Evolution of the intensification of food provision (Smil, 1991).

	<i>Energy Input (GJ/ha)</i>	<i>Food Harvest (GJ/ha)</i>	<i>Density (people/km²)</i>
Foraging	0.001	0.003 – 0.006	0.01 – 0.9
Pastoralism	0.01	0.03 – 0.05	0.8 – 2.7
Shifting agriculture	0.4 – 1.5	10 - 25	10 - 60
Traditional farming	0.5 – 2.0	10 - 35	100 - 950
Modern agriculture	5.0-60	29 - 100	800- 2000

Settlement densities can be orders of magnitude higher than agricultural rates, although residential densities in some urban areas are only marginally higher than the farmland densities in the most intensively cultivated agricultural areas (compare 2500 people/km² in Los Angeles suburbs with 2000 peasants/km² of arable land in Sichuan, China). However, maximum residential densities of about 90,000 people/km² (the centre of Hong Kong) translate into an anthropomass of 36 MJ/m² (Smil, 1991). This is roughly 200 times higher than the density of large herbivorous ungulates in Africa's richest ecosystem.

Territoriality of modern urban populations has no energetic foundation (all food comes from outside), but energetic reasons alone are insufficient to explain the pre-industrial quest for a defensible territory (Lopreato, 1984).

Urbanised territories dominate the surrounding environment in a number of ways. The growth of cities, absorbing and transforming nearby natural ecosystems and agricultural lands, negatively influences the local and regional biodiversity. This process leads to the changing of the nature of land surfaces, and therefore its reflection and absorption of solar radiation and aerodynamic properties, that in turn leads to raising urban temperatures and the changing of the local climate, creating urban heat islands. (Landsberg, 1981; Lo et al., 1997; Kalnay and Ming, 2003). In the latter work, the impact of land use changes caused by urbanisation on Global warming is estimated by comparing surface temperatures in the continental US with their trends over the past 50 years. The result was that half of the observed decrease in the diurnal temperature range is due to urban land use changes. The

estimate of 0.27°C mean surface warming changes per century due to land use changes is twice as high as previously estimated, based on urbanization alone. The “urban heat island” effect occurs at night, when the buildings etc. release heat absorbed during day. In addition, metropolitan agglomerations influence the local and global environment through their consumption of non-native resources and their concentrated production of waste and consumable.

Therefore, we can say that although the total area of urbanised territories is relatively small (~1-2% in 1990s), they play an ever-increasing role in Global Change in general and in the GCC in particular.

1. Urban areas emit (in accordance with different estimations) between 78% (O’Meara, 1999) to 97% (IPPC SRES, 2000) of all anthropogenic carbon emissions. Up to 60% of these emission come from the transportation and building sectors, while the rest are from industry. Of course, all of these emissions are “spread” and mixed in the entire atmosphere over 3 – 4 months’ period, but they are generated by namely urban point sources.
2. Cities transform the natural territories they occupy, partially obliterating vegetation and soil, partially modifying them. By the same token, urbanisation changes the structure and function of the local carbon flows within these territories. Note that the process often involves considerably larger territories than the exact city areas.
3. Cities consume a lot of organic carbon in the form of food and other agricultural products, as well as wood, etc., produced, as a rule, far from the urban territories, transforming them into other forms of carbon (faeces, exhaled CO₂, residues of food processing, dead organics of “green zones”, etc.) in the process of urban and purely human metabolism. In other words, cities destroy the spatial entity of the processes of production and decomposition of living matter that is typical for natural ecosystems. Note that this entity provides the closure of any local carbon cycle.

The final statement may be illustrated by the following example (Solecki and Rosenzweig, 2001): the New York metropolitan area annually consumes the equivalent of 800,000 ha of wheat, or, approximately the total amount of wheat grown yearly in the state of Nebraska.

2.4. The city as a specific heterotrophic ecosystem. Carbon balance in urbanised territories.

From an ecological point of view, any city (and especially an industrial one) is a heterotrophic system that is supported by external inflows of energy, food, water and other substances. Thermodynamically, any city (and generally, any urbanised territory) is an open system that is far from thermodynamic equilibrium. Therefore, the concepts and methods of thermodynamics of open systems can be used for the analysis of city metabolism. Note, that all matter and energy needed for a city's functioning are collected from external territories that are significantly larger than the area of the city itself and very often are located quite far away. The heterotrophic ecosystem "city" differs very much from a natural heterotrophic ecosystem, because:

1. A city has a more intensive metabolism per area unit, requiring a significant inflow of artificial energy (in the form of fossil fuel and electricity).
2. During the process of its own metabolism, a city consumes larger amounts of various materials: food, water, wood, metals, etc. i.e., all that Pimentel et al. (1973) have called "grey energy".
3. A city also emits (as the products of its metabolism) larger volumes of, and more toxic, substances, than natural territories, from which they were originally produced (especially various synthetic substances).

Therefore, considering all of the above, the state, structure and composition of input and output flows play a more important role for the ecosystem "city" than for such a natural ecosystem as forest. Many cities have wide green belts, (consisting of trees, shrubs, lawns, as well as ponds and lakes) so it may be said that a certain autotrophic component is present in the ecosystem "city". However, it does not play any significant role in the mechanisms operating within the city. While the green belts are very important from a purely recreational and aesthetic point of view, they also smooth air-temperature fluctuations in a city and reduce noise and other pollution, while serving as habitats for small animals and birds. It is not "charge free", however, to support their functioning since the labour and fuel spent on irrigation, lawn management, tree planting and care etc. increases the energy and monetary expenses of a city. For instance, the annual

subsidies in fuel, fertilisers, labour, etc. required maintaining a lawn in the Madison metropolitan area (Wisconsin, USA) is equal to 22 GJ/ha (Odum, 1983), which is approximately equal to the artificial energy input for a maize field. Loucks et al. in his unpublished report (cited by Odum, 1983) has compared the parameters of the local carbon cycles within the Madison-metropolitan “green area” (the ecosystem located on urbanised territory) and the neighbouring “natural” forest. The annual net production of the natural ecosystem is equal to 400 tonsC/km², while the same value for urbanised territory is 350 tonsC/km². However, the latter value is calculated for the whole area. If one assumes that approximately 30% of the urbanised territory is covered with buildings, i.e. by concrete and other “non-penetrated” surfaces, then only 70% functions as an ecosystem, resulting in an “effective” productivity equal to $350/0.7 = 500$ tonsC/km² (in the case of Madison, the “green city area” was equal to 70% for the years 1960s).

It is obvious that buildings, roads, concrete and asphalt do not cover the whole surface of an urbanised territory. There are comparatively large fragments covered by trees, shrubs and grass in the form of parks, gardens, lawns, etc. All of this is called the “green city area” or the “free city space”. The green area is a mosaic of many quasi-natural micro-ecosystems, and it plays the main role in the biological part of the local carbon cycle of the ecosystem “city”.

As another example of estimating a city’s “green areas”, Nowak and Crane (2002) found that the average tree cover of urban areas in the continental US doubled between 1969 and 1994, and currently occupies 3.5% of land, which constitutes 27.1%. It seems that there is some contradiction between this estimation, and Loucks’ values for Madison’s metropolitan area in the 1960s (70%). The simplest explanation for this discrepancy is that there is a lot of uncertainty in the basic definitions of what exactly does urbanised area, city area, metropolitan area, and “green area” mean. Nowak and Crane, for example, consider only forested areas, while Loucks included all types of vegetation into the “green area”. Another explanation concerns the possibility of spatial and temporal shifts in these estimations. Nowak and Crane’s average results relate to the whole territory of the continental US, while Louck’s values relate only to Madison metropolitan area. Note that Nowak and Crane estimate the percentage of “green area” in Wisconsin as 26%.

Concerning the temporal shift, we must keep in mind the classic concept of “open city space”, developed by E. P. Odum (1971), where he showed that for a typical American city, the free space was about 70% in the 1970s, while if there is no urban planning, this space is reduced to 16% by the year 2000. However, with planning, this value increases to 31%. Later on, we shall use namely this value as a basic one for highly industrialised and economy-in-transition regions.

Returning to the estimation of plants’ productivity in the city ecosystem, 500 tonsC/km², we can explain such an increase by taking into account the fact that fertilisers uptake by a city ecosystem is equal to 140 tons /km².year.

However, there is another explanation of this effect (Gregg et al., 2003). The authors study the urbanisation effects on tree growth in the vicinity of New York City. It is obvious that plants in urban ecosystem are exposed to higher rates of nutrient and base-cation deposition, warmer temperatures and increased CO₂ concentrations than plants in rural areas. This all should, in principal, increase plant growth, and the authors found urban plant biomass to be double that of rural sites with the same areas. A reason for such an increase in biomass is, according to the authors, higher ozone (O₃) exposures reduced the plant growth at rural sites. Soils, temperature, CO₂ concentration, nutrients, urban air pollutants and microclimate could not account for the increased tree growth in the city. If we agree with the last statement (*à propos*, this is an argument on behalf of our assumption that "urbanised" and "natural" ecosystems differ from each other insignificantly with respect to productivity), then the “ozone hypothesis” seems very doubtful. The observed phenomenon of biomass increasing can in fact be explained by not only the higher growth rates of plants in the city, but also by the following.

Indeed, if we write a simple balance equation for the living biomass:

$$\frac{dB}{dt} = P - \frac{1}{\tau} B ,$$

where B is the biomass, P is the productivity (or growth rate), and τ is the mean lifespan of plants, then in a steady state $B^* = \tau P^*$. We see that an increase in biomass can therefore be a consequence of either an increase in τ or in P , or in both values. The first mechanism, i.e. an increase in τ , appears to us the more realistic. In fact, any city ecosystem is a cultivated one and resembles a park, rather than a forest. As a result, the competition

within a city ecosystem is significantly weakened, and the lifespan of its living matter increases. An illustration of this thesis could be the fact that animals in a zoo live much longer than in nature.

Note that our point of view is implicitly confirmed by Nowak and Crane (2000). In accordance with their estimates, the carbon storage in urban forests with their relatively low tree cover (25.1 tC/ha in average for US) is less than in natural forest stands (53.5 tC/ha). The gross sequestration rate, i.e., the fraction of the gross annual production accumulated in wood, in urban forests, 0.8 tC/ha-year, is also less than in natural ones (for instance, 1.0 tC/ha-year for a 25-year old natural regeneration spruce-fir forest with 0.1 kgC/m² cover, (Birdsey, 1996), although the difference is insignificant.

However, on a per-unit tree cover basis, carbon storage by urban tree and gross sequestration may be greater than in natural forests, 92.5 tC/ha and 3 tC/ha-year, due to a larger proportion of large trees and the more open structure (that leads to the weakness of competition) in urban forests (Nowak, 1994).

It is interesting to compare these estimations with Bazilevich's estimations for Russian forests (Bazilevich et al., 1986). In accordance with Bazilevich, the characteristics of the boreal coniferous forests of North America are very close to the equivalent in the European part of Russia (and the first are very close to the average values for the continental US). The total production of the Russian forests is equal to an average of 5 tC/ha-year, about 50% of which is wood. Therefore, we can say that the sequestration rate of Russian natural forests with almost 100% cover is 2.5 tC/ha-year. Biomass storage by Russian forests is on average 150 tC/ha, of which about 65% , i.e., 97 tC/ha, is wood. It is interesting that these estimates differ from Nowak and Crane' s (2002), but are very close to the values for Chicago's urban forests made by Nowak (1994). Note that if we assume that the average values, 25.1 tC/ha and 0.8 tC/ha-year, were estimated for the entire urban area, with forest cover on average 27.1%, then, recalculating these density estimations for properly forested area (assuming 100% cover), we obtain: $25.1 \text{ tC/ha} : 0.271 = 92.6 \text{ tC/ha}$ and $(0.8 \text{ tC/ha-year}) : 0.271 = 3 \text{ tC/ha-year}$. Firstly, we note the agreement between the two Nowak's estimations, and secondly, their closeness to Bazilevich's values for natural

forests. This allows us to assume that all these discrepancies are a consequence of the different methods of estimation. Moreover, this is one more argument in favour of our following hypothesis, which is as follows:

With respect to productivity (and, possibly, to the storage of living and dead biomass), "urbanised" and "natural" ecosystems differ from each other insignificantly.

However, they are not the same regarding outflows of carbon. Carbon outflow from the natural ecosystem is practically zero, while for the urbanised one, it is equal to $250 \text{ tonsC/km}^2 \cdot \text{year}$, i.e. to half of annual ecosystem production. The carbon in the form of wood, falling leaves and cut grass is exported to the neighbouring regions, thereby it is included into the cycle of the corresponding natural ecosystem. Also, carbon flows in natural ecosystem are generally vertical (from the atmosphere and reversed into the atmosphere); but in an urbanised ecosystem, half of the vertical flow passes through in a horizontal direction, where the organic matter is transported either into other ecosystems with different decay conditions, or via rivers to the ocean. Therefore, urbanisation changes the structure of the local carbon flows.

Thus, we may state that urbanised territories are:

1. The main source of anthropogenic carbon;
2. A powerful transformer of flows within local carbon cycles.

Finally, we need to discuss urbanisation phenomena from an environmental point of view (see also McDonnell and Pickett, 1990). In this article, urban areas are defined as those with population densities greater than 620 persons *per km*². In accordance with this definition, in 1989, 74% of the US population (203 million people) lived in urban areas, and it is predicted that more than 80% will do so by the year 2025. Cropland, pastures and forests are constantly being converted into urban territories. The urban area has increased by 3.6 million hectares, and by 5.2 million hectares between 1970-80. The structure of metropolitan areas and their fringes consists of a variety of components, from completely built-up areas to natural (extensively managed by people, city parks, lakes, ponds, streams etc.) and semi-natural areas. It is intuitively clear as to what the difference is between "urban" and "rural" ecosystems, nevertheless to draw a sharp boundary between them is very difficult. Certainly, we may take into consideration the "gradient" concept,

which is defined as environmental variation ordered in space, in such a way that spatial patterns impose on the structure and functioning of ecosystems at different scales (populations, communities, ecosystems). The steepness of the gradient is determined by the degree of environmental change. When we deal with a single environmental variable or parameter, then by moving along the gradient, we can define the border point as that with a maximal rate of change of this parameter. But how must we deal with this, when there are two or more relevant parameters? A weighting problem now appears, which is also difficult to solve. McDonnell and Pickett (1990) consider the study of ecosystem structure and function along urban-rural gradients as an unexploited opportunity for ecology. The complexity of this phenomenon is due to the spatial interactions between the various anthropogenic factors, and between anthropogenic and natural factors. Unfortunately, this problem is still far from being resolved, and because of the uncertainty in the definition of the border between urban and rural ecosystems, we shall set the area of an urban ecosystem as some percentage of the total city area. The latter is determined, using standard statistical data.

2.5. Carbon balance in urbanised territories and the role of human metabolism: global scale.

Today there are many different models that describe the various aspects of the GCC. Frequently, they operate at high spatial resolutions, with detailed descriptions of the metabolism of both natural and artificial civilisers systems. However, as a rule they do not consider the contribution of urban territories to the GCC. Moreover, in most studies of the global carbon balance, which serve as a basement for the calibration of the GCC models, the role of urban areas is omitted. As for the proper human metabolism, it seems at first glance, and is a common belief, that the contribution of the metabolic process of *Homo sapiens*, considered a biological species populating the biosphere of our planet, to the global carbon balance is negligible. Unfortunately, almost all these models (with the possible exception of the Moscow Biosphere Model - Krapivin et al., 1982) also do not take into account human metabolism.

The first attempt to estimate the contribution of urbanisation to the GCC was made by Bramryd (1980). In his opinion, most urban territories,

covering a substantial part of the planet, have more carbon stored per unit area than natural ecosystems. This includes carbon transported into the cities and stored in building etc., but most of this flow is transformed into waste. Bramryd has estimated (at the corresponding time horizon) that the storage of organic carbon in the soils and vegetation of urban territories, and also in people and pets, and the carbon fluxes from mineralisation, incineration (rapid oxidation of carbon) and the landfilling of solid waste, are accompanied by processes similar to ones in peatlands. For instance, the global input of carbon into solid waste (sludge and industrial waste) is estimated to be 0.16 Gt per year (1 Gt = 10^9 t).

Long-term accumulated organic carbon in urban territories can be divided into four main groups:

1. *Biomass in humans and animals.* With an assumed mean individual weight of 50 kg, and taking into account that dry matter (containing 50% carbon) is about 30%, then the carbon content of one individual is equal to 7.5 kgC. For a world population of six billion, the total amount of carbon is therefore $45 \cdot 10^{12}$ gC. It is interesting to compare this value with Whittaker and Likens' (1973) estimates of the total biomass of all animals, $906 \cdot 10^{12}$ gC, and the biomass of land animals, $457 \cdot 10^{12}$ gC.

Let us now attempt to estimate the role of human biological metabolism on the global carbon balance and compare this value with its other components. We know from physiological studies (see, for example, *Space Biology and Medicine*, v. II (2), 1994, where these data were obtained from very detailed experiments within closed spaces) that under the condition of moderate work activity, a single individual of 70 kg standard weight exhales $0.4 \text{ m}^3 \text{ CO}_2$ per day, corresponding to a total of 216 gC per day. Approximately 115 gC is emitted with faeces and other discharges. This leads to annual amounts of approximately 79 kgC and 42 kgC, respectively. With a current world population of six billion individuals (with an average weight of 50 kg), the components of *biological* metabolism of mankind are equal to ~ 0.34 GtC per year and ~ 0.18 Gt per year, respectively, giving a total of 0.52 GtC per year.

Since it is impossible to imagine humans without pet animals (we assume that dogs have a clear dominance), then we must add to the value

above the dogs' biomass. We assume that 0.06 dogs *per capita* is a reasonable average for the world (with 1.5 kgC per dog) (Bramryd, 1980). Thus, the estimation of the biomass of pets for six billion people is $0.54 \cdot 10^6$ tons C. All of these dogs produce annually about $5 \cdot 10^6$ tons C in faeces (it seems that this Bramryd's estimation is very overstated) and exhale about $3.6 \cdot 10^6$ tons of C in the form of CO₂. Adding these values to the values for human metabolism, we obtain: $0.52 + 0.01 = 0.53$ GtC *per year*.

We will now compare this value with the other components of the global carbon balance (see Table 2.2). Undoubtedly, the value 0.53 GtC/year is of a global scale and can be added to the table.

Table 2.2. The components of the GCB and emissions and uptake values estimated for 1988. (Svirezhev et al., 1997).

<i>Industrial emission</i>	<i>5.89 Gt C/year</i>
Deforestation	1.36 Gt C/year
Soil erosion	0.98 Gt C/year
Terrestrial biota uptake	3.91 Gt C/year
Ocean uptake	1.02 Gt C/year
Residue in the atmosphere	3.31 Gt C/year.

2. *Biomass in trees and other plants.* The mean global estimate of living plant biomass in towns, 3.5 kg dry weight (1.75 kg C) *per m*² of open (“green”) area, was made by Bolin *et al* (1979). The mean NPP of vegetation was also estimated in this work as 0.25 kg C/m² · year, or 250 tons C/km² · year. Both estimations seem understated, and Bramryd (1980) has doubled them. This appears to be more realistic, if we keep in mind that Loucks' estimation of the NPP in Madison metropolitan “green” area was 500 tons C/km² · year. Then, estimating the global urban area in 1980 as $2 \cdot 10^6$ km², and assuming that 50% belongs to “green area”, we find that urban territories may contain 3.5 GtC in living vegetation biomass, while a global figure for net plant assimilation of carbon in urban territories is approximately 0.5 GtC/year. It is interesting that if we compare this value with the estimate for human metabolism, 0.53 GtC/year, we find that they are very close. This coincidence may be considered as an argument on behalf of the following statement: *an urbanised territory with its population is a special ecosystem,*

which is in a state of equilibrium with respect to the carbon exchange between the atmosphere and the ecosystem, if the civilization metabolism (industrial and transport CO₂ emissions) are excluded.

3. *Carbon in construction material, furniture, books.* Extensive amounts of carbon are accumulated for long time periods in building constructions, furniture, books and other articles made of organic materials. These values were estimated within the framework of the “Nuclear Winter” problem (see, for example, Svirezhev et al. 1985), when it was necessary to estimate the amounts of fuel materials in cities.

The following estimates (for the 80s) are:

a) about 3 Gt of organic carbon fixed in houses in the whole of Europe, North America, Japan, and Australia;

b) about 0.4 Gt of organic carbon in other countries.

4. *Carbon in solid waste.* Most products of forestry and agriculture are turned sooner or later into garbage. Solid waste is either deposited in sanitary landfills or incinerated. Carbon stored in landfills experiences slow decomposition rates and is gradually released as a result of microbiological activity. Estimates for different regions are shown in Table 2.3 (Bramryd, 1980). Approximately 50 – 60 million tons of C are released into the atmosphere by burning, while about 100 – 110 million tons of C are deposited in landfills with the following slow release into the atmosphere.

Table 2. 3. Solid-waste production in different parts of the world.

<i>Region</i>	<i>Solid-waste per capita (tons carbon)</i>	<i>Solid-waste per year (million tons carbon)</i>
Heavy industrialised parts of Europe	0.15	20.6
Less industrialised parts of Europe	0.06	19.7
United States	0.30	64.6
Canada	0.30	6.0
South America	0.05	18.0
Africa	0.008	3.5
Asia (except Japan)	0.004	9.3
Japan	0.15	18.0
Australia, New Zealand	0.13	2.0
Others in South Pacific	0.006	0.03
Total	1.158	161.73

5. *Organic carbon accumulated in landfills and soil carbon.* Landfills are often regarded as long-term accumulators of carbon and in this respect can be compared with natural peatland ecosystems. According to Bramryd, one-third of the organic carbon is still unmineralised after 30 years.

Using the exponential model of the decomposition of organic matter,

$$N(t) = N_0 \exp(-t / \tau)$$

where τ is the residence time of carbon in the landfill, we obtain: $(1/3) = \exp(-30/\tau)$, whence $\tau = -30/\ln(1/3) \approx 27.3$ years. The remaining carbon is bound in long-lived humus and will remain unmineralised for a very long time. What concerns organic carbon accumulated in urban area soils, Bramryd estimates this value to be 21,000 tons C *per* km². We shall, however, use another estimation based on Bazilevich's data.

Returning to the local carbon balance of urban areas, Bramryd states that most of the annual biomass production is burned or transported from the area of production. The accumulation of new material is slow, but municipalities often apply organic fertilizer. However, organic matter is transported and being accumulated in landfills, hence recycling is less than in the natural ecosystem. Generally speaking, his point of view is very close to ours.

2. 6. Maps of population density and areas of urbanised territories.

It is clear that one of the most important variables when determining the total contribution of urbanised territories to the GCC – at global, regional and local levels – is their area. Unfortunately, even if we can estimate the urban (city, metropolitan) area for current (or past) times using existing national and regional statistics, the prognoses of this value vary greatly, indeed. For example, information found in statistical reports, such as the UN Report “World of cities, 2001”, operates with population data and provides future prognoses. There are other prognoses in the literature, but they all only deal with population values as well, and this is a common situation. Nevertheless, there is one standard demographic variable that contains both spatial and population information: population density, that is population/area, which results in such standard tools for demographic studies as the maps of the population density. These maps are drawn at both global and regional

scales. For instance, the global population density map, shown above in Fig. 2.3, makes use of data describing the estimated population in 1994 of 219 countries, subdivided into polygons that were assigned to 5 by 5 minute quadrilaterals, resulting in 5.6 billion people, spread over 132 million km² of land. In fact, such maps are simply the graphical representation of probabilistic distribution, describing the percentage of population *versus* percentage of occupied land area.

Using Tobler's "Map of the Global Population" in grid format, Small and Cohen (1999) build a so-called Spatial Localisation Function (SLF). If the cumulative sum of population is plotted as a function of the cumulative land area that it occupies for monotonous increasing local density, it is possible to quantify the localisation of human population on the Globe. This is a Lorenz curve for the spatial distribution of human population or the SLF. The localisation of human population apparent in Fig. 2.3 reveals the extent to which the Earth's landmasses ($1.32 \cdot 10^8$ km²) are characterised by several populous regions with a higher contiguous population density and by large regions with much lower mean population densities. The corresponding SLF are shown in Fig. 2.4. For comparison, the populous areas were divided into seven sub-regions of relatively contiguous population separated by regions of sparse population. Note that this subdivision is similar to the standard UN Regional subdivision (see UN, 2001). These "density constrained" SLF, constructed for regions with local densities greater than 10 people per km², are also represented in Fig. 2.4.

The elimination of scarcely populated areas results in a more uniform distribution of population within the remaining land area, indicated by the regional SLFs having less curvature than the global SLF. The regional SLFs indicate that while the South central and East Asian regions are by far the most densely populated, they are also the least spatially localised of the regions. North America, by comparison, is much less densely populated on average, but is far more spatially localised.

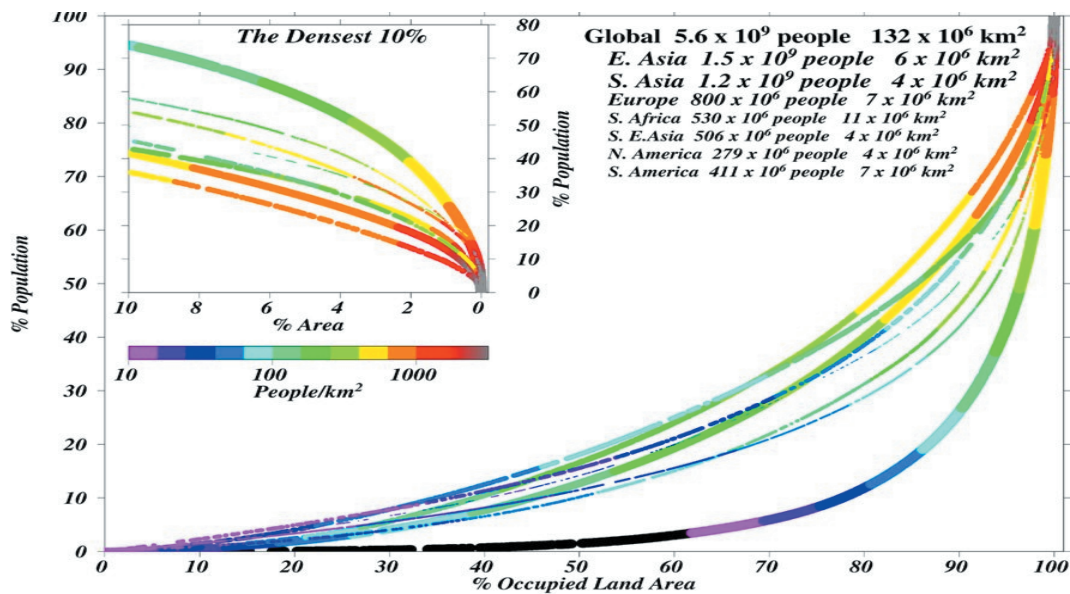


Fig. 2.4. Spatial Localization Functions (SLF) for the global human population and for seven populous sub-regions. Each curve shows the cumulative fraction of the population with cumulative fraction of land area for increasing population density. The thick global curve is the most concave because it covers all ice-free land area, including many sparsely populated areas. Regional curves (thickness proportional to total population) include only areas that are populated at local densities greater than 10 people/km². The insert shows the most densely populated 10% of land areas enlarged and inverted. The figure indicates that 50% of the world's population occupies less than 4% of the ice-free land area at densities greater than 300 people/km², while in Eastern Asia 42% of the total population occupies 10% of the populated land area at densities greater than 700 people/km². *Source:* Small and Cohen (1999).

The shown most densely populated 10% makes it obvious that 50% of the total world population occupies less than 4% of the ice-free land area, with densities greater than 300 persons *per* km². Asia stands out here, especially Eastern Asia, where 42% of the population occupies 10% of the populated land area at densities greater than 700 persons *per* km². Deviating slightly from our main topic, we shall note that to study the spatial distribution of population and the land on which the people live, in an attempt to connect these two values numerically, is one of interesting approaches. The authors, Small and Cohen (1999), believe that understanding the relationship between humans and the environment can be obtained by studying their distribution on the Earth's surface as well as interactive feedbacks between those two entities. It is also specifically stated in their article that climate and ecological zones serve as constraints on the localisation of the densest populations.

However, the results tell us that human population is more localised with respect to land forms, distances to major water bodies and elevation, then with respect to climatic parameters, such as temperature, precipitation and their variability. When looking over a global scale, localisation becomes blunt with respect to climate.

In another article by Miller and Small (2003), this concept is developed as a way of looking specifically at urban areas. The authors acknowledge the importance of studying rapid urbanisation issues, since they understand that urban growth is represented mostly by dense settlement over relatively small areas. They construct a similar curve describing the cumulative percentage of human population as a function of cumulative percentage of occupied land area (see Fig. 2.5). This curve is an illustration of the non-uniformity of population distribution over land area, and its curvature indicates the degree of the non-uniformity.

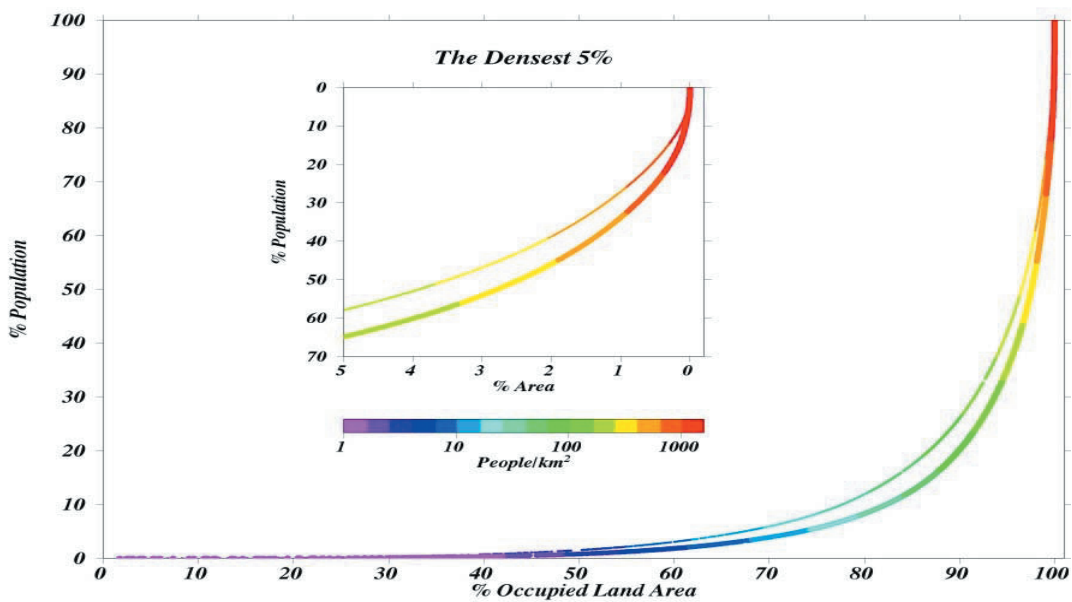


Fig. 2.5. Global distribution of human population on Earth's ice-free land area in 1990. The curve shows the cumulative percentage of human population as a function of the cumulative percentage of occupied land area. If human population were uniformly distributed, the percentage of population would equal the percentage of land area and the curve would be straight. Curvature indicates the degree of localization of population in dense settlements. This curve, compiled from 127,105 census estimates worldwide, indicates that 50% of the human population occupied less than 3% of Earth's potentially habitable land area (excluding Antarctica) as population densities exceeding 500 people/km². Source: Miller and Small (2003).

It is obvious that if we know the density threshold that determines when a territory becomes urbanised then we may estimate the percent of urbanised area.

The problem, however, is how to define the urban.

2.7. Urbanised territories: different definitions and a concept of the threshold density.

In the previous section, we used the expression “urban (or urbanised) area (territory)” many times. However, in spite of the intuitive obviousness of this term, it remains a typical “fuzzy” definition with a high degree of uncertainty.

For instance, in accordance with the definition provided by the US Census Bureau (www.demographia.com), an urbanised area is a densely populated area (built up area) with a population density of more than 1,000 inhabitants per square mile (or 386 persons per square kilometre) and a population of more than 50,000¹. Thus, the minimal city area and its characteristic size are equal to 130 km² and 12 km, respectively. This definition is independent of corporate city or regional government boundaries.

An urbanised area is considerably different from a metropolitan area. The latter typically includes large tracts of non-urbanised (non-developed) land. For example, the Los Angeles metropolitan area (Consolidated Metropolitan Statistical Area) covers more than 34,000 square miles, only 2,000 of which belong to the Los Angeles urbanised area.

Therefore, in accordance with the US Census Bureau’s concept, only approximately 6% of the whole metropolitan belongs to the proper urban area.

At first glance, this definition (with necessary regional corrections) could be used as an operational one in our investigation. But, when we started to analyse the different sources of information (especially non-American), we were forced to relinquish this idea because the definition of “city” in regions with different economies and traditions is extremely undetermined. Moreover, if we look again at the above cited works that

¹ Certainly these threshold values differ from each other for different countries and especially for different regions, such Africa, Latin America, Asia, etc.

generally operate with the US statistics, we see that many authors use the term “metropolitan area” as a synonym for the term “urban area” and *vice versa*.

Generally speaking, there is a great deal of uncertainty in all definitions, one way or the other, concerning urbanisation (city area, urban(ised) area, and metropolitan area). This is seen very clearly if we deal with official statistical reports, containing different demographic information (see Appendix II).

For example, when we deal with the Arab statistical yearbooks, we see that their definition of city area differs dramatically from the conventional one, with the concept of urban area rather based on the ancient structure of a city, the so-called “*Medina*”. As a rule, Arab statistical yearbooks offer information about the areas of *wilayas* (**Algeria**, 1991), *governorates* (**Egypt**, 1996), *districts* (**Kuwait**, 1990, 1997), *provinces* and *prefectures* (**Morocco**, 1993), taking into account both rural and urban areas, i.e. data of a higher hierarchical level (see the reference list from **Algeria**, 1991 to **Zaire**, 1994 in Appendix II).

Many attempts have been made to find universal definitions (for instance, UNESCO in 1973), but none were totally successful. It is intuitively clear that the definition of urbanisation must not be based upon local conditions alone, since it may influence changes in the areas located remotely from the city. From this follows that a definition has to be connected with the population size of some locality, called a city. For instance, settlements with more than 2500 inhabitants are urban areas in the USA; while 2000 inhabitants living in contiguous housing form an urban area in France and in the Netherlands it is municipalities with 2000 or more inhabitants, etc. However, if we operate with a continuous distribution of population density, then this definition is not operable, since it does not automatically allow us to separate the “city location” in the continuous density map. In this case, an application of the concept of “threshold density” is more natural. For instance, if this threshold is equal to 430 persons *per km*², then in 1995, 97% of the Belgian territory was urbanised (HABITAT, 1996). Later on we shall apply namely this concept to estimating of area of some urbanised territories.

Hence, we could use the “directive” definition of the threshold density when this value is given *ad hoc*. The problem is that even if in the USA there is an official definition of urbanised territory, there may be no such definition in other regions, for instance, in Europe where these definitions vary from one country to another. It seems at first glance that we could estimate this threshold using the national and regional urban statistics (see Appendix II). Indeed, by calculating the population densities for all cities in this database and selecting the cities with minimal density for each region we do obtain some empirical estimation of the threshold densities (see Table 2.4).

We believe that it is sufficient to examine this table to see that our attempt was unsuccessful. Even if we exclude such marginal values as 3 persons per square kilometre in Kuhmo (Finland) and 44 pers/km² in Puerto Princesa (the Philippines), then the threshold density varies from 26 pers/km² in the EU to 732 pers/km² in Latin America. Note that the US minimal density, 546 pers/km² in Kansas-City, is greater than the standard value, 386 pers/km².

Table 2.4. Cities with minimal population density.

<i>Region</i>	<i>Population Density, $D = N_u / S_u$ (pers/km²)</i>	<i>Cities</i>
Africa	405-1418	Stellenbosch (South Africa)+other SA cities,
	1554	Beira (Mosambique)
Arab Countries	231	Kuwait (Kuwait)
	395	Ramla S.D. (Israel)
China	431	Huhehot,
	560	Zhuhai
Asia and Pacifica	44-364	Puerto Princesa (the Philippines)+ other Philippine cities,
	376	Islamabad (Pakistan)
Countries with Economy in Transition	36-80	Cesky Crymlov (Czech Republic)+other Czech cities,
	86	Banska Bystrica (Slovak Republic),
US, Canada, Australia and New Zealand	546	Kansas-City (USA)
	599	Colorado Springs (USA)
Highly Industrialised Countries in Europe	3-26	Kuhmo (Finland)+other Finish cities,
	27	Berwick-Upon-Tweed (UK)
Latin America and the Caribbean	732	Cajamarca (Peru),
	3840	San Salvador (El Salvador)

On the one hand, it is intuitively clear that the threshold value (by an order of magnitude) must be equal to hundreds and even thousands

(especially for the Far Eastern and Latin American cities) persons per square kilometre, while the empirical method gives us much lower values, for instance, 3 pers/km² for Europe and 44 pers/km² for Asia. What is the reason for such a contradiction? The point is that to designate the boundary between urban and rural territories with respect to population density is a very hard problem, while the absence of a strong, formal definition generates a fuzziness in the boundary. As a result, territories with very low densities are included in national statistics as urban ones. This is verified by the following example.

Let each settlement occupy a certain territory that belongs to one of two classes, urbanised or rural, and be characterised by its population density. We assume that each of these settlements belongs to one of two corresponding distributions with respect to population density: either “urban” or “rural”. It is natural to assume that all cities belong to the “urban” distribution. Let us for simplicity assume that both distributions are normal and the above considerations are valid within a given region. An application of the standard Kolmogorov – Smirnov test (Stuart and Ord, 1987) to the *complete* sampling of cities, belonging to a given region, shows that the test is fulfilled only for African, Chinese, Latin American and Caribbean cities. For other regions, the test is not fulfilled even for relatively low values of significance. The situation is not significantly improved if we change from the densities to their logarithms, i.e., from the normal to log-normal distribution. The violation of the test for Asia and Pacifica, Countries with Economy in Transition, and Highly Industrialised Countries in Europe occurs at the expense of cities with low densities; cities with high densities violate the test in the Arabian region (Damascus, $D = 38,462$ pers/km²; Cairo, 28,332; Beirut, 22,388 and Alexandria, 9311 pers/km²), and in the USA, Canada, Australia and New Zealand regions (New York, 9260 pers/km²). Therefore, we can say that cities with low and super-high densities must be deleted from the sampling, and that the rest of the cities belong to the “urban” population with a very high probability. The deletion of Arabian megapolises may be explained by the fuzziness of the definition of urban territories in Arabian countries (see above). Concerning New York City, it represents a very special urban organism altogether.

We see that the preliminary – before the construction of regression and other statistical models – sampling distribution must be truncated wherever the tails of these empirical distributions must be cut. A criterion of the operation is the threshold value of population density. Nevertheless, the problem “how to do this using statistical methods and this statistical information” remains. In order to resolve it, we suggest an algorithm that will be described in the following chapter.

2.8. Correlation between urban population and urban area: models.

The two main macroscopic variables defining the state of a city (urban territory) are its population, N_u , and its area or size (from an ecological point of view, this area is the area of the population), S_u . The simplest model of the system “city” is then given by a functional dependence, $S_u = F(N_u)$, which may also be time dependent. In the plane $\{S_u, N_u\}$, the curve $S_u = F(N_u)$ is the trajectory of the system starting at an initial point $\{S_u^0, N_u^0\}$ (see Fig. 2.6).

The problem is how to find a concrete form of this function. The simplest solution is to determine the regression between these variables using statistical data. However, although the correlation may be high, caution is still required, since the “functional” city and the “administrative” city often do not coincide (we have already met this situation above). Nevertheless, assuming that the city has a circular form with a characteristic radius R (in km), Tobler (1975) obtained the empirical relationship $R = 0.035N_u^{0.44}$ (apparently, under the strong influence of the “allometric” paradigm, which is very popular in population biology). In other regions, the scaling coefficient, $\alpha = 0.035$, is generally smaller, resulting in more compact cities, but the exponent, $\beta = 0.44$, appears stable. The empirical data from which this relation was inferred covers settlement sizes ranging from 150 to over a million persons, with a very high level of correlation. It is interesting that some archaeologists use a similar formula to estimate the former population of excavation sites. The coefficient of proportionality, α , may also change with time. For example, in the US it appears to have changed since 1945 when the impact of the automobile affected sub-urbanisation (Tobler, 1975).

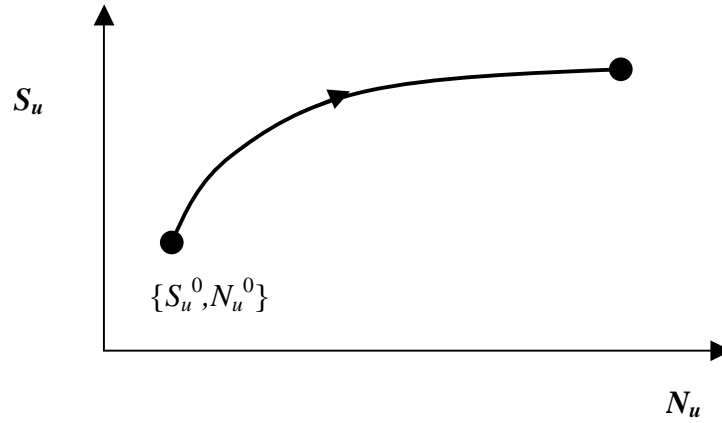


Fig. 2.6. Trajectory of the city evolution.

Note also that since $S_u \sim R^2$, if a city has a compact form, then Tobler's formula can be re-written as $S_u \sim N_u^{0.88}$. By taking into account Tobler's result that the exponent, $\beta = 0.44$, is very stable, and the value 0.88 is very close to one, we see that linear regression may be a suitable model for relating the dependence of a city's area with its population. Moreover, statistical estimation theory is especially well developed for linear regression models. It is for this reason that for now on, we shall use linear regression models.

We assume that there is some threshold value (although it can be different for different countries and regions) of population density, D^* , such that territories with a population density $D \geq D^*$ are considered urbanised. Then, if we have, for example, a map of population density with the resolution 12km x 12km or higher, by selecting all domains with $D \geq D^*$ and calculating their areas, we obtain an estimation of the area of urbanised territories at a regional or global level. Note that the Tobler et al. map was constructed with a resolution approximately equal to 10km x 10km (5'x5'), i.e., the resolution is sufficient.

Of course, instead of the direct use of this map, we can use the Cohen – Small distributions. It is obvious that a map of population density is a graphical representation of the function of local density, $D(x, y)$, where x and y are the co-ordinates of this location. Let a domain, Ω , in the co-ordinates plane be a given region with an area equal to $S_t = \iint_{\Omega} dx dy$. The total

population of the region is then given by $N_i = \iint_{\Omega} D(x, y) dx dy$. To construct the Cohen – Small distribution, we determine in the plane $\{x, y\}$ a family of isolines corresponding to different densities, $0, D_1, \dots, D_i, \dots, D^*, \dots$ etc., where each line bounds the domain Ω_i , in which $D < D_i$. Calculating two consequences

$$S_i / S_t = \frac{1}{S_t} \iint_{\Omega_i} dx dy \quad \text{and} \quad N_i / N_t = \frac{1}{N_t} \iint_{\Omega_i} D(x, y) dx dy, \quad (1)$$

we obtain the dependence of the percentage of population on the percentage of occupied territory, i.e., the Cohen – Small distribution. It is very visible, when we use this distribution in the modification of Miller and Small (2003) – see above Fig. 2.5.

The estimation of urban area using the Cohen – Small distribution is very sensible with respect to the threshold value of density. Indeed, if we return to the original Cohen – Small distributions (see Fig. 2.4) and estimate the percentage of urbanised area (using the 400-persons threshold), we find that, for example, in the USA for the year 2000, urbanised territories occupied 1.55% of the total land area, close to the statistical value of 1.7%. Meanwhile, the equivalent value for India with the same threshold is equal to approximately 10%, which is not realistic. This, however, may be a consequence of a special form of Cohen – Small distribution. We will attempt to show that it is a general problem for any distribution. The fact is that population densities in urbanised territories are very high – much more than the mean population density of a country or region. Therefore, when we estimate urban areas, we operate within the tails of the distributions that are as a rule known with a very low accuracy when dealing with sampling distributions.

Generally speaking, for our purposes, it is more convenient to use another distribution, $p(D)$, where the value $p(D)\Delta D$ is the relative area (percent with respect to the total area, S_t) of such a domain, the population density of which lies between D and $D + \Delta D$.

It is obvious that the normalising condition below must hold:

$$\int_0^{\infty} p(D) dD = 1. \quad (2)$$

We define the function $p(D)$ up to infinity (by zero). An urbanised area is then defined as:

$$S_u = S_t \cdot \int_{D^*}^{\infty} p(D) dD \quad (3)$$

where D^* is the threshold density of population for urbanised territories. The mean population density is equal to:

$$\hat{D} = N_t / S_t = \int_0^{\infty} D p(D) dD. \quad (4)$$

If the proportion of a population inhabiting urbanised territories is known (k_u)

then

$$k_u \hat{D} = \int_{D^*}^{\infty} D p(D) dD. \quad (5)$$

So, if the distribution $p(D)$ belongs to the class of two-parametric distribution, and its type is known, then there is no problem to estimate the urbanised area if we know the total population, N_t , the percent of urban population, k_u , and the density threshold, D^* , for a given region.

In their classic monograph, Kendall and Stuart (1958) have indicated that the spatial distribution of population density for different species (including *Homo sapiens*) is close to the two-parametric gamma-distribution:

$$p(D) = \frac{1}{\Gamma(\alpha)\beta} \left(\frac{D}{\beta} \right)^{\alpha-1} \exp(-D/\beta) \quad (6)$$

where $\Gamma(\alpha)$ is Euler's gamma-function, $\alpha > 0$ determines the form of distribution and β is a scale factor (see Fig. 2.7). Note that Vaughn (1987) successfully applied this distribution for the description of population densities in a city centre.

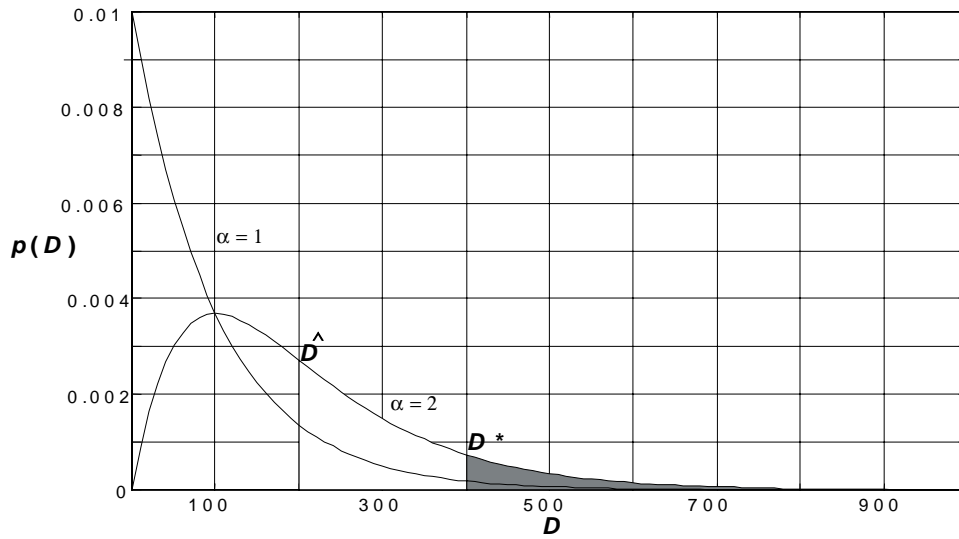


Fig. 2.7. Γ - distribution as the distribution with density $p(D)$.

Equalities (4) and (5) can be used to estimate these parameters. After such calculations, we obtain:

$$\hat{D} = \alpha\beta \text{ and } k_u = \frac{\Gamma(\alpha+1; \alpha\lambda)}{\Gamma(\alpha+1)}, \quad \lambda = \frac{D^*}{\hat{D}} \quad (7)$$

where $\Gamma(\alpha+1; \alpha\lambda)$ is the incomplete Euler function. Finally, knowing the parameters α and β for each region, the percentage of urbanised territory in this region is calculated as:

$$s_u = S_u / S_t = \frac{\Gamma(\alpha; \alpha\lambda)}{\Gamma(\alpha)} . \quad (8)$$

For instance, the area of the grey domain in Fig. 2.7 is equal to s_u .

As a first approximation, we assume that the value of the critical population density is the same for all regions, i.e. $D^* = 400$ persons per square kilometre. Therefore, for instance, in the continental USA for the year 2000 ($\hat{D} = 29, k_u = 0.76$), $s_u \approx 1.45\%$ (which is close to the statistical estimation, 1.7%), and for India ($\hat{D} = 318, k_u = 0.27$), $s_u \approx 9\%$. The latter estimation will be more realistic if D^* is increased. For instance, assuming that the ratio $\hat{D} / D^* = 0.075$ is constant for all regions, then (for India) the estimation of $s_u \approx 0.9\%$.

2.9. Other city models: a short overview.

The cities and the conformities of their growth are very interesting dynamic objects, and it is natural that this fact has generated many different attempts to develop a model of urban (city) growth (evolution). The first class of urban models are the so-called “mechanistic” models, i.e. wherever the growth is determined by some *attractiveness potential* of the city that, in turn, generates migration flows from the surrounding rural territories. The classic example of such type of models is the Allen – Sanglier’s model (1979), the attractiveness potential of which is introduced as an analogue of physical potential. Generally speaking, the problem of a city’s attractiveness for people is far from being completely resolved. There are many discussions about this: What is a city? Why is a city? Why do people actually desire to live in cities? Van Houtum and Ernste (2001) have collected many citations concerned with this topic. For instance, J. Donald (1999), notes that: (1) “*A city has always stood, not only for the vanities, the squalor and the injustice of human society, but also for the aspiration to civilized society*”, (2) “*A city does not exist outside of the imagination, a city is made real through imagination*”, (3) “*The city forces citizens to repress emotional involvement with others and instead to use formal more distant logical criteria, in interaction with others*”, or as R. Sennet states in *Le Monde Diplomatique* (16.02.2001): “*A city is a place where people can learn to live with strangers, to enter into the experiences and interests of unfamiliar lives. Sameness stultifies the mind: diversity stimulates and expands it. The city can allow people to develop a richer, more complex sense of themselves. This is a power of strangeness: freedom from arbitrary definition and identification*”.

The second class of models constitutes urban economic models. As a rule, these models are developed within the frameworks of classic economic theory: landowners and households (trading of their housing prices and transportation costs) aim to maximize their economic return. This is the main principle of the well-developed theory of land rent and land market clearing. That is, any parcel of land (physical and localisation qualities) will be used to earn the highest rent.

These models use equilibrium concepts to describe urban spatial structures, using sometimes demand and sometimes bid-rent functions to model the distribution of land to its users. The models assume a monocentric pattern of employment location. It is problematic to integrate these models with dynamic ecological models (Wingo, 1961; Alonso, 1964).

Another sort of economic models constitutes spatial disaggregated intersectoral input-output models based on the classic Leontieff's input-output model (see Leontieff, 1967). These determine the spatial allocation of economic flows between sectors with the costs of transport dependant upon location. The presence of high spatial aggregation, relying entirely on cross sectional equilibrium, makes them unsuitable for integration with ecological models, based on other spatial details.

It is obvious that in economical models, the general behavior principally depends on the individual choice of the agents of economical processes. For instance, the approach applied in so-called "discrete-choice" models (McFadden, 1978) is a little more flexible and uses random-utility theory to model consumer choices amongst discrete location alternatives that provide utilities. Unfortunately, the major and common limitation of most urban models is the fact that they represent the spatial choice behaviour of households and businesses, and are aggregate and static. Special micromodels are therefore required for the description of these individual reactions that are then averaged to obtain some macrocharacteristics (Mackett, 1992; Wegener, 1994). These models represent individuals, and directly model the choices of job locations based on their occupation and location etc., using Monte Carlo simulation (suitable for systems where decisions are made at the individual unit level and interactions are complex within the system).

The third class is formed by integrated models using a more dynamic approach: today those are "CUF II" (Landis and Zhang, 1967) and "UrbanSim" (Alberti and Waddell, 2000; Waddell, 2000). They use highly spatially disaggregated representations of the urban landscape and GIS to integrate the attributes of land. In "CUF II", land use change is estimated as a transitional probability based on the surrounding land characteristics. The "UrbanSim" model (framework, simulating evolution of metropolitan areas by dynamic interactions between socio-economic and ecological processes) was

developed to predict three types of human-induced environmental stressors: land conversion (a set of spatial metrics of urban development with ecological patterns of parcels and neighborhoods used to represent it), resource use and emissions. Using a spatially explicit process-based landscape modelling approach, ecosystem processes are simulated and represent land cover interactions over regional scale. Ecological changes (modelled as an input of the urban ecological model to physical-geographical parameters) will feed back on the choices of households and business locations, and land and resource availability.

A very special class of models are “landscape ecology models”, that are based on the dynamics of species populations, communities and ecosystems. Initially developed for the non-urban environment to study the processes creating observed patterns, these have been used over the last decades for urban studies. The major questions are the following: What are the fluxes of matter and energy within urban ecosystems? How does the spatial structure of ecological, physical and socio-economic factors in a city affect an ecosystem’s functioning? Most landscape spatially explicit models are grid-based. Vegetation cover was initially exported from climatic models (Holdridge’s life zones classification system), and was later replaced by simulations of the biological dynamics of vegetation and its interaction with soil and topography. Traditional population models (“gap models”) are replaced by transition probability models (Botkin and Breveridge, 1997).

Wu and Loucks (1995) define the following three sorts of ecological models.

1. Individual-based models that simulate a property of an organism and the mechanisms of its interaction with the environment.
2. Process-based landscape models (mass balance) that simulate the flows of water and nutrients, and biotic responses influencing changes in spatial patterns.
3. Stochastic landscape models that describe changes in spatial patterns based on the characteristics of a given cell, the structure of a patch to which the cell belongs and conditional transitional probability.

The poorly understood aspects of the development of urban systems are the ways in which local interactions affect the global composition and dynamics of the whole region. Hence, one may state that urban ecosystems

(structured as cumulative and aggregate) possess fundamental features of complex and self-organising systems. The agents making decisions are subject to changed rules based upon new information. The local behaviour of multiple actors therefore leads to different global patterns. Uncertainty is extremely important to consider in these non-equilibrium systems, since the evolution paths are affected by any change in the past trends. It is not surprising that since the 1960's, a variety of new urban models have been introduced. These include the whole arsenal of typical methods used in the theory of complex systems: catastrophe theory (Wilson, 1976), theory of dynamic chaos (Wilson, 1981), theory of dissipative structures (Allen and Sanglier, 1979), fractals (White and Engelen, 1993), cellular automata (Tobler, 1979; White and Engelen, 1997), theory of self-organization (Schweitzer, 1997), all of which emphasize the dynamics of the urban form and its relationship to generating processes.

Special models describe the morphology of urban growth. For instance, an analogy with the growth of cancer cells is widely used (Gordon and Wong, 1985). Urban sprawl is often associated with the decentralisation of settlement and appearance of new centres (polycentric urban form hypothesis). However, many economic models suggest that a monocentric city structure is better for the economy and effectiveness of transportation (under the assumption that exponential population-density gradients are negative in many cities).

To detect and quantify urbanisation gradients using landscape pattern analysis (Luck and Wu, 2002), the location of urbanization centres may be estimated using multiple indexes. The classic models of urban morphology are:

1. The concentric zone theory (central business area in the middle with the rings of various land use);
2. The sector theory (concentric zones modified by transportation);
3. The multiple nuclei theory (patchy urban pattern formed by multiple centres of specialised land use nativities).

Human activities produce landscape fragmentation. Gradient analysis and landscape pattern analysis are the methods used for quantitative spatial analysis. For instance, the gradient analysis is integrated with landscape pattern metrics to characterize urbanisation pattern of Phoenix, USA. The

results tell us that the degree of human impact on the urban landscape depends upon the distance from the urban centre. An urbanisation centre was clearly identifiable, as having the smallest mean patch size and the highest patch richness, patch density, patch size coefficient of variation, landscape shape index and area-weighted mean shape index.

2.10. Setting of a problem.

Since the main variable, determining the role of urbanised territories in the GCC, is their area, we must forecast the dynamics of area of the urbanised territories for given regions of the Globe. Unfortunately, we do not know how to resolve the problem by some direct way. Nevertheless, if there is a close correlation of this value with another value, the dynamics of which are known with greater accuracy, then the mentioned above problem could be resolved. We believe that the best candidate for this role is urban population. Hence, we must construct the functions $S_u^i = F_i(N_u^i)$, where $N_u^i = N_u^i(t)$ is a given function of time, for all considered regions. We shall use two methods. The first is purely statistical, based on the construction of a regression of S_u^i with respect to N_u^i . We must first “clean” the original national statistic’s data, since these data are influenced by not only urban, but also rural contributions. The second method is based on the use of the two-parametric Γ -distribution. As shown earlier, urbanised areas may be described through the quantiles of this distribution. Since its parameters depend upon such demographic characteristics as the mean population densities and the density threshold corresponding to an urban territory, by the same token we will obtain the dependence of urban area on urban population.

Hence, we have the probable dynamics of urban areas for different regions. However, the urbanised territories are not homogenous in relation to carbon storage and fluxes. For instance, cities contain both build-up areas and “green” areas (parks, lawns, etc.). It is natural that if the first are indifferent in relation to atmospheric carbon, then the second actively participates in the carbon exchange between the surface and atmosphere. Therefore, we must know how to estimate the city’s “green” area that is covered by vegetation and participates in the carbon exchange between the atmosphere and urbanised territory, and between the latter and neighbouring

territories, covered by “natural” ecosystems. Note that the dynamics of this “green” area depends upon the growth of the total city area as well as other processes, for instance, “*favelisation*”, i.e. the growth of informal settlements. The latter is very important for the case of Third World cities.

Since one of the most important constituents of urbanisation is the replacement of natural ecosystems by built-up areas, we must know three parameters dealing with the “natural” ecosystems surrounding a city. These are the net primary production, and the storages of living biomass and dead organic matter (humus). We shall use Bazilevich's biomes data for this. These estimates depend upon the type of model that describes the distribution of cities over the regional territory. We shall use two models. The first is a random distribution one, and the second takes into account the spatial correlation between the location of a city and certain types of biome. In other words, we shall try to formalise a well-known principle: “ A fish is looking for where it is deeper, and man is looking for where it is better”.

The general model will be a combination of these partial models.

3 MODELS DESCRIBING THE AREA OF URBANISED TERRITORIES AS A FUNCTION OF THEIR POPULATIONS

3.1. Demographic prognoses.

As we mentioned in Section 2.6, one of the main variables determining the role of urbanised territories in the GCC is their area. However, the information to be found in statistical reports, such as the UN Report “The state of the World’s cities, 2001” (UN, 2001), only contains such demographic data as the current total and urban populations and their predicted values, where they are determined for six standard UN regions (Fig. 3.1).

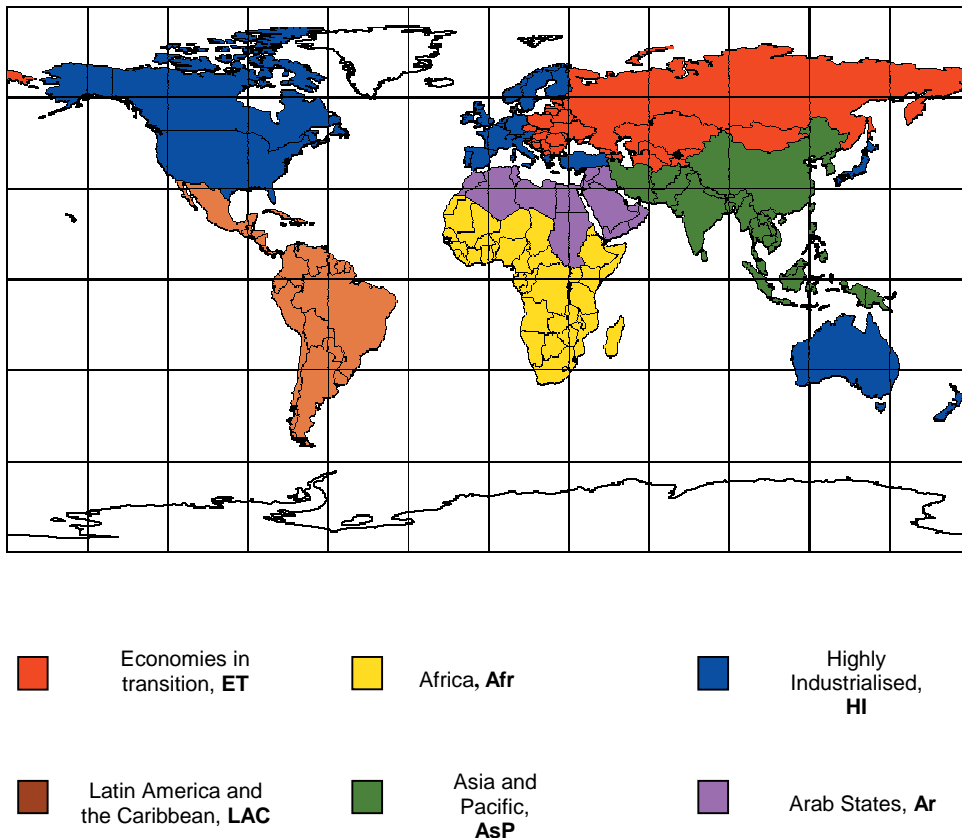


Fig. 3.1. The six world regions of the UN standard division.

An example of the probable dynamics of total and urban populations, in this case for the Latin America and the Caribbean region (LAC), in accordance with the report is presented in Fig. 3.2.

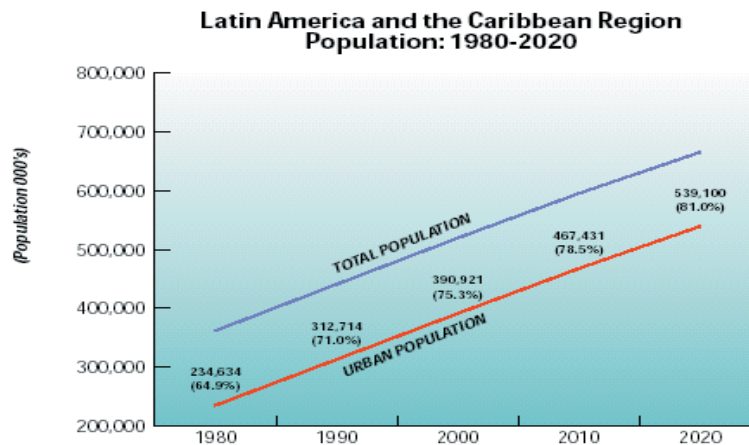


Fig. 3.2. The real and prognostic dynamics of total and urban populations for the Latin America and Caribbean region.

The prognoses for other regions and for the whole world are represented in Appendix I. Nevertheless, these data need some correction. This correction was necessary, since there are serious doubts about the accuracy of prognoses for such important demographic characteristics as total regional populations. For instance, in accordance with the data from this book for a region such as the Highly Industrialised, which includes Western Europe, USA, Canada, Australia; Japan, etc. the total population in 2000 is equal to 597 million people. However, if we use other (more detailed) demographic sources (UN, 2000), we obtain an estimate of 883 million. By taking this into account, we shall use the statistical data and prognoses for the total country population from other sources (UN, 1992; Svirezhev et al.,1997). These prognoses are described in more detail in Appendix I. However, in order to estimate the percentages of urbanised populations for the world's regions, we shall use data from the book "The state of the World's cities, 2001" with the corresponding corrections and extrapolations.

In order to show the degree of difference between these two prognoses, we present the dynamics of world and regional population in Figs. 3.3 and 3.4. It is interesting that even though the prognoses for world population do not differ very much from each other (Fig. 3.3), the regional prognoses are very different, especially for regions such as the Afr and the ET. Note that we compare only the prognoses that have been made for the regions that coincide with the UN and our regional divisions (for the latter, see below). It seems to us that our prognoses are less dramatic than the UN results.

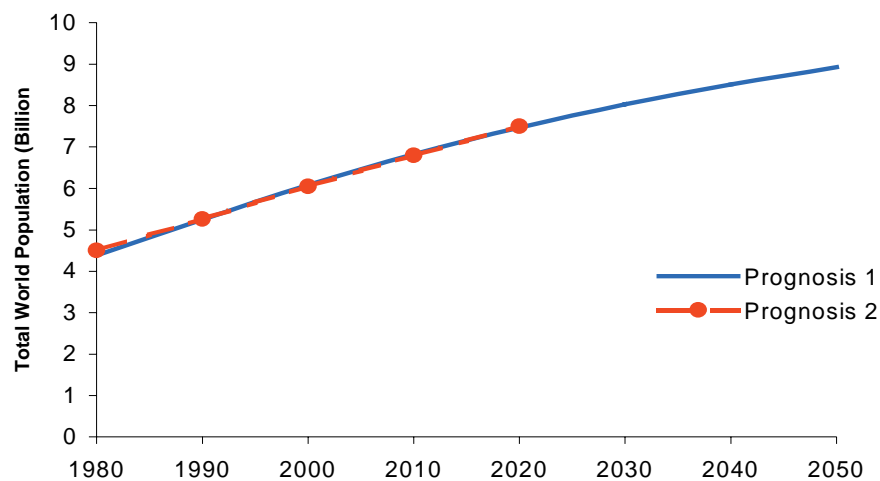


Fig. 3.3. Dynamics of the total world population.
 Prognosis 1 (Svirezhev et al.,1997),
 Prognosis 2 (UN, 2001).

It is obvious that the area of urbanised territory depends on the size of population of a city and on other social, environment, etc. parameters. *We will assume that the first one is the most important, and will neglect the dependence on the other parameters.* We must therefore obtain the functional dependence relating the area of an urbanised territory to its population.

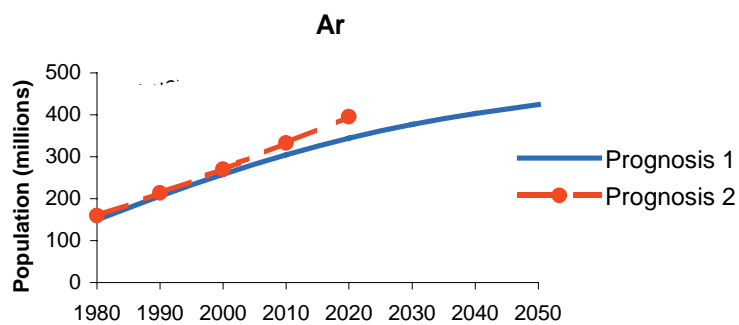
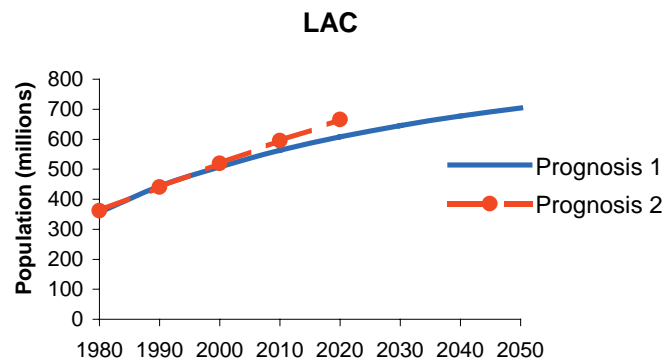
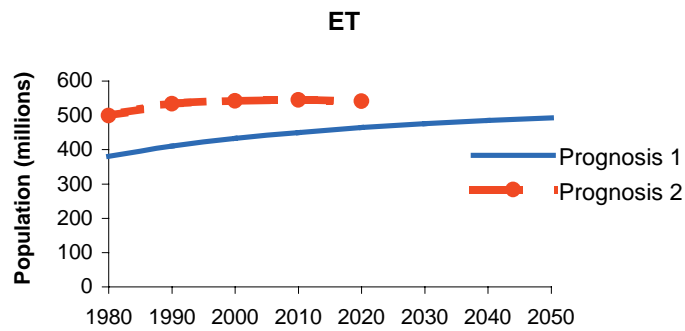
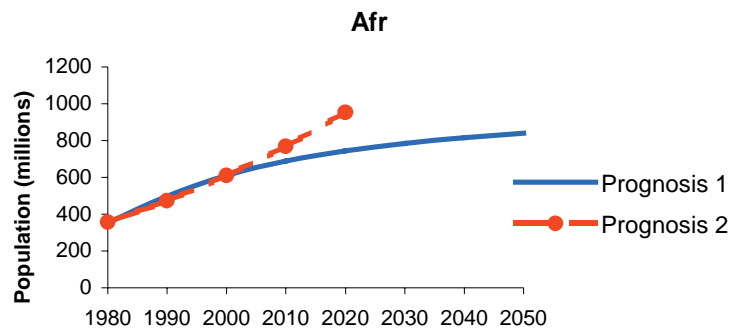


Fig. 3.4. Dynamics of the total regional population.
 Prognosis 1 (Svirezhev et al.,1997),
 Prognosis 2 (UN, 2001).

3.2. Regression model: “cleaning” of original information.

In accordance with our assumption that there is a functional relationship between urban area and urban population, we will now develop the appropriate regression model.

We analyse the statistics for more than one thousand cities distributed around the World (see Appendix II), implementing the following procedure for each region. Data dealing with population and area of cities for the 1990s are collected from different sources (see the references from Algeria, 2001 to Zair, 1994). These data are ordered with respect to the corresponding urban populations, ensuring no noticeable gaps in this ordination. The representability of the data, R_s , is defined as the ratio of the sampling urban population to the total urban population in a corresponding region. This value varies from 10-11% in the ET and the Ar countries, to 37-38% in the HI ones.

The reason why data are sparse for the Ar region is that the definition of a city area differs dramatically from the conventional one, as mentioned earlier (see Section 2.7). The low representability in the ET could be explained by the long period of political and economic instability. Naturally, few data were collected and systematised during those years, and it has only been in the last few years that local governments have begun to publish their own statistical yearbooks (see for example Bulgaria, 1999, 2001; Belarus, 2002; Croatia, 2001).

On the other hand, a long history of data collection and processing exists in HI countries. In Europe for example, “Statistisches Jahrbuch deutscher Städte“ was first published in 1890 and covers many indexes, including „the city area“, which is important for us.

The first attempt to construct equations of linear regression between the i^{th} city area, S_i , and its urban populations, N_i for all UN regions was unsuccessful: the coefficient of correlation, R , that measures the quality of “best” linear approximation, was very low, especially in two regions: the AsP ($R^2 = 0.18$) and the HI ($R^2 = 0.46$). The situation did not improve when we used logarithmic scales, i.e., constructed the regression between $\ln S_i$ to $\ln N_i$. What are reasons for this failure?

The first reason (as we already mentioned in Section 2.7) is that the original sampling is a mixture of three sets, such that the settlements in the sampling may belong to both urbanised and rural territories, as well as to super-megapolises. Therefore, in order to operate with the sampling, we must “clean” it, that is to initially delete settlements that belong to the “rural” and “super-megapolis” sets. Note that we divide the two regions that gave the worst results, AsP and HI, into two sub-regions: the AsP region is divided into China and the Far-Eastern Asian countries including Japan, while the HI region is divided into the Western European countries, and the USA, Canada, Australia and New Zealand. The reasons for such sub-divisions will be explained below.

We first delete from the samplings of the Ar and UCA regions all cities with densities higher than 5,566 and 6,056 pers/km², respectively (Damascus, Cairo, Beirut, Alexandria and New York). Secondly, assuming that rural and urban settlements differ from each other by the population density, $D_i = N_i / S_i$, we shall consider the eight sample distributions of D_i for each region. If we estimate the closeness of these distributions to normal ones (using the Kolmogorov-Smirnov test), we see that they are closer to a lognormal distribution (i.e. the distribution of $\ln D_i$ is closer to the normal one than the distribution of D_i). Nevertheless, the confidence level is still very low, requiring further cleaning of the sampling by removing the tail of the distribution corresponding to lowest densities. We therefore suggest the following two algorithms to undertake this. In the first method, we consequently delete the cities with minimal densities, each time testing the remaining sampling by Kolmogorov-Smirnov test. The process is continued until the desired confidence level (99%) is reached. The resulting minimal $D_{\min} = D^*$ is the threshold value of density separating urban and rural settlements. Thus, we will for now on use the truncated regional sampling distributions, whose tails have been cut. The resulting border values are shown in Table 3.1, the regional divisions corresponding to Fig. 3.6 (see below).

The second method is based on the following statistical statement: sampling values situated outside the interval $\mu \mp 2.58\sigma$, where μ is the sampling mean of $\ln D_i$ -distribution, and σ is its sampling variance, do not

belong to the normally distributed parent population within a 99% probability. The border values, i.e. the minimum and maximum density, $D_{\min} = \exp(\mu - 2.58\sigma)$ and $D_{\max} = \exp(\mu + 2.58\sigma)$, corresponding to this interval, are also shown in Table 3.1. Comparing the estimations of density thresholds obtained using these two algorithms, we see that they give similar results (with the possible exception of the minimal density for the ET region and maximal for the LAC). Therefore, in order to truncate the sampling distributions we use the border values determined by the first method, but when we apply the Γ -model (see Section 3.6.), the minimal threshold density, $D_{\min} = D^*$ (one of the leading parameters) will be taken from the results of the second method, i.e. from the second column of Table 3.1.

Table 3.1. Minimal and maximal population densities (pers/km²) and the corresponding cities.

<i>Region</i>	<i>1st method, D_{min} and D_{max}</i>	<i>2nd method, D_{min} and D_{max}</i>
Africa (Afr)	405 (Stellenbosch)	364
	23,952 (Onitsha)	37,756
Arabian Countries (Ar)	231 (Kuwait)	265
	5,566 (Port Said)	9,312
China (Cn)	431 (Huhehot)	317
	4,296 (Shijiazhuang)	5,628
Asia and Pacific (AsP)	787 (Legaspi)	586
	52,570 (Hong Kong)	57,807
Latin America and Caribbean (LAC)	732 (Cajamarca)	913
	28,491 (Lima)	51,066
Countries with Economy in Transition (ET)	260 (Pomaz)	229
	26,871 (Beograd)	23,826
Highly Industrialised Countries in Europe (HI)	111 (Harrogate)	95
	10,755 (Geneva)	8,468
US, Canada, Australia and New Zealand (UCA)	546 (Kansas-City)	351
	6,056 (San Francisco)	8,596

Initially, we determine the regression between city area to urban population for the six UN regions. However, in the two regions, AsP and HI, we find that the sampling points form two separate clouds in each region (Fig. 3.5).

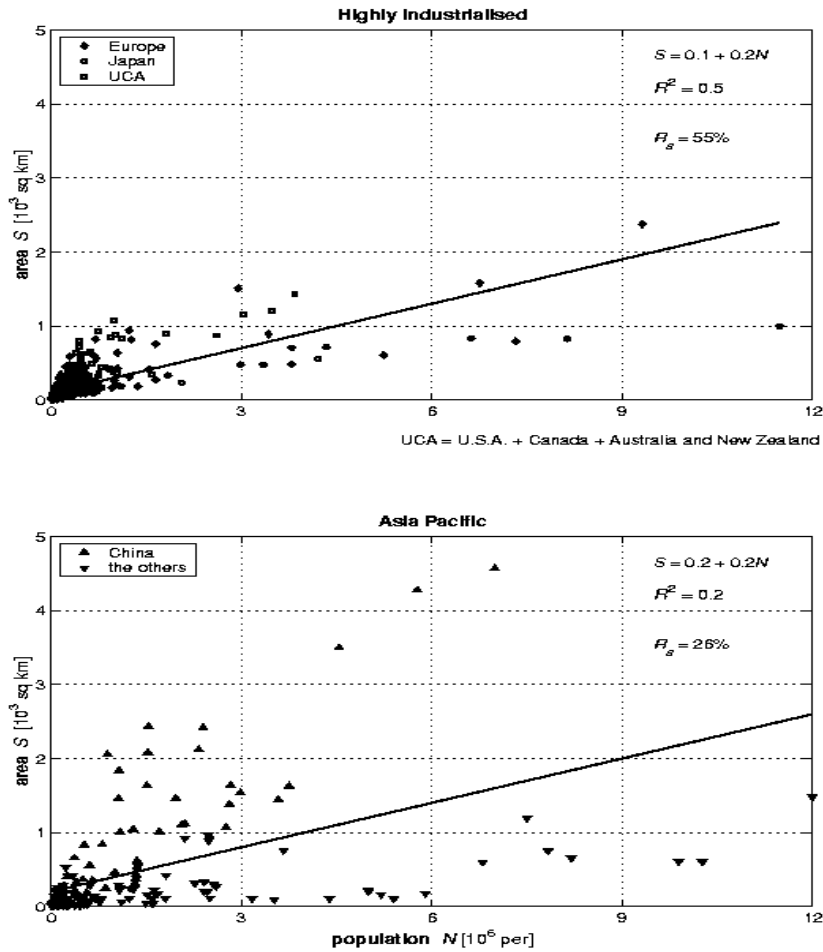


Fig. 3.5. Regression equation $S = a + bN$, correlation coefficient, R , and representabilities, R_s , for two selected world regions (HI and AsP) in the 1990s.

In the AsP region, these clouds are formed by Chinese and all other cities, respectively. In the HI region, Australian, New Zealand, US and Canadian cities form one cloud, while the other is formed by European cities. In each case, separate regression curves correspond to each cloud. This demonstrates that the UN regional subdivision, which mainly takes into account political and economic factors and does not consider culture-specific urban life styles, is not applicable in all cases. For instance, in accordance with the UN classification, Japan belongs to the HI region, although the Japanese life style is closer to that of Asian and Pacific countries. For this reason, we include Japan in the AsP region. Similarly, Israel's ancient cities follow the Arabian tradition, and are therefore included in the Ar region.

As for China, it is a country with a strongly planned process of city growth. Therefore, in the new AsP region, Japan is included and China is

excluded, the latter forming a new region, Cn. The subdivision of the HI region corresponds to the classic concept of the “Old” and “New” World. As a result, the HI region will contain only European countries, while the USA, Canada, Australia and New Zealand will form another new region, UCA. The new division of the World is shown in Fig. 3.6.

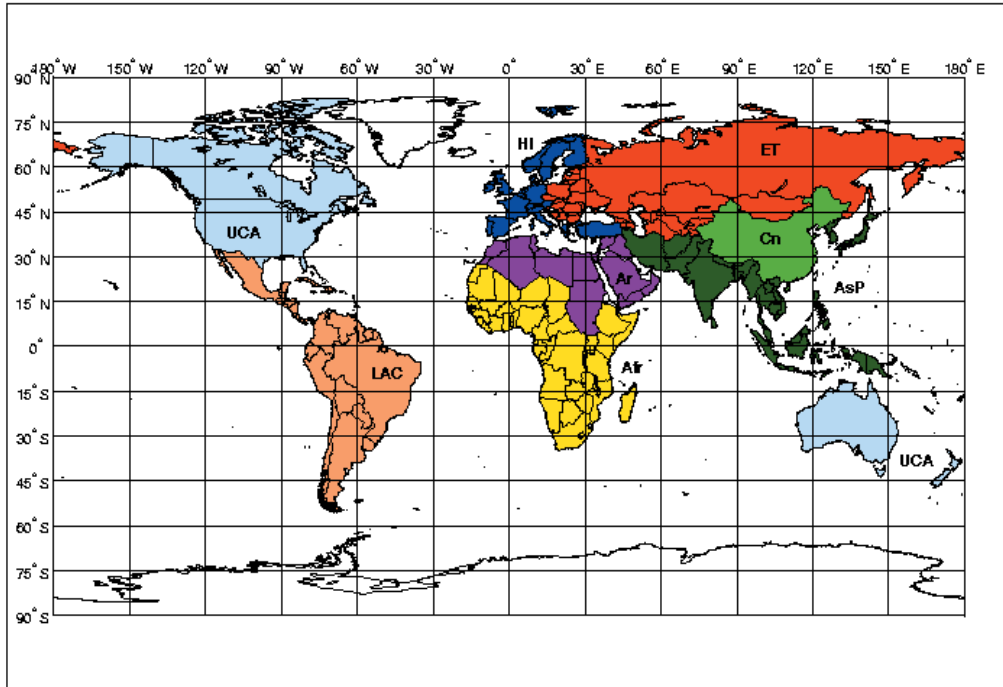


Fig. 3.6. The eight regions of proposed subdivision, to be applied in this work.

3.3. Regression models for the eight regions.

The linear regressions of urban area, S , versus urban population, N , for each of the eight regions are shown in Fig. 3.6. The coefficient of correlation, R , that measures the quality of the “best” linear approximation, increases significantly for the two new pairs of regions (Cn/AsP and HI/UCA). For instance, the values of R^2 , that were equal to 0.2 and 0.5 for the “old” AsP and HI regions, increase to 0.6-0.7 for the “new” regions, namely AsP, Cn, HI and UCA. It should also be mentioned that, since the constant term, a , in the equations of linear regression is small, it may be considered to a sufficient degree of certainty that the inverse value of the density of urban population is proportional to the slope, b , of the regression line. Hence, all regions may be divided between two groups, namely regions with relatively low urban

population densities (Cn, Ar, UCA, HI; Fig. 3.7 left) and those with higher densities (AsP, Afr, LAC and ET; Fig. 3.7 right).

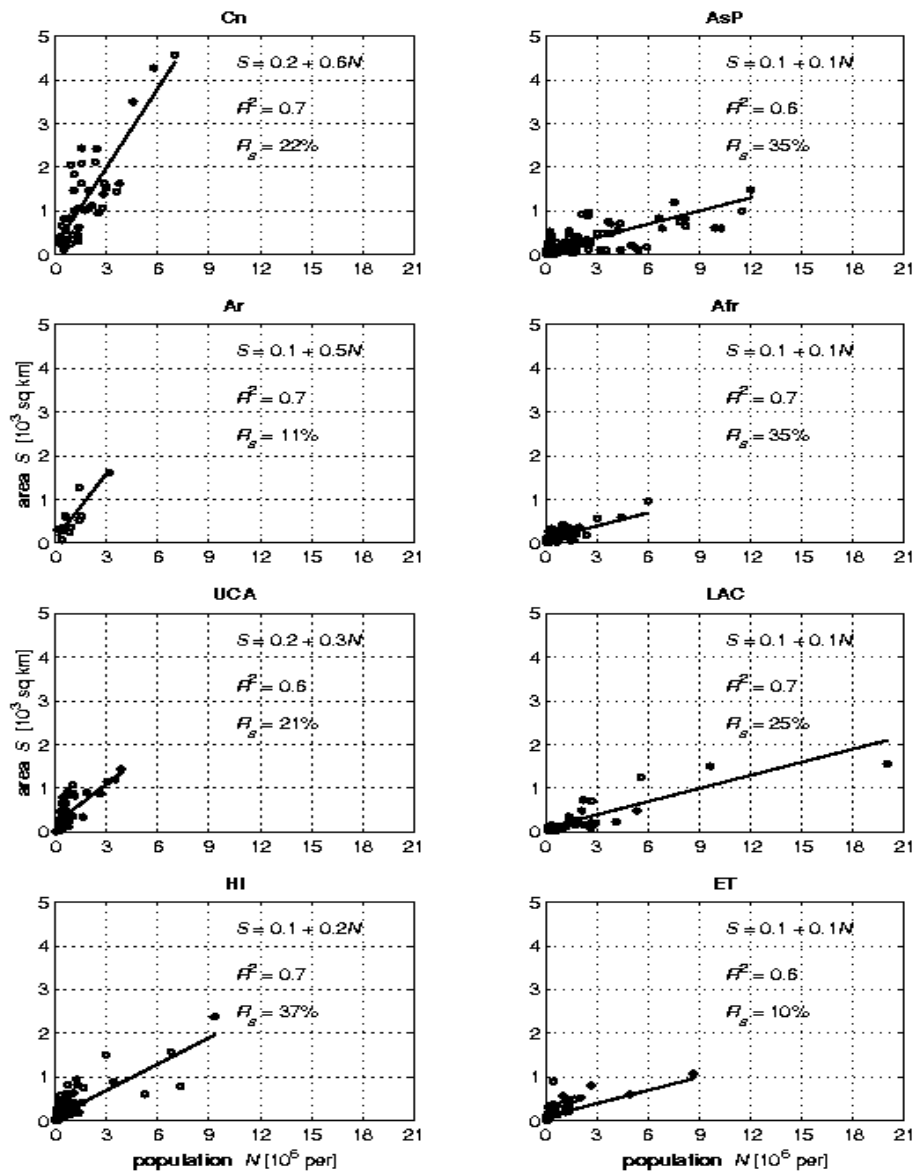


Fig. 3.7. Regression equation, $S = a + bN$, correlation coefficient, R , and representabilities, R_s , for eight world regions in the 1990s (○: a city), $S=S_i$, $N=N_i$.

In fact, the urban population density in the higher group can exceed that of the lower by 2–6 times. It is therefore obvious that the regions belonging to the different groups have principally different life styles, for example, HI and AsP. However, if the measure of urban population density, $1/b$ [1000 pers/km²], in the left group is approximately equal to 0.1, then in the right group, it varies greatly from 0.2 for HI to 0.6 for Cn. Paradoxically, Chinese cities are more spacious than cities of other regions. This may be

explained by the fact that the classic structure of a Chinese city consists of densely populated residential quarters and enormous squares and monuments (Knapp, R. G., 1989, Chinese cities, 1985).

In the previous chapter we discussed Tobler's regression model, described by the equation $\ln S_u = \alpha + \beta \ln N_u$. We tried to develop such a model using our data, i.e., to construct the regression in logarithmic scale. Unfortunately, in all cases, the R^2 -criterion was worse than for regression in the linear scale. As an example, the logarithmic-scale regression for the AsP region is shown in Fig. 3.8.

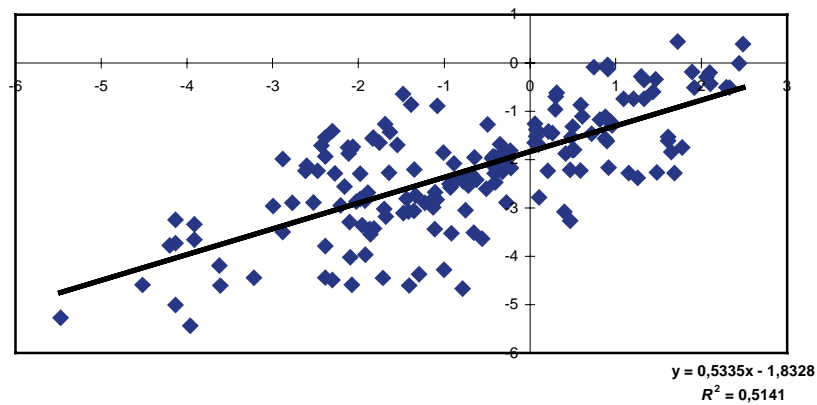


Fig. 3.8. Logarithmic-scale regression for the AsP region

$$[x = \ln N_i (\text{in million}), y = \ln S_i (\text{in thousands km}^2), R^2 = 0.51].$$

For comparison, the correlation coefficient of the regression in the linear scale

$$\text{is } R^2 = 0.6.$$

3.4. Regional urbanised area as a function of its population.

We have shown that a reliable linear relationship exists between urban area and population, such that for each region, the area, S_i , of the i^{th} city is

related to its population, N_i , by the following linear equation:

$$S_i = a + bN_i + \varepsilon_i, \quad (1)$$

where a and b are the coefficients of the corresponding linear regression for each region, and ε_i is the random error. We assume that the distribution of ε_i is normal and symmetrical with respect to zero. If the total number of cities

equals n , by summing Eqs. (1) from $i = 1$ to n we obtain:

$$\sum_{i=1}^n S_i = a \cdot n + b \sum_{i=1}^n N_i + \sum_{i=1}^n \varepsilon_i . \quad (2)$$

Summable ε_i -values will cancel each other, since they are symmetric with respect to zero. As a result, for sufficiently large n , their sum will tend to zero, and they can be neglected in Eq. (2). Since $S_u = \sum_{i=1}^n S_i$ is the total area

of urbanised territories and $N_u = \sum_{i=1}^n N_i$ is the total urban population, Eq. (2)

may be rewritten as:

$$S_u = an + bN_u , \quad (3)$$

where the values a , b and N_u are known, but n is unknown. Because our statistical data contains information about m ($m < n$) cities, i.e. we only have a sample from the parent population, the question therefore is how to statistically estimate the parameter n .

Note that if the distribution of N_i is normal, then the mean of the parent population, \hat{N}_u , and the sampling mean, \hat{N}_u^m , are related as (Stuart and Ord, 1987)

$$\hat{N}_u = \hat{N}_u^m \pm \frac{t_p \sigma_m}{\sqrt{m}} \quad (4)$$

where $\hat{N}_u = (1/n) \sum_{i=1}^n N_i$ is the mean of the parent population,

$\hat{N}_u^m = (1/m) \sum_{j=1}^m N_j$ is the sampling mean, $\sigma_m^2 = (1/(m-1)) \sum_{j=1}^m (N_j - \hat{N}_u^m)^2$ is the

sampling variance, and t_p is the value of the normal criterion for a desired level of confidence, p . For instance, if $p = 95\%$, then $t_p \approx 1.96$. Later on we will use this level of confidence.

It is obvious that the size of the total urban population is $N_u = n \cdot \hat{N}_u$. By multiplying both sides of Eq. (4) by n we obtain:

$$N_u = \frac{n}{m} N_u^m \pm \frac{n}{m} t_p \sigma_m \sqrt{m} , \quad (5)$$

where $N_u^m = \sum_{j=1}^m N_j$ is the known value. By resolving Eq. (5) with respect to n , we obtain:

$$n = \frac{mN_u}{N_u^m \mp t_p \sigma_m \sqrt{m}}. \quad (6)$$

This expression gives us the confidence interval for n . In other words, we can say that within a probability of $p\%$, the real value of n lies within the interval $[n_{\min}, n_{\max}]$, where

$$n_{\max} = \frac{mN_u}{N_u^m - t_p \sigma_m \sqrt{m}}, \quad n_{\min} = \frac{mN_u}{N_u^m + t_p \sigma_m \sqrt{m}}. \quad (7)$$

The real value of S_u will be within the interval $[(S_u)_{\min}, (S_u)_{\max}]$ with the same probability. Using Eq. (3) we immediately obtain the expressions for the calculation of $(S_u)_{\min}$ and $(S_u)_{\max}$:

$$S_{\min} = an_{\min} + bN_u, \quad S_{\max} = an_{\max} + bN_u. \quad (8)$$

Therefore, we can now estimate the area of the urbanised territories, but only for the year for which statistical data are available. Formally, we can use the regression model to forecast the future dynamics of urbanised territories, if we know the dynamics of urban populations. Formulas (8) define a corridor of the prognosis (see below). However, it is necessary to define which constraints must be imposed on the forecasting algorithm (predictor) in order that it will be correct.

3.5. Construction of a statistical predictor.

In order to use our regression model for predictions, i.e., to extrapolate it into the future, we must formulate additional assumptions (constraints) on the possible dynamics of urban population growth and the corresponding growth of the area of urbanised territories. We assume that:

1. In the course of urbanisation in a given region, the total number of cities does not change, only their population grows. In other words, $n = \text{const}$ and as a consequence, n_{\min} and n_{\max} are also constant.
2. The linear relationship (1) between a city's area and its population holds for each city of a given region.

Let all cities of a given region expand with the same relative growth rate, $r(t)$, such that:

$$\frac{dN_i}{dt} = r(t)N_i. \quad (9)$$

This is another strong assumption, in which all cities grow identically, but independently from each other. Generally speaking, this assumption is far from obvious. Nevertheless, as it was shown by Ioannides and Overman (2003), this independence holds for US city growth processes, despite some variation in growth rates as a function of city population. That is, in this case, city growth rates are identically distributed independently of city population. Hence, we can fully suppose that for each region, city growth rates are $r_i(t) = r(t)$.

A solution of Eq. (9) is

$$N_i(t) = N_i(t_0) \cdot \exp\left\{\int_{t_0}^t r(\tau) d\tau\right\} = N_i(t_0) \cdot F(t). \quad (10)$$

By substituting solution (10) into (6), we arrive at

$$n(t) = \frac{mN_u(t_0)F(t)}{N_u^m(t_0)F(t) + t_p \sigma_m(t)\sqrt{m}}, \quad (11)$$

where

$$\begin{aligned} \sigma_m^2(t) &= \frac{1}{m-1} \sum_{j=1}^m \left[N_j(t_0)F(t) - \frac{1}{m} \sum_{j=1}^m N_j(t_0)F(t) \right]^2 = \\ &= \frac{F^2(t)}{m-1} \sum_{j=1}^m \left[N_j(t_0) - \frac{1}{m} \sum_{j=1}^m N_j(t_0) \right]^2 = F^2(t) \cdot \sigma_m^2(t_0), \end{aligned}$$

from which it immediately follows that $n(t) = n(t_0)$. Therefore, if the dynamics of urban population are described by the model of exponential growth (Eq. (9)), then $n(t) = const$.

In order to clarify the second assumption, we may consider any of the graphs shown in Fig. 3.5. In fact, all graphs serve as typical “moment photos” of a region at the initial time t_0 , i.e., the year when our statistical data were collected. A simplified version of the Fig. 3.7 is presented in Fig. 3.9. It is

obvious that, if the representative points move parallel to the line $S_i = a + bN_i$, then the new states at $t > t_0$ are described by the same regression model as the initial states. This implies that the statistical regression model, $S_i = a + bN_i$, with the same coefficients, a and b , can be used for any year in future. This is a typical example of *similar* growth.

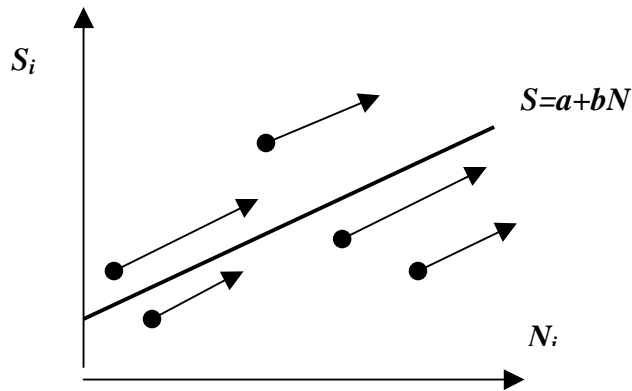


Fig. 3.9. The assumption about *similar* growth of urbanised areas: (●) states of cities at the year t_0 , (→) states of cities in the next years t , $t > t_0$.

Therefore, using the regional statistical estimations for the coefficients a and b , and the 95% confidence interval for cities' number, $[n_{\min}, n_{\max}]$, we can predict the admissible value of the regional urban area, S_u (corresponding to $n_{avg} \in [n_{\min}, n_{\max}]$), and its $p\%$ confidence interval for any year, if the regional prognosis of urban population is given. In Fig. 3.10, the dynamics of corridors for admissible values of S_u within the 95% confidence interval are shown for all regions. The regional dynamics of urban population and their prognoses are taken from Appendix I. After this, the corresponding values of N (at 1990) are substituted into (7) to calculate n_{\min} and n_{\max} , followed by the calculation of $(S_u)_{\min}$ and $(S_u)_{\max}$, using Eqs. (8). It is noted that these corridors are relatively narrow i.e., our prognoses for urban area

are sufficiently accurate, only if the demographic prognoses of urban population are accurate.

One can see that the most rapid growth of urbanised territories takes place in the Cn, Ar and AsP regions, while in the other regions there is almost no change. The maximal widths of confidence corridor are for the HI and ET regions. This can be explained by a very high diversity of cities with respect to their population, and the low representability of statistical data in the ET region ($R_s = 10\%$). Nevertheless, biased estimates of the mean for the urbanised area (the lines within a corridor in Fig. 3.10 described by the expression $(S_u)_{avg} = an_{avg} + bN_u$, where $n_{avg} = mN_u / N_u^m$) are sufficiently accurate for their dynamics. The bias of n_{avg} is a consequence of the non-linear transformation from the confidence interval for N_u into the interval for S_u given by Eqs. (8). Therefore, the statistical predictor and its confidence corridor (corresponding to 95% level) are described by the following linear equations:

$$(S_u) = an_{avg} + bN_u, \quad (S_u)_{min} = an_{min} + bN_u, \quad (S_u)_{max} = an_{max} + bN_u. \quad (12)$$

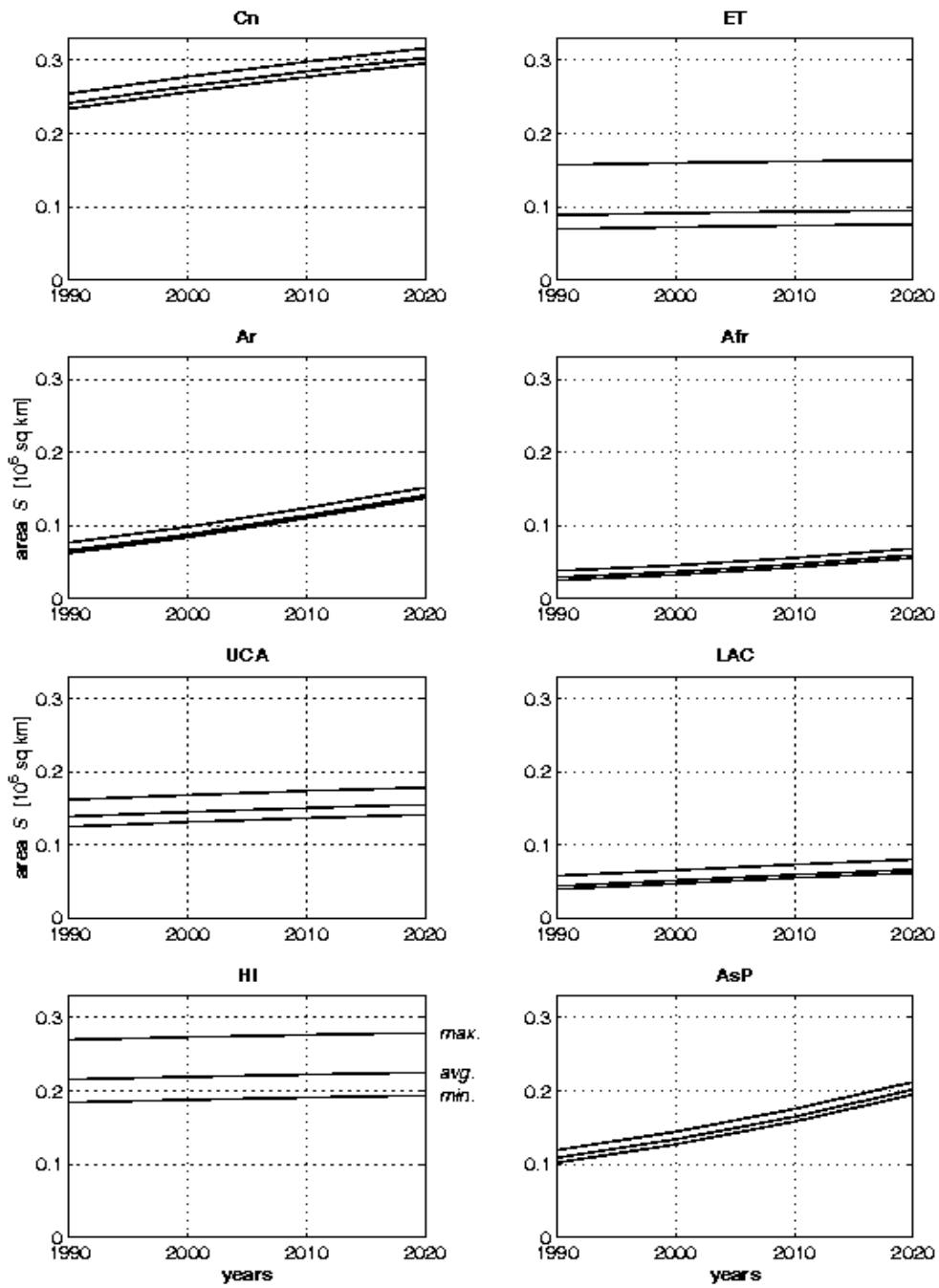


Fig. 3.10. Dynamics of regional urbanised area (in 10^6 km^2) for the eight world regions between 1990-2020, including the 95% confidence interval.

Regional values of the coefficients a and b , and the parameters $n_{\min}, n_{\text{avg}}, n_{\max}$ are listed in Table 3.2.

Table 3.2. Values of a, b and $n_{\min}, n_{\text{avg}}, n_{\max}$ for different regions.

<i>Region</i>	<i>Afr</i>	<i>Ar</i>	<i>Cn</i>	<i>AsP</i>	<i>LAC</i>	<i>ET</i>	<i>HI</i>	<i>UCA</i>
a	0.1	0.1	0.2	0.1	0.1	0.1	0.1	0.2
b	0.1	0.5	0.6	0.1	0.1	0.1	0.2	0.3
n_{\min}	121	75	152	356	81	349	1500	283
n_{avg}	163	109	200	440	123	550	1808	352
n_{\max}	251	199	256	577	256	1295	2276	468

In Fig. 3.10, we restricted our predictions from 1990 until 2020, but also showed the confidence corridors of the predicted dynamics. In Tables 3.3 and 3.4, and Figs. 3.11 and 3.12, we show the average predicted dynamics of the areas of urbanised territories at the regional level, but for the time interval 1980 to 2050.

Table 3.3. Dynamics of the urban area for the regions, in 10^3 km^2 .

<i>Year</i>	<i>1980</i>	<i>1990</i>	<i>2000</i>	<i>2010</i>	<i>2020</i>	<i>2030</i>	<i>2040</i>	<i>2050</i>
<i>Region</i>								
Afr	24.5	30.3	37.2	44.1	50.7	57.0	62.9	68.5
Ar	44.6	63.7	83.7	104.5	124.2	143.0	158.2	170.4
Cn	202.4	244.8	298.2	361.9	437.2	507.9	571.9	625.6
AsP	88.6	104.7	126.9	153.9	185.9	216.3	244.2	268.8
LAC	35.4	43.8	50.5	56.5	61.6	65.6	68.7	71.5
ET	78.4	82.2	85.5	88.4	91.0	93.0	94.1	95.0
HI	242.4	247.0	252.1	257.2	262.2	266.8	271.1	275.2
UCA	132.4	139.9	147.7	155.3	162.3	168.4	173.6	178.3

If we now look at the dynamics of the relative world urban area constructed for the average and maximal values of the number of cities, n_{avg} and n_{\max} (Fig. 3.13), we can see that even for the maximum estimate of n , the value of the relative urban area is less than the estimation of other authors.

For instance, for the year 1985 we have $s_u(\max) = 0.81\%$ in comparison with 1.2% proposed by Miller (1988).

Table 3.4. Dynamics of the relative urban area for the regions, in %.

<i>Year</i>	1980	1990	2000	2010	2020	2030	2040	
<i>Region</i>								
Afr	0.12	0.15	0.18	0.21	0.24	0.28	0.30	0.33
Ar	0.30	0.54	0.71	0.89	1.06	1.22	1.35	1.45
Cn	2.11	2.56	3.11	3.77	4.56	5.29	5.96	6.52
AsP	0.72	0.85	1.03	1.25	1.51	1.76	1.99	2.19
LAC	0.17	0.21	0.25	0.28	0.30	0.32	0.34	0.35
ET	0.31	0.33	0.34	0.35	0.36	0.37	0.38	0.38
HI	5.62	5.73	5.85	5.97	6.08	6.19	6.29	6.35
UCA	0.48	0.51	0.54	0.57	0.59	0.62	0.64	0.64

We believe that the reason for such a discrepancy (and we have already mentioned this) relates to the “fuzziness” of the definition of urban(ised) territory. In our case, we most likely deal with the summarised area of all cities of each given region, i.e., with some minimal estimation. It is natural that any city will influence a greater territory than it actually occupies, resulting in that namely this summed territory (i.e. the proper city territory + the territory of its influence) being defined as an urban(ised) territory. Comparing our estimation and that of Miller (1988), we could have boldly increased our values by two times. Nevertheless, we shall not do this and will continue to use our original values, by simply considering them to be minimal ones.

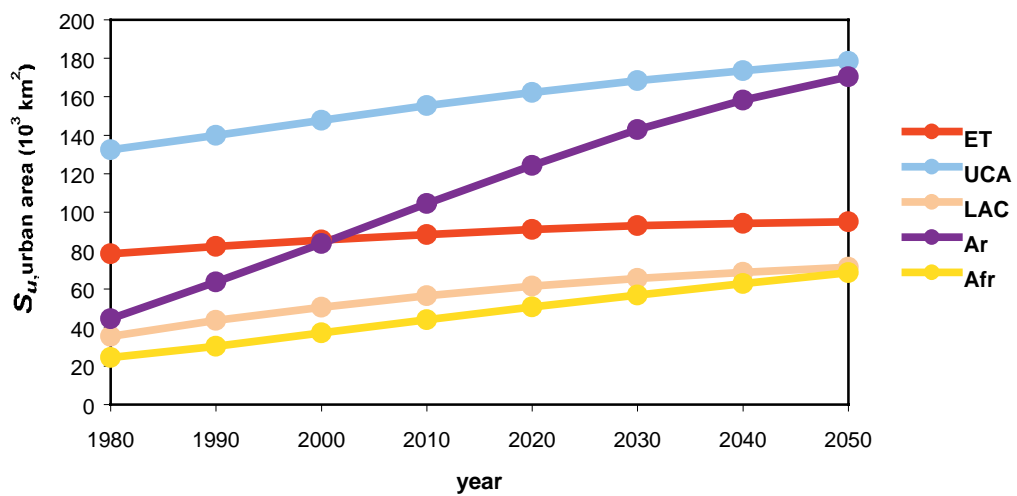
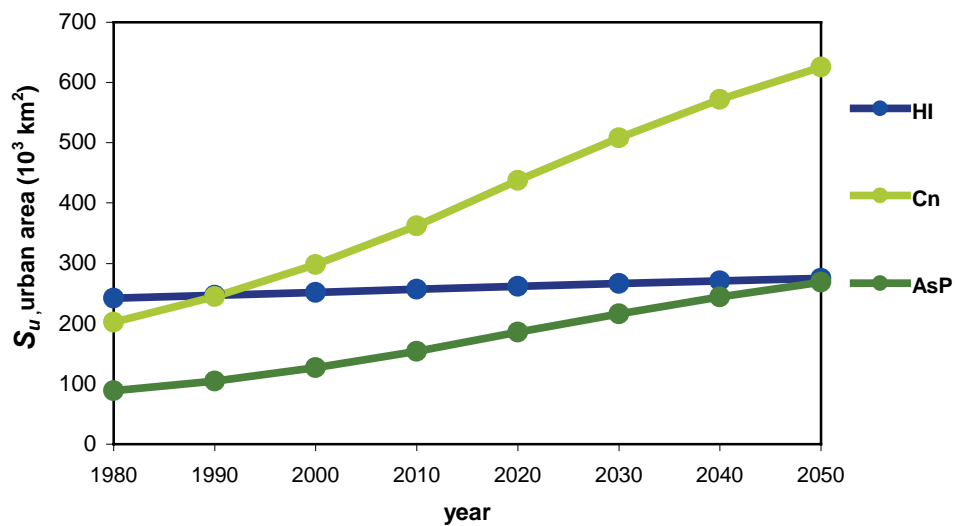


Fig. 3.11. Dynamics of the regional urban area (in 10^3 km^2) for the eight world regions between 1980-2050.

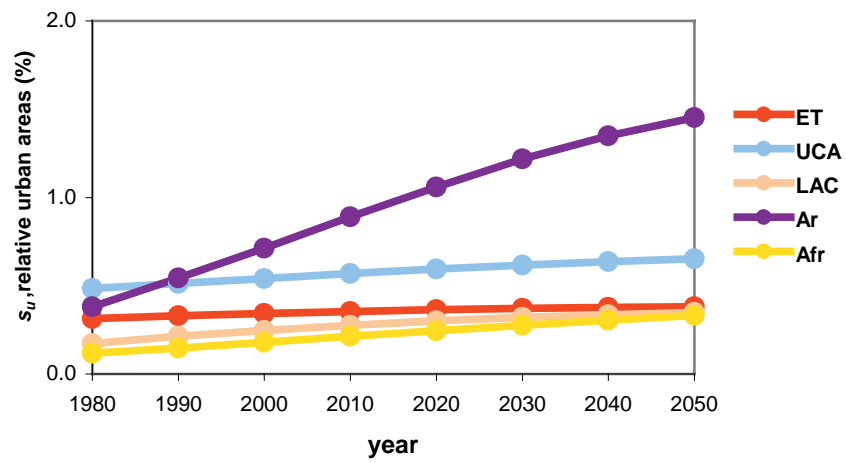
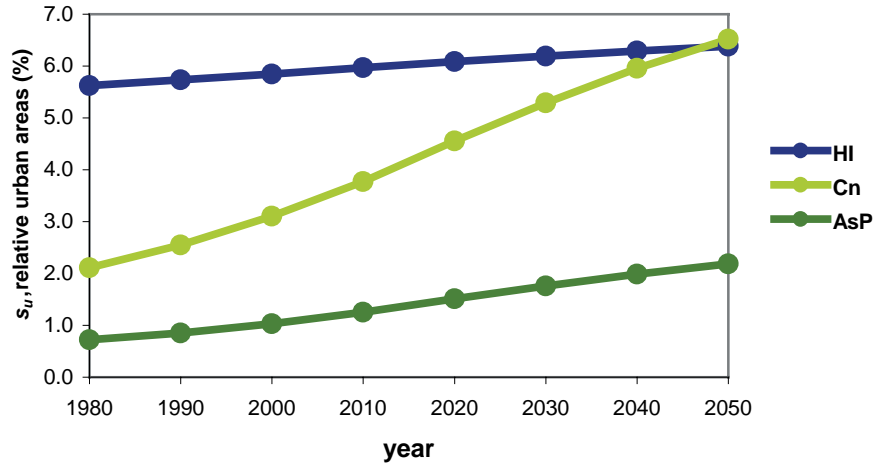


Fig. 3.12. Dynamics of the relative urban area (in % of the total regional area) for the eight world regions between 1980-2050.

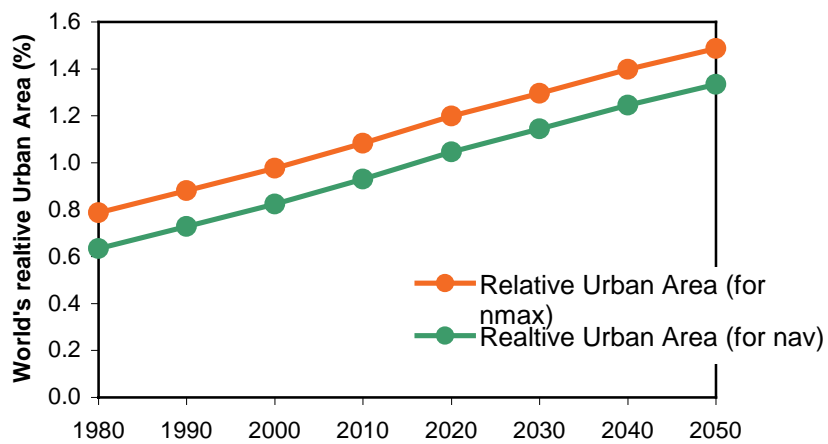


Fig. 3.13. Dynamics of the relative world urban area (in % of the total world area) between 1980-2050.

3.6. Construction of a predictor based on the Γ -distribution.

In order to construct another type of predictor, i.e., a functional relationship connecting the area of urbanised territory and its population, we may use some parametric distribution, the parameters of which are some function of urban population, and, possibly, other demographic characteristics. We already mentioned such a method in the previous chapter (Section 2.7), when we considered the possibility of applying the Γ -distribution to the description of the empirical distribution of population density with respect to populated areas.

We assume that the distribution of population density is described by

$$p(D) = \frac{1}{\Gamma(\alpha)\beta} \left(\frac{D}{\beta}\right)^{\alpha-1} \exp(-D/\beta) \quad (13)$$

where $\Gamma(\alpha)$ is Euler's gamma-function. This determines a fraction of the total area populated with a density range between D and $D + \Delta D$. This share is equal to $p(D)\Delta D$. As shown in Section 2.7, the parameters α and β are determined by using such demographic characteristics as total population, N_t , urban population, N_u , the population density threshold for urbanised territories, D^* , and the total area of region, S_t . We describe this further using

$$k_u = N_u / N_t = \frac{\Gamma(\alpha + 1; \alpha\lambda)}{\Gamma(\alpha + 1)} \quad \text{and} \quad \hat{D} = N_t / S_t = \alpha\beta, \quad (14)$$

where $\lambda = D^* / \hat{D}$ and $\Gamma(\alpha + 1; \alpha\lambda)$ is the incomplete Euler function (Ryzhik and Gradstein, 1962). Finally, knowing the parameters α and β for each region, the share of urbanised territory (in relation to the total area) in this region is calculated as:

$$s_u = S_u / S_t = \frac{\Gamma(\alpha, \alpha\lambda)}{\Gamma(\alpha)}, \quad (15)$$

or, using the various relations for gamma-functions from Ryzhik and Gradstein, we obtain:

$$s_u = k_u - \frac{(\alpha\lambda)^\alpha e^{-\alpha\lambda}}{\Gamma(\alpha + 1)}. \quad (16)$$

If the values of λ and k_u are known (see Table 3.5), then the values of α are found as solutions of the functional equation (13, left). We presume that the values of the density threshold do not change with time. This is plausible if we assume that within each region, the style of urban life, traditions, structure and form of cities and dwelling, etc. do not change over the course of the considered time.

Substituting the inferred values of α into Eqs. (15) or (16), we obtain the relative areas of urbanised territory (in % of the total regional area) for each region (see Table 3.6 and Fig. 3.14).

In Fig. 3.15, the world dynamics of relative area of urbanised territory, calculated by the Γ - model, are presented. We see that in this model, the percentage of the world's urban area in the year 1985 is about 3%, which is very close to the estimation made by Small and Cohen (1999) for the year 1990.

It would be interesting to compare these two models (regression and Γ - models). However, because of the large difference in the order of magnitude of the dynamics of the urbanised territory relative area obtained by each method, it is difficult to do so. To resolve this problem, we suggest the following method for the equalisation of these magnitudes and demonstrate it using the example of Africa.

In 1990, the total area of African cities was 0.15% of the total area of this region. At this time, the Γ - model gives the value of 1.21%. Therefore, what changes must we apply to the Γ - model to obtain the 0.15% value? The answer is evident: we have to increase the threshold density, D^* , by 7.9 times, from 364 until 2,875 pers/km². This causes the increase in λ , since $\lambda = D^* / \ddot{D}$ (see formula (14)), and respectively, the decrease in α from 0.095 (see Table 2.5) to 0.0107, and the subsequent decrease in s_u from 1,21% to 0.15%. We show this in Fig. 3.16, where we superpose the points corresponding to the year 1990 for the regression and Γ - models, and then multiply the values of λ from Table 3.5 by the same coefficient, 7.9, to calculate the values of s_u for the other years.

Table 3.5. Values of $k_u = N_u / N_t$, $\lambda = D^* / \hat{D}$, and α .

Year		1980	1990	2000	2010	2020	2030	2040	2050
Region									
Afr	k_u	0.232	0.281	0.343	0.404	0.462	0.518	0.571	0.621
	λ	21.4	15.2	12.3	10.9	10.1	9.62	9.24	8.97
	α	0.073	0.091	0.096	0.093	0.085	0.078	0.067	0.058
Ar	k_u	0.449	0.512	0.564	0.614	0.658	0.701	0.731	0.752
	λ	20.7	15.1	12.0	10.2	9.075	8.26	7.73	7.32
	α	0.041	0.048	0.052	0.052	0.050	0.047	0.044	0.042
Cn	k_u	0.272	0.302	0.342	0.391	0.449	0.496	0.538	0.567
	λ	3.06	2.69	2.42	2.22	2.06	1.94	1.85	1.77
	α	0.74	0.82	0.87	0.85	0.80	0.73	0.67	0.63
AsP	k_u	0.302	0.331	0.370	0.419	0.478	0.526	0.565	0.595
	λ	4.875	3.93	3.21	2.74	2.42	2.19	2.02	1.89
	α	0.33	0.41	0.48	0.52	0.53	0.51	0.50	0.49
LAC	k_u	0.649	0.710	0.753	0.785	0.810	0.825	0.833	0.841
	λ	52.5	42.2	36.8	33.2	30.7	29.0	27.6	26.5
	α	0.0084	0.0082	0.0078	0.0074	0.0080	0.0078	0.0067	0.0067
ET	k_u	0.613	0.663	0.705	0.742	0.775	0.799	0.806	0.812
	λ	15.0	13.9	13.2	12.7	12.3	12.0	11.8	11.6
	α	0.031	0.031	0.028	0.024	0.022	0.020	0.019	0.019
HI	k_u	0.757	0.769	0.784	0.802	0.819	0.833	0.846	0.858
	λ	1.01	0.951	0.901	0.860	0.824	0.794	0.767	0.74
	α	0.77	0.83	0.85	0.80	0.73	0.67	0.60	0.55
UCA	k_u	0.768	0.780	0.795	0.813	0.830	0.845	0.857	0.869
	λ	35.6	32.2	29.5	27.5	26.0	24.7	23.9	23.15
	α	0.0075	0.0079	0.0079	0.0077	0.0073	0.0069	0.0066	0.0062

Table 3.6. Dynamics of the relative area of a region, S_u , in % (Γ -model).

Year	1980	1990	2000	2010	2020	2030	2040	2050
Region								
Afr	0.73	1,21	1.74	2.18	2.56	2.82	3.06	3.20
Ar	1.21	1.77	2.33	2.80	3.16	3.45	3.62	3.75
Cn	6.24	7.88	9.66	11.7	13.8	15.6	17.0	18.2
AsP	4.13	5.51	7.48	9.64	11.8	13.8	15.5	16.9
LAC	0.54	0.66	0.73	0.78	0.85	0.86	0.87	0.88
ET	1.90	2.05	2.05	2.15	2.17	2.15	2.15	2.17
HI	34.7	37.2	39.2	40.1	40.5	40.7	40.3	40.0
UCA	0.75	0.81	0.87	0.91	0.92	0.93	0.94	0.93

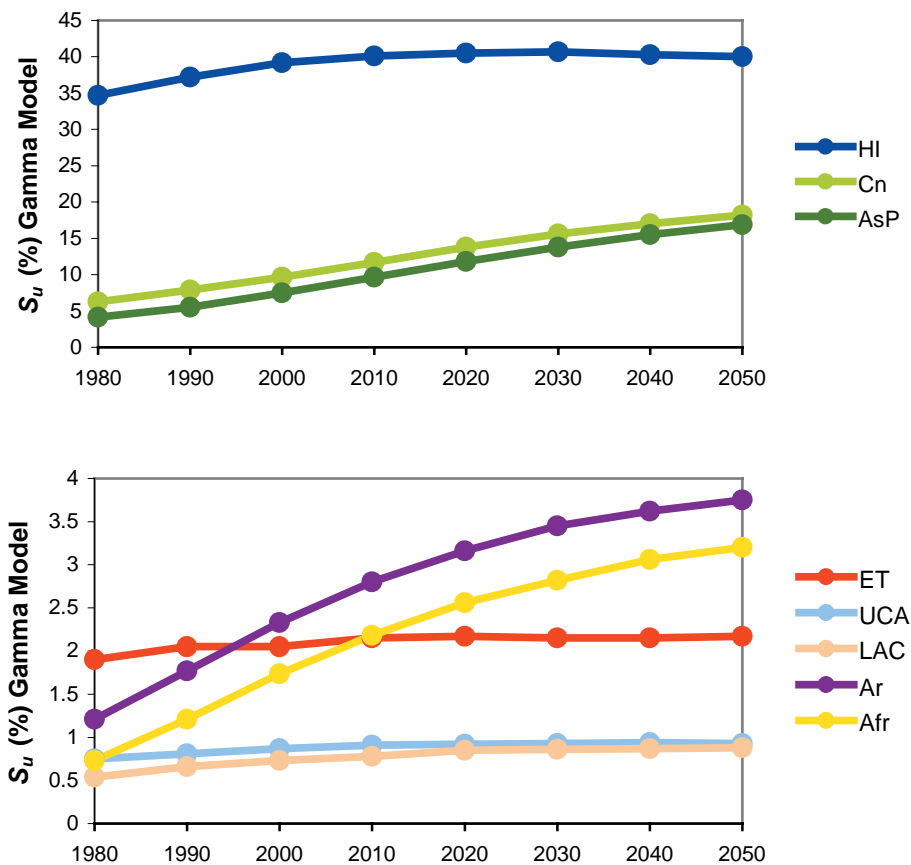


Fig. 3.14. Dynamics of the relative urban areas (% of the total regional area) for the eight world regions between 1980-2050 (Γ - model).

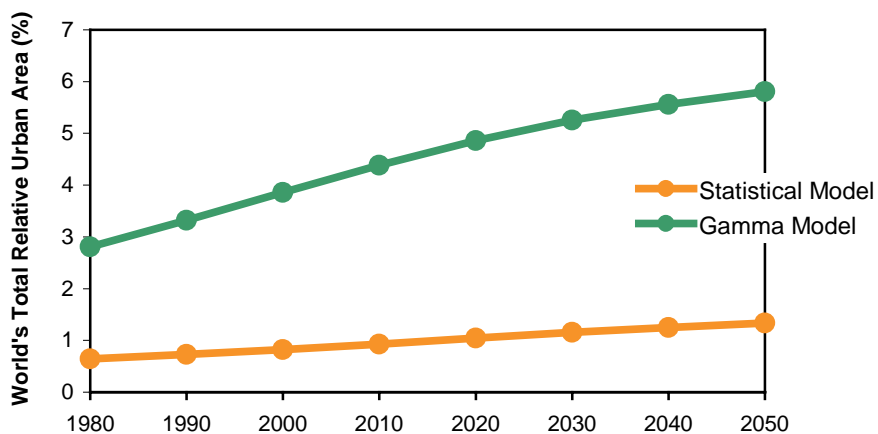


Fig. 3.15. Dynamics of the relative world urban area (in % of the total world area) between 1980-2050.

Similarly, there is no problem to construct the comparative dynamics of the relative urbanised areas for the other regions (see Figs. 3.17 – 3.18).

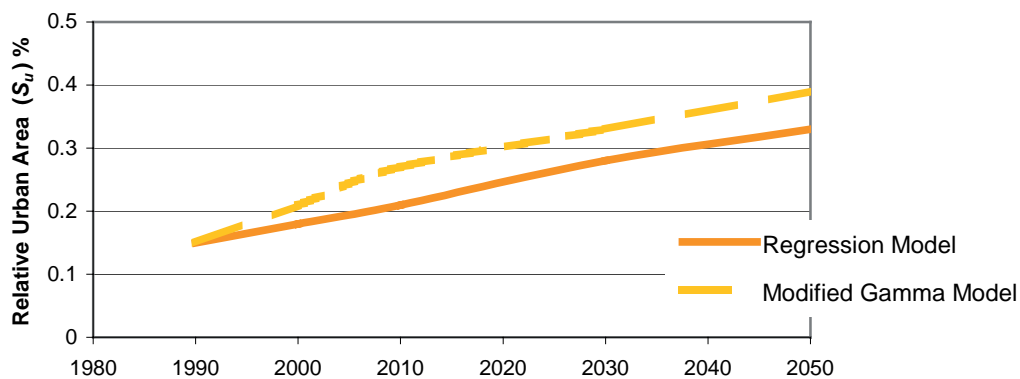


Fig. 3.16. Comparative dynamics of the relative urban areas in the Africa region, obtained by the regression model and the modified Γ - model.

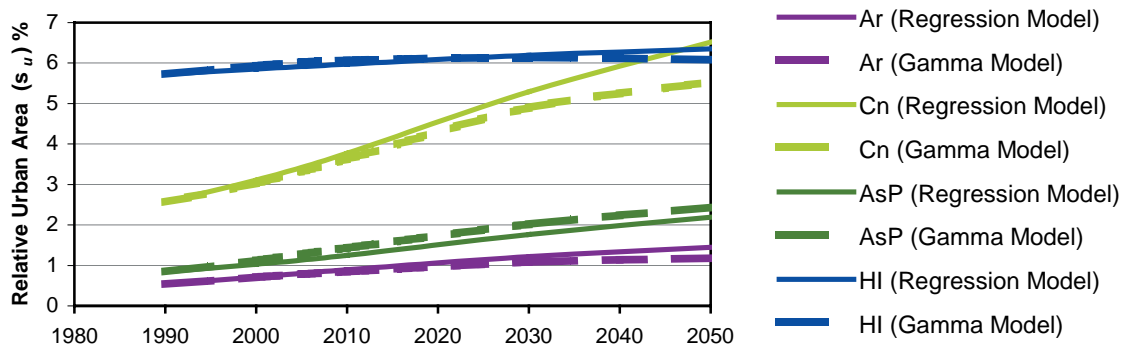


Fig. 3.17. Comparative dynamics of the relative urban areas in the Ar, Cn, AsP, and HI regions, obtained by the regression model and the modified Γ - model.

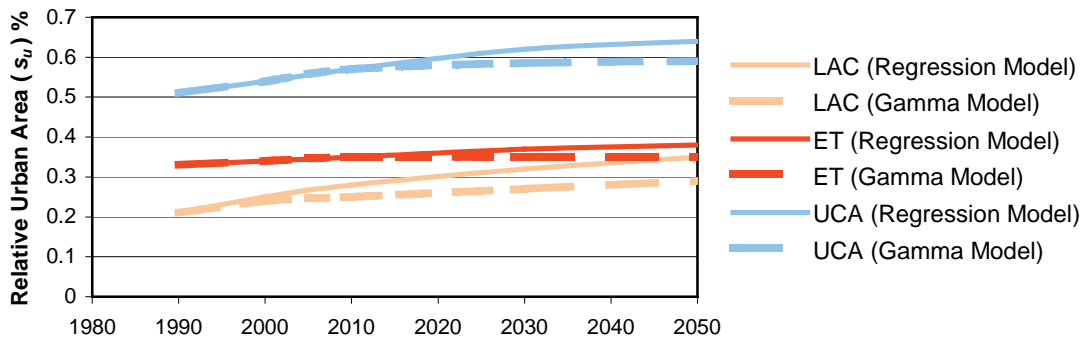


Fig. 3.18. Comparative dynamics of the relative urban areas in the LAC, ET, and UCA regions, obtained by the regression model and the modified Γ - model.

Comparing these graphs, we see that the Γ -model infers dynamics of urbanisation that are possibly very similar to more realistic dynamics. They are, on the one hand, a result of the generalisation of concrete statistical data, while on the other, are a consequence of statistical extrapolation to a near future. It is natural that the use of a model based on the two-parametric Γ -distribution is more attractive, since these parameters are integral indicators that combine demographic characteristics, such as the threshold density, which in turn is connected with life quality (“to have plenty of room is better”), and also with a city structure (the number of sky-scrapers in a city). Therefore, by changing the threshold density in accordance with some scenarios, we can study the dynamics of urbanised areas as a function of such scenarios.

It is interesting to compare how the threshold densities must be changed in order to equalise the values of relative areas estimated using both the regression and Γ -models (see Table 3.7).

Table 3.7. Comparative values of the threshold densities (in pers/km²) for the original (D^*) and modified (D_m^*) Γ -models.

<i>Region</i>	<i>Afr</i>	<i>Ar</i>	<i>Cn</i>	<i>AsP</i>	<i>LAC</i>	<i>ET</i>	<i>HI</i>	<i>UCA</i>
D^*	364	265	317	586	913	229	95	351
D_m^*	2,875	860	931	3,608	2,812	1,400	478	556

We see that the threshold densities in the modified Γ -model most likely correspond to the densities of the proper cities rather than the urbanised territory (see for instance Appendix II). This is one more argument confirming our hypothesis that the national statistics deal rather with the stable, traditional parts of a city's territories, that are naturally less than the territories that include growing outskirts.

3.7. Summary and conclusions on the dynamics of UT.

Comparing all these dynamics of the relative regional urban areas (see Table 3.8), we can say that regions such as the Afr, Ar, Cn and AsP manifest fast increasing areas of urbanised territory. For instance, urban area in the Africa region will increase 3-4 times during the 80 years (between 1980 and 2050), while, during the same time, the HI, ET and UCA regions will experience insignificant increases in urban area. If one compares the results produced by the two forecast models, the most dramatic growth of relative urban areas is shown by the regression model for the Ar region (almost 5 times increase), while the Γ -model forecasts the most dramatic growth for the Afr region (more than 4 times increase). Both models coincide with regards to the insignificant increase of the urban areas of the ET; HI and UCA, and relatively moderate increase (2 fold) for the LAC region.

Table 3.8. Increase in the relative urban area, from the regression and Γ -model (multiples of the 1980 situation).

<i>Region</i>	<i>Afr</i>	<i>Ar</i>	<i>Cn</i>	<i>AsP</i>	<i>LAC</i>	<i>ET</i>	<i>HI</i>	<i>UCA</i>
Regression	2.75	4.83	2.96	3.04	2.05	1.23	1.13	1.33
Gamma-model	4.38	3.10	2.91	4.09	1.63	1.14	1.15	1.24

Finally, when we estimate the contribution of urbanised territories into the GCC, we shall use the absolute values of urban area obtained using the statistical model (note that namely this variable is important in the procedure), as the minimal estimation, and correspondingly, the values obtained from the Γ -model, as the maximal one.

4 CARBON CYCLE IN URBANISED TERRITORIES. THEIR ROLE IN THE GLOBAL CARBON CYCLE

4.1. Introduction.

Until now we have not properly considered the elements of the carbon cycle in urbanised territories. Nevertheless, we already know how to estimate one of the most important variables in the regional carbon cycle – the total area of urbanised territories – using only standard demographic statistical data and their prognostic values. However, in relation to the carbon cycle, the total city area cannot be considered as homogenous. For example, while a “building up” area is disconnected from the carbon cycle, another, so-called “green” area continues to participate in the processes of carbon accumulation and exchange with the city’s natural environment (although, probably, with altered characteristics). Apparently, it is possible to describe the alteration of land-use in urban territory by the change of the relationship between these two areas.

4.2. Estimation of the city’s green area.

It is obvious that buildings, roads, concrete and asphalt do not cover the whole surface of an urbanised territory. There are also comparatively large segments of land covered by trees, shrubs and grass in the form of parks, gardens, lawns, etc. All of these are called the “green city area” or the “free city space”. The green area is a mosaic of many quasi-natural micro-ecosystems and plays the main role in the biological part of the local carbon cycle of the ecosystem “city”.

In the 1970s, E.P. Odum suggested the new concept of “city open space plan” (see Odum, 1971). He showed that for a typical American city, the open or free space was 71% in the 1970s. If no urban planning is applied, then the free space will be reduced to 16% by the year 2000. However, with planning this value increases to 33% (see Table 4.1).

The table contrasts the consequences of planned and unplanned land use in a 45,000-acre area near a large eastern US city that in 1970 had

approximately 20,000 people, but was projected to grow to 110,000 or perhaps 150,000 people by the year 2000.

Table 4.1. Comparison of unplanned and planned (optimal land use) development of a rapidly growing urban area (from Odum, 1971)*.

	<i>Year 1970, Population 20,000</i>	<i>Projected Year 2000, Population 110,000</i>	<i>Projected Year 2000, Population 110,000</i>
	Current	Unplanned Development	Optimal Use Plan
Developed Area	13,000 acres	38,000 acres	30,000 acres
Residential	7,500	26,000	21,300
Commercial	500	700	630
Industrial	70	300	70
Institutional	2,500	5,500	3,000
Roads	2,500	5,500	5,000
Free Space ("undeveloped area")	32,000	7,000	15,000
Waste disposal parks	0	0	1,000
Recreations parks	500	2,000	5,000
Farming & forestry	11,500	0	2,000
Natural areas	20,000	5,000	7,000
Total area	45,000	45,000	45,000
Per cent free space	71%	16%	33%

* Data adapted from a plan for a Maryland urban area.

As shown in column 3, judicious planning of residential and other development can preserve a third of the area as free space, including adequate space for efficient semi-natural tertiary treatment of both industrial and domestic wastes in ponds and well-planned landfills located in a large free space waste disposal park.

Hence, we assume that the relative "green" area, p_g , for the UCA region is 33% ($p_g = 0.33$). For Germany on the other hand, free space in a city is estimated to be 18.2% (a mean value calculated for 116 German cities; DE, 1997), but this does not take into account the vegetation of residence quarters. For the European cities overall, 5% of the residence quarters' area

is covered by woodland, and 25% by grass (Lazic et al, 2002). Since residence quarters comprise 38% of a total city space, we obtain a value of $(18.2+0.38\cdot(5+25))\% = 29.6\% \approx 30\%$ ($p_g = 0.3$) for the green city area of German cities in the 1990s. We will assume that this value may be taken as a relative estimate of city green areas for the HI and UCA regions.

Therefore, we may divide the total territory of a city into two parts. The first is the area occupied by buildings, roads etc., i.e. covered by artificial surfaces without vegetation. This is the “built-up area”. “Free city space” belongs to the second part. Their fractions are equal to p_1 and p_2 , correspondingly, where $p_1 + p_2 = 1$. We assume that *the value of p_1 must be the same for the cities of all eight regions*. The following concept justifies this assumption.

Any city is a complex social system, and its spatial structure is adjusted for the normal functioning of a city. Therefore, integral structural characteristics such as the relative area occupied by various subsystems that provide the normal functioning of a city (industry, service, municipal institutions, roads, etc.) must be general system invariant. It does neither depend (or, only weakly depends) upon the economic status of the region, nor upon its specific cultural characteristics. Also, since we have already assumed that any city grows *similarly*, then the invariant does not depend on time either.

Therefore, while the relative part of the “built-up” area remains constant, the “free space” area can be redistributed between the “green” and the area occupied by so-called “informal” low-income settlements, abundant in the developing world. We assume that the territory of informal settlements can expand only at the expense of the green territories. This is explained by the fact that parks and other urban recreation areas usually belong to municipalities, where the property rights are perhaps not as strict compared with private ownership. The free city space area, p_2 , can therefore be represented as:

$$p_2 = p_f + p_g = fp_2 + (1-f)p_2 \quad (1)$$

where $p_f = fp_2$ is the fraction of city area occupied by informal settlements and $p_g = (1-f)p_2$ is the fraction of green (covered by vegetation) area. From

the previous discussion, $p_2 = 0.3$, while f is the coefficient of “favelisation” ($0 < f < 1$). It is obvious that for the HI and UCA regions, $f = 0$.

Nowadays, informal settlements are an ordinary phenomenon of urbanisation in many regions of the World. These settlements, like inner-city slums, are called *favelas* or *tugurios* in Latin America, *chawls* in India, *medinas* in the Arab world, and shop-house tenements in South-East Asia. From now on, we shall use the common word *favelas*. Regarding their role in the carbon cycle, on the one hand, *favelas* do not have any green plants on their territory, while on the other, they tend to produce lower emissions, and have a more compact structure than conventional built-up areas.

Unfortunately, it is a difficult problem to collect reliable statistics on *favelas*' areas. The existing sources are very scarce (for instance UN, 2001), therefore, we had to make several additional assumptions. As a result, the following average estimations of the percentages of *favelas* area and f (coefficient of *favelisation*) are presented in Table 4.2.

Table 4.2. Relative green, p_g , and favelas, p_f , areas within a city.

Region		Ar	Asp	Cn	LAC	ET	HI	
p_f (%)	15	10	12	1	20	1	0	0
p_g (%)	15	20	18	29	10	29	30	30
f	0.50	0.33	0.40	0.03	0.67	0.03	0.0	0.0

We cannot provide a detailed prognosis of *favelas* dynamics. Therefore, the simplest hypothesis is that the value of f does not change during the process of the growth of urbanised territories.

Finally, for each region j ($j = 1, 2, \dots, 8$) the area of an urbanised territory S^j (from now on for simplicity we will omit the sub-index “ u ”) can be presented as a sum of three items:

$$S^j = S_b^j + S_g^j + S_f^j, \quad (2)$$

where $S_b^j = (1 - p_2)S^j = 0.7S^j$ is the built-up area, $S_g^j = p_g^j S^j = p_2(1 - f^j)S^j = 0.3(1 - f^j)S^j$ is the green area and $S_f^j = p_2 f^j S^j = 0.3 f^j S^j$ is the area occupied by *favelas*.

4.3. Losses of organic carbon as a result of urbanisation: a land use model.

Let the area of urbanised territory of the j^{th} region in the year t be equal to $S^j(t)$. The annual increments of $S^j(t)$ are then expressed as $dS^j(t) = S^j(t) - S^j(t-1)$. We assume that in the process of urbanisation, some natural (or similar) ecosystem with local densities of living biomass, $(B^j)^*$, and dead organic matter (humus), $(D^j)^*$, is replaced by the “built-up” area. The annual rate of this “sprawling” is $dS^j(t)$. We assume that all living biomass is completely destroyed, relatively quickly decomposed, and emitted into the atmosphere in the form of CO_2 . Since any building and road constructions are accompanied by the destruction of soil structure, its fragmentation and the increase in its aeration will likewise result in the destruction of soil humus that will also be emitted into the atmosphere as CO_2 . This is a typical process of *land conversion*.

However, the area $dS^j(t)$ is involved partially in this process: its $(p_g^j)^{\text{th}}$ -fraction (green area) remains, as before, occupied by natural ecosystems. Thus, the annual amount of carbon emitted by the j^{th} region, i.e., the annual carbon outflow, is equal to:

$$dC_l^j(t) = (1 - p_g^j) dS^j(t) \cdot [(B^j)^* + (D^j)^*] \quad (3)$$

where $(1 - p_g^j) = 0.7 + 0.3f^j$, and the values for f^j are taken from Table 4.2.

4.4. Redistribution of carbon flows by “urbanised” ecosystem. The total balance of carbon flows.

Let us assume that the areas of urbanised territories are constant, i.e., $dS^j(t) = 0$. It is obvious that the balance of natural carbon (if we exclude the anthropogenic carbon emission) in any territory is only determined by difference between the annual amount of atmospheric carbon accumulated by vegetation located in this territory (uptake of atmospheric CO_2 by terrestrial

vegetation), and the carbon emitted by the area *via* the process of the decomposition of dead organic matter.

In an ecosystem at equilibrium, the balance is equal to zero since production and decomposition would balance each other. However, while in natural ecosystems these flows are balanced, this balance is disturbed in ecosystems located within the green area of urbanised territories (“city” or “urbanised” ecosystems). As mentioned above, about 50% of carbon ($k_e = 0.5$), accumulated as the annual net primary production (NPP) of “urbanised” ecosystems, is removed from and transported to either other ecosystems with different decay conditions, or through rivers to the ocean. As a result, the local balance of carbon is disturbed and the urbanised territory starts to operate as a “carbon sink”. Thus, carbon is not accumulated within the territory but is instead horizontally redistributed to other areas. Generally speaking, urbanisation changes the structure of local carbon flows. All these flows are shown (for clearness) in Fig. 4.1. The power of the carbon sink can be estimated for all regions. Let k_e^j be the share of organic carbon exported from the “urbanised” ecosystem of j^{th} region into neighbouring territories, and $S_g^j = p_g^j S^j(t)$ be the green area of the urbanised territory. The annual balance of natural carbon between the atmosphere and urbanised territory of j^{th} region will therefore be equal to:

$$\begin{aligned} dC_s^j(t) &= \underbrace{(NPP^j)^* \cdot S_g^j(t)}_{\text{production}} - \underbrace{(1 - k_e^j) \cdot (NPP^j)^* \cdot S_g^j(t)}_{\text{decomposition}} = \\ &= k_e^j p_g^j S^j(t) \cdot (NPP^j)^*, \end{aligned} \quad (4)$$

where $(NPP^j)^*$ is some mean value of the annual NPP of the corresponding regional natural ecosystems, $S^j(t)$ is the area of urbanised territory and $p_g^j = 0.3(1 - f^j)$ is its green fraction.

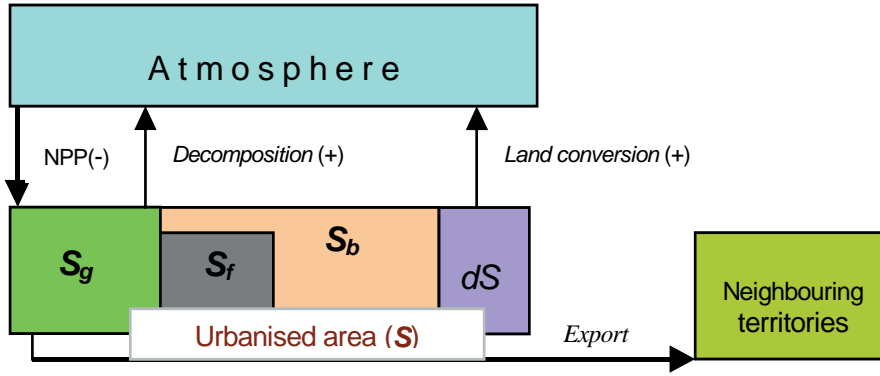


Fig. 4.1. Carbon flows in an “urbanised” ecosystem.

Flows: 1. Production „NPP” = $(NPP)^* S_g$, 2. „Decomposition”=

$$= (1 - k_e)(NPP)^* S_g,$$

3. “Land conversion”, $dC_l = (B^* + D^*)dS$, 4. “Export” = $k_e(NPP)^* S_g$.

The $(NPP)^*$, B^* and D^* are the local stationary values of the NPP, living biomass and humus, correspondingly; the coefficient k_e is a fraction of dead organic matter exported from the “urban” ecosystem into neighbouring territories.

Areas: 1. S_g - „Green” area (park zone), 2. S_f – area occupied by favelas,

3. S_b – built-up area, 4. dS – annual increment of urbanised area,

$$S = S_g + S_f + S_b - \text{total urbanised area.}$$

Although, we have estimated k_e^j to be equal to 50%, this value may vary for different regions. As it may be problematic to explicitly estimate the regional values, we assume that $k_e^j = 0.5$ for all regions.

However, in reality urbanised territories are expanding, hence $dS^j(t) \neq 0$. This term, expressing the dynamics of urbanised territories, should be taken into account within the general expression for the total annual balance of carbon, dC_{tot}^j :

$$dC_{tot}^j(t) = dC_l^j(t) - dC_s^j(t) = (0.7 + 0.3f^j)dS^j(t) \cdot [(B^j)^* + (D^j)^*] - 0.3k_e^j(1 - f^j)S^j(t) \cdot (NPP^j)^*. \quad (5)$$

This formula represents the local carbon balance, namely, the one for a given territory. It is obvious that, if $dC_{tot}^j > 0$, then the given territory is a source of carbon, while if $dC_{tot}^j < 0$, then it is a sink. If $dC_{tot}^j = 0$ then the territory is neutral with respect to the GCC.

Note that our definition of sink (and source) rather differs from that used, for instance, by Prentice et al. (2001). The point is that in the “Prentice-like” definition a sink is considered as a system that accumulates matter, whereas we consider a sink as a system that “sucks” matter from the environment. For instance, a through-flow system, the mass of which will not necessary increase, is, from our point of view, always a sink; whereas in accordance with the “Prentice-like” definition, it is a sink if and only if its mass increases. It appears to us then, that our definition is closer to the standard physical definition than the “Prentice-like” one.

We emphasise that these considerations apply only to natural, non-anthropogenic carbon flows.

4.5. Estimation of the NPP, living biomass and humus for different regions.

In order to estimate the values of NPP^* and (B^*+D^*) , we use Bazilevich's global data set (Bazilevich, 1979), applying the smoothing and correction procedure of Svirezhev (2002). The elementary unit of the database is a biome. A list of all main biomes is represented in Table 4.3.

Tab. 4.3. Different types of global vegetation (biomes).

1. <i>Polar desert, polar tundra</i>	16. <i>Dry steppe</i>
2. <i>Tundra</i>	17. <i>Sub-boreal desert</i>
3. <i>Mountainous tundra</i>	18. <i>Sub-boreal saline desert</i>
4. <i>Forest tundra</i>	19. <i>Subtropical semi-desert</i>
5. <i>North taiga</i>	20. <i>Subtropical desert</i>
6. <i>Middle taiga</i>	21. <i>Mountainous desert</i>
7. <i>South taiga</i>	22. <i>Alpine and Sub-alpine meadows</i>
8. <i>Temperate mixed forest</i>	23. <i>Evergreen tropical rain forest</i>
9. <i>Aspen-Birch lower taiga</i>	24. <i>Deciduous tropical forest</i>
10. <i>Deciduous forest</i>	25. <i>Tropical xerophyte woodland</i>
11. <i>Subtropical deciduous and coniferous forest</i>	26. <i>Tropical savannah</i>
12. <i>Xerophyte woods and shrubs</i>	27. <i>Tropical desert</i>
13. <i>Forest steppe</i>	28. <i>Mangrove forest</i>
14. <i>Temperate dry steppe (including mountainous)</i>	29. <i>Saline land</i>
15. <i>Savannah</i>	30. <i>Subtropical and tropical woodland and tugaj shrubs</i>

A geographical explication of these biomes (Bazilevich's biome map) is shown in Fig. 4.2. The regional borders and the domains with urbanised population are also presented in this figure.

In addition we present in Table 4.4 the data for NPP and the densities of living biomass and dead organic matter (humus) for the main biomes.

It is obvious that the borders of biomes do not coincide with the borders of states, UN regions or urbanised territories. In addition, we have to take into account that the distribution of urbanised territories in a region is not homogeneous (see for instance Fig. 4.2).

Using the map shown in Fig. 4.2, we can construct the so-called *biome's portrait* of a region, that is the percentages of area that is occupied by every biome, π_k^j ($\sum_1^{30} \pi_k^j = 1$). We can then calculate the regional means of productivity, living biomass and humus as

$$(NPP^*)^j = \sum_{k=1}^{30} \pi_k^j (NPP^*)_k, \quad (B^*)^j = \sum_{k=1}^{30} \pi_k^j (B^*)_k, \quad (D^*)^j = \sum_{k=1}^{30} \pi_k^j (D^*)_k, \quad (6)$$

where the values of NPP^* , B^* and D^* are taken from Table 4.4. Results of these calculations are shown in Table 4.5.

If we then use these data in Eqs. (3) – (5) to estimate the corresponding carbon flows in urbanised territories, this utterly implies that we assume that in every region, its cities are geographically distributed (over the surface of the region) *randomly*. We shall name this type of spatial distribution *Model I*.

Nevertheless, if we look at the red points representing city distribution in Fig. 4.2, we can see that these points are not completely randomly located but are attracted to domains that are more suitable for human conditions (local climate, vegetation, soil, etc). It is natural that in a certain sense, all these factors are reflected by integral parameters such as the productivity of the local vegetation, its living biomass, and the storage of dead organic matter. If we superimpose on the biome's map a sufficiently fine grid (so that each cell contains not more than a single red point) then we can construct the biome's portrait of a regional urban territory.

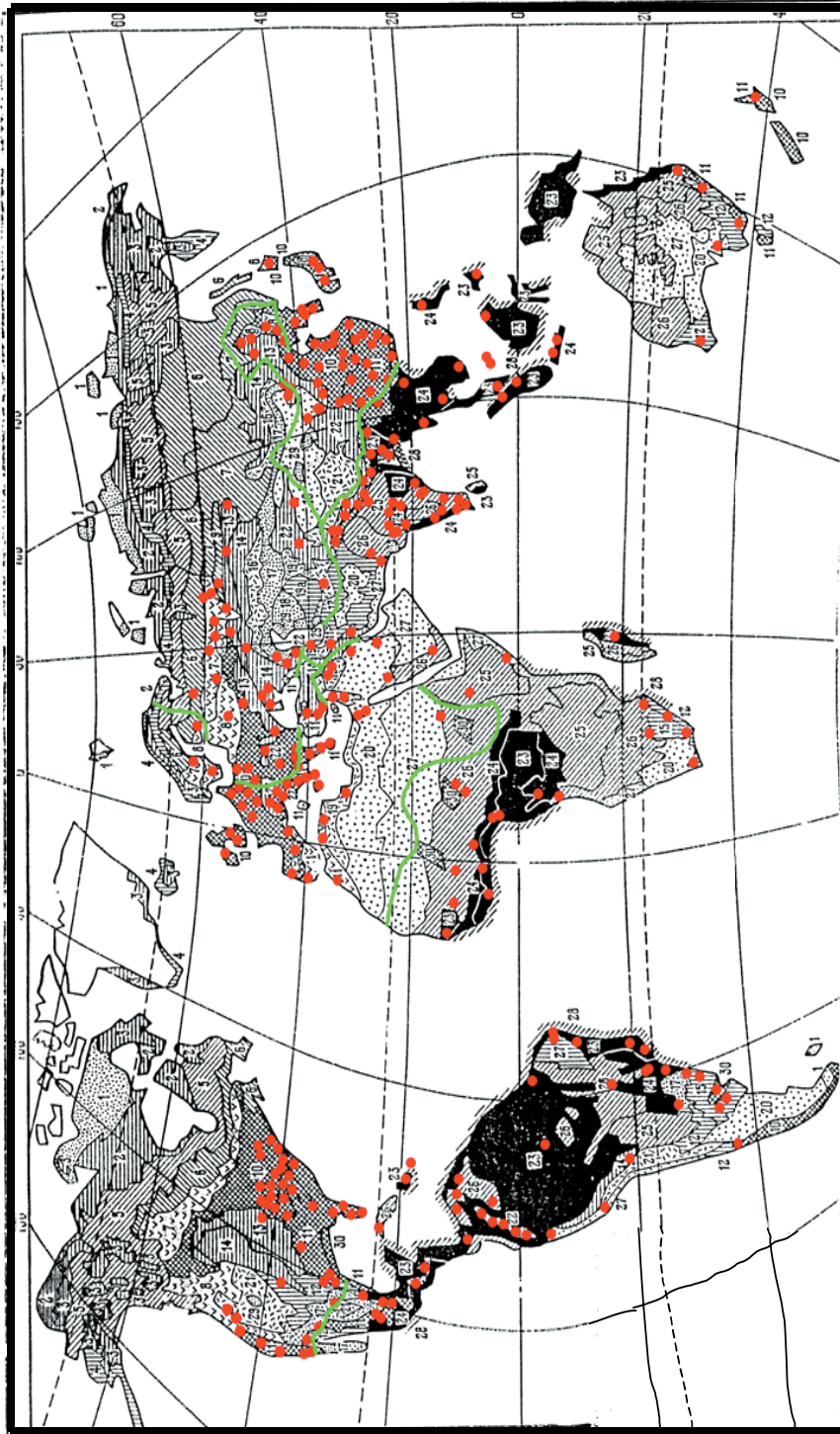


Fig. 4.2. Bazilevich's biome map. The biomes numbering is shown in Table 4.3.

Table 4.4. Annual net primary production, P^* (10^3 tons C /($\text{km}^2 \cdot \text{year}$), density of living biomass, B^* (10^3 tons C /(km^2), and density of dead organic matter, D^* (kilotons C /(km^2 , in 1m soil); **a** - biome type, **b** - biome area ($\times 10^6$ km^2). Biomes n° 9 and n° 28 are not included because of the smallness of their territories. *Source:* Svirezhev (2002).

a	b	P*	B*	D*	a	b	P*	B*	D*
1	2.55	0.068	0.148	0.938	16	2.66	0.15	0.32	7.04
2	2.93	0.144	0.76	3.08	17	2.08	0.18	0.45	6.8
3	2.23	0.15	0.76	3.06	18	2.59	0.096	0.18	4.56
4	1.55	0.26	1.5	5.02	19	1.99	0.14	0.32	4.94
5	5.45	0.22	3.2	4.52	20	7.16	0.044	0.096	0.87
6	5.73	0.25	6.2	6.06	21	1.15	0.18	0.32	9.49
7	6.60	0.26	7.4	11.5	22	3.54	0.3	0.76	13.4
8	2.12	0.35	8.0	16.1	23	10.4	1.3	18.0	13.4
10	7.21	0.53	15.0	16.9	24	7.81	0.95	16.0	13.1
11	5.75	0.71	14.2	14.4	25	9.18	0.54	2.4	10.6
12	3.91	0.23	1.5	8.4	26	17.1	0.5	2.4	10.2
13	3.72	0.3	0.76	23.3	27	11.5	0.068	0.144	1.4
14	4.29	0.32	0.76	18.1	29	0.37	0.068	0.15	2.75
15	1.66	0.44	1.5	14.8	30	0.9	0.78	16.0	12.1

Table 4.5. Annual regional means for the net primary production (NPP^* , in 10^3 tonsC/ km^2 per year), and the sum of specific living biomass and dead organic matter – humus ($B^* + D^*$, in 10^3 tonsC/ km^2): *Model I.*

Region	Afr	Ar	AsP	Cn	LAC	ET	HI	UCA
NPP^*	0.80	0.24	0.82	0.34	0.72	0.31	0.50	0.53
$B^* + D^*$	21.8	7.4	24.5	19.4	23.3	13.2	23.8	22.9

For this we have to calculate the percentage of urban area that is occupied by every biome, $(\pi_u)_k^j \left(\sum_1^{30} (\pi_u)_k^j = 1 \right)$. These portraits for each of the eight regions are represented in Table 4.6. Note that the number of cells covering each region is rather high and adequate: for instance, the Afr region is covered by 155 cells, the UCA by 340 cells, and even a relatively small region such as the HI contains 62 cells.

Table 4.6. The biome's portraits of urbanised territories of the different regions.

The fractions $(\pi_u)_k^j$ is expressed in %.

Biome	Region	Afr	Ar	AsP	Cn	LAC	ET	HI	UCA
6. Middle taiga							4.0	3.1	
7. South taiga							23.3	3.0	
8. Temperate mixed forest							11.6	5.8	2.2
10. Deciduous forest				8.5	42.9		19.6	67.6	13.2
10. Subtropical deciduous & coniferous forest			15.3	17.0	42.9	15.6		11.8	62.9
12. Xerophyte woods & shrubs		3.8		2.1					6.1
13. Forest steppe					4.8		11.7		2.1
14. Temperate dry steppe				2.1		6.3	19.0	2.8	1.8
15. Savannah		11.5				9.4			
16. Dry steppe							3.8		
17. Subboreal desert						6.2			5.9
18. Subboreal saline desert							2.7		
19. Subtropical semi-desert			30.8	2.2					
20. Subtropical desert			30.8						1.9
22. Alpine & subalpine meadows					4.8	12.5	3.9	5.9	
23. Evergreen tropic rain forest		26.9		10.6		21.9			
24. Deciduous tropical forest		3.8		14.9		6.3			3.9
25. Tropical xerophyte woodland		11.5		23.0					
26. Tropical savannah		38.5	15.4	6.4		12.5			
27. Tropical desert		3.8	7.7			6.2			
29. Saline land					4.8	3.1			
30. Tropical & subtropical woodland & tugaj				12.8					

We now calculate the weighting means of productivity, living biomass and humus for the urbanised territory of each j^{th} region:

$$(NPP_u^*)^j = \sum_{k=1}^{30} (\pi_u)_k^j (NPP^*)_k, \quad (B_u^*)^j = \sum_{k=1}^{30} (\pi_u)_k^j (B^*)_k, \quad (D_u^*)^j = \sum_{k=1}^{30} (\pi_u)_k^j (D^*)_k \quad (7)$$

Results of these calculations are shown in Table 4.7.

Table 4.7. Means of the net primary production (in 10^3 tons C/ km² per year), and the sum of specific living biomass and dead organic matter – humus (in 10^3 tons C/ km²) for urbanised territories: *Model II*.

Region	Afr	Ar	AsP	Cn	LAC	ET	HI	UCA
NPP_u^*	0.70	0.25	0.72	0.56	0.66	0.33	0.50	0.56
$B_u^* + D_u^*$	18.2	8.4	23.3	27.9	20.6	21.0	28.7	24.0

If we substitute these data into Eqs. (3) – (5), when $(NPP_u^*)^j \Rightarrow (NPP^*)^j$, and calculate the carbon flows, then we implicitly use a model where the cities are randomly distributed only over the urbanised territory (*Model II*). By the same token, we assume that in the process of urbanisation, humans prefer to master (with the coefficients of preference) only those domains that are similar (with respect to a biome’s portrait) to other domains that had been mastered by this time.

If we compare the data in Tables 4.5 and 4.7, we can see that for almost all regions (except Cn and ET) the values of NPP^* and $B^* + D^*$, that were estimated using both models, do not significantly differ from each other, although in “tropical” regions as the Afr, AsP and LAC, there is a tendency for attraction towards more “moderate” locations that is manifested in a decrease in the NPP values. If we neglect this shift, we can say that in all these regions, cities are distributed over their territories almost randomly.

As for the Cn region, then the significant deviation from the random model is simply explained in that 4/5 of China’s territory is unpopulated semi- and full desert, hence it is natural that Chinese cities are “attracted” to more productive territories.

The ET region is characterised by a significant shift of the living biomass and humus storage in the direction of their greater values that is observed in the urbanised territories of this region. If we take into account that the ET region is mainly the territory of the former USSR, then it is also simply explained from a historical point of view (Soloviev, 1959). Briefly, because of the large distances and poorly developed transport network, each Russian city needed its own food supply; hence they would be surrounded by an agricultural ring. In turn, agriculture requires fertile soil. The latter is characterised by a high value of humus, maintained by the abundance of living biomass (for example, the famous Chernozem belt of Russia).

4.6. Losses of carbon as a result of urbanisation, export of carbon into neighbouring territories, and the total carbon balance in urbanised areas. I. Regression model.

We now have the necessary information to calculate the losses of carbon as a result of land conversion during the course of urbanisation in the nearest future. Using Eq. (3), in which the annual increment of urban area, $dS^j(t)$, is determined by the regression model of Chapter II, and the total biomass and humus storage, $(B^j)^* + (D^j)^*$, corresponds to *Model I* (the random distribution of cities in a given region), we obtain the dynamics of the annual losses of organic carbon (see Tab. 4.8 and Fig. 4.3). The carbon emissions as a result of land conversion are equal to the corresponding losses of organic carbon. The emissions monotonously decrease for the LAC and ET regions. This is a result of “saturation” in the process of the cities’ growth that occurred in 80-90s of last century. As for the ET region, the sharp deceleration of the cities growth was caused by the general economic processes associated with collapse of the USSR.

The increase in carbon emissions in the other regions points to the accelerating process of urbanisation. However, acceleration quickly stops between the years 2000 – 2010 in the Afr, Ar, UCA and HI regions as saturation occurs, although this may be because of different reasons. In the Cn and AsP regions, saturation occurs later, between the years 2020 – 2030.

After this turning point, the emissions from all of these regions begin to drop, corresponding in general to the deceleration of urbanisation.

Tab. 4.8. Regional carbon balance of urbanised territories (in 10^6 tonsC per year).

Regression model.

Year		1980	1990	2000	2010	2020	2030	2040	2050
Region									
Afr	dC_l	8.56	10.72	12.89	12.78	12.15	11.64	11.00	10.37
	dC_s	1.47	1.82	2.23	2.23	3.04	3.42	3.77	4.11
	dC_t	7.09	8.91	10.66	10.66	9.11	8.22	7.23	6.26
Ar	dC_l	10.88	11.34	11.80	12.33	11.68	11.09	9.01	7.25
	dC_s	1.08	1.54	2.02	2.52	3.00	3.45	3.82	4.11
	dC_t	9.81	9.81	9.79	9.81	8.68	7.64	5.19	3.14
Cn	dC_l	43.27	58.41	73.54	87.81	103.73	97.37	88.18	73.90
	dC_s	10.01	12.11	14.75	17.90	21.63	25.13	28.29	30.95
	dC_t	33.26	46.30	58.79	69.91	82.10	72.24	59.89	42.96
AsP	dC_l	19.91	32.28	44.65	54.22	64.36	61.04	56.14	49.35
	dC_s	6.54	7.72	9.36	11.36	13.72	15.96	18.03	19.84
	dC_t	13.37	24.55	35.28	42.87	50.64	45.07	38.12	29.51
LAC	dC_l	20.78	17.48	14.19	12.55	10.62	8.36	6.54	5.82
	dC_s	1.26	1.56	1.80	2.01	2.19	2.34	2.45	2.55
	dC_t	19.52	15.92	12.38	10.53	8.43	6.02	4.09	3.27
ET	dC_l	4.17	3.63	3.08	2.71	2.43	1.90	1.01	0.87
	dC_s	3.53	3.71	3.86	3.99	4.10	4.20	4.24	4.29
	dC_t	0.64	-0.08	-0.77	-1.28	-1.67	-2.30	-3.23	-3.42
HI	dC_l	7.12	7.76	8.39	8.52	8.38	7.70	7.21	6.67
	dC_s	18.18	18.53	18.90	19.29	19.67	20.01	20.34	20.64
	dC_t	-11.06	-10.77	-10.51	-10.77	-11.29	-12.31	-13.13	-13.97
UCA	dC_l	11.41	11.98	12.55	12.19	11.10	9.78	8.34	7.59
	dC_s	10.53	11.12	11.74	12.35	12.90	13.38	13.80	14.17
	dC_t	0.88	0.86	0.81	-0.16	-1.80	-3.60	-5.46	-6.59
World	dC_l	107.58	133.86	160.15	182.41	204.98	191.39	171.88	147.55
	dC_s	23.89	28.46	34.02	40.43	47.69	54.49	60.60	65.84
	dC_t	83.69	105.41	126.13	141.98	157.29	136.90	111.28	81.71

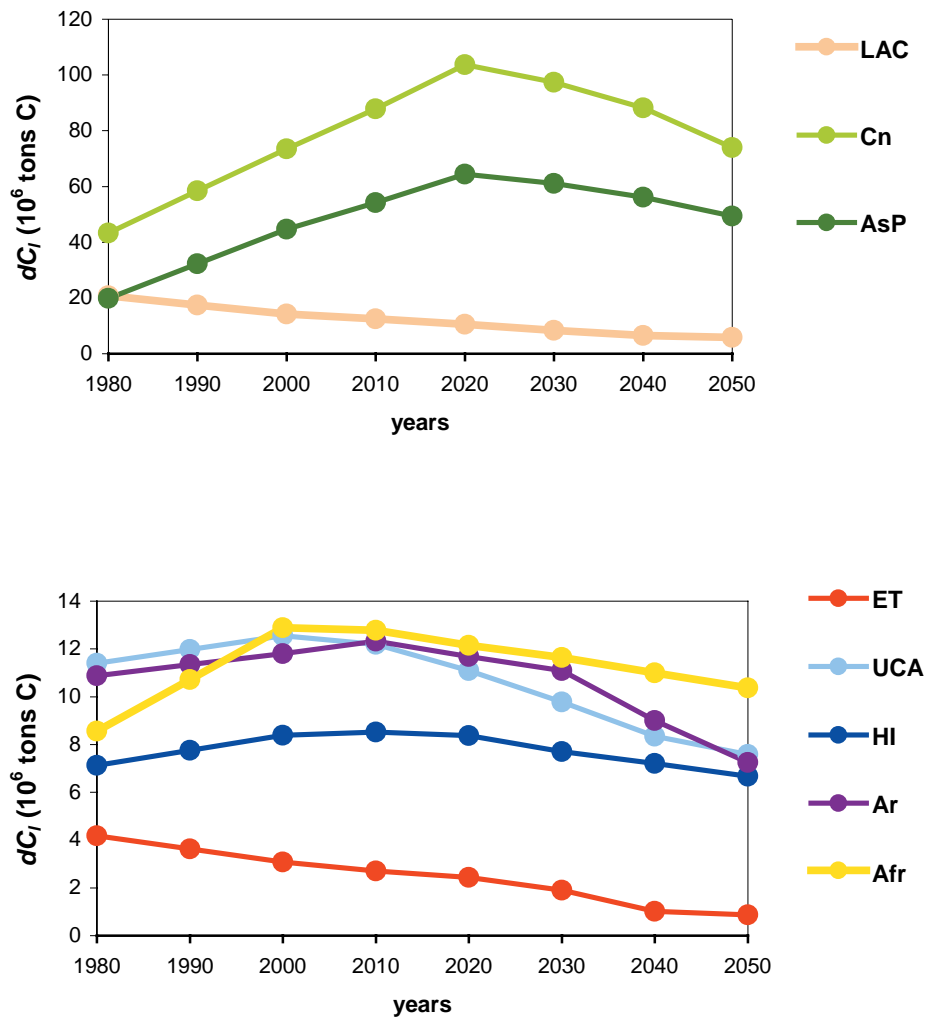


Fig. 4.3. Annual carbon emission as a result of urbanisation between 1980-2050.

The world dynamics of “urbanisation” emissions are shown in Fig. 4.4 (see also Tab. 4.8). We see that the annual carbon emission by urbanised territories, caused by land conversion in the process of their growth, will attain a maximum of 205MtC between ca. 2020-2030. Emission will then slowly decrease, such that by the year 2050 it will equal ca. 150 MtC. Maximal contributions to this emission are given by two regions: Cn and AsP.

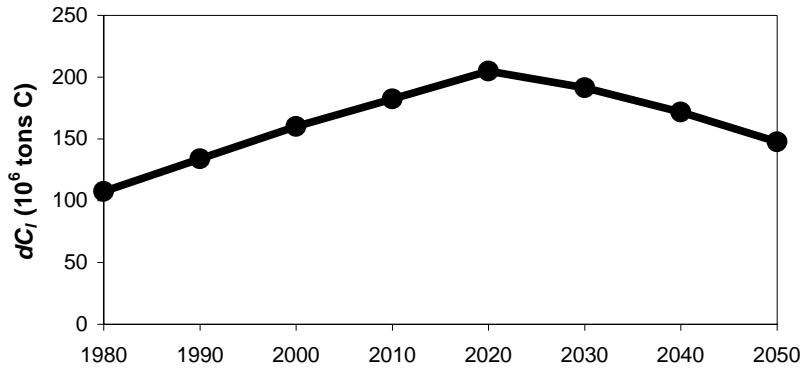


Fig. 4.4. World annual emission of carbon as a result of land conversion during the process of urbanisation between 1980-2050.

Note that these results differ insignificantly from the results presented in our earlier article (Svirejeva et al., 2004). This may be explained by the fact that in the earlier work, we used other demographic data and prognoses (UN, 2001).

In the next step, using Eq. (4), we can estimate the annual sink of carbon into the ecosystems of the regional urbanised territory – the carbon sequestration rate (see Table 4.8 and Fig. 4.5). Since $k_e^j = 0.5$, the latter is equal to the annual export of organic carbon (in the form of dead organic matter) out of the urbanised territory's green areas to neighbouring natural ecosystems.

At the first stage (up to the year 2015) the maximum amount of organic carbon is horizontally exported by the urbanised territories of the HI region. However, after this the export rate from the Cn region becomes the highest. Nevertheless, the AsP export, which is growing almost as fast as the Cn rate, does not exceed the HI rate till 2050. Four regions (Afr, ET, LAC and Ar) demonstrate almost the same dynamics of carbon export, although, the amounts of exported carbon are minimal in these regions.

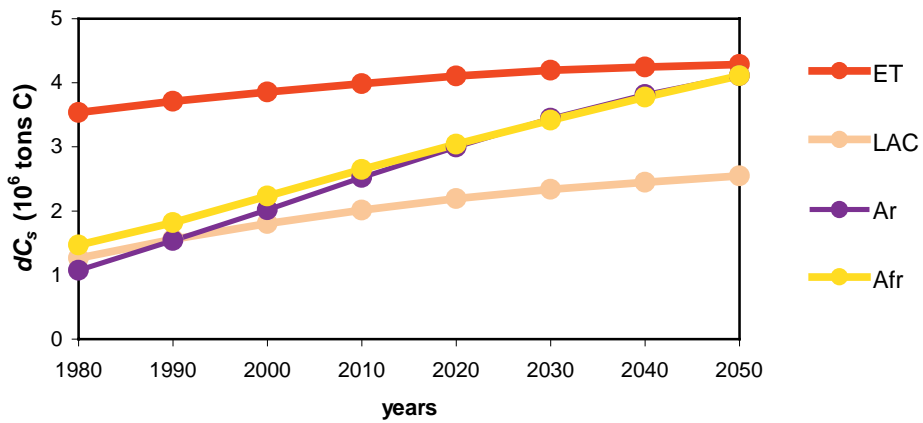
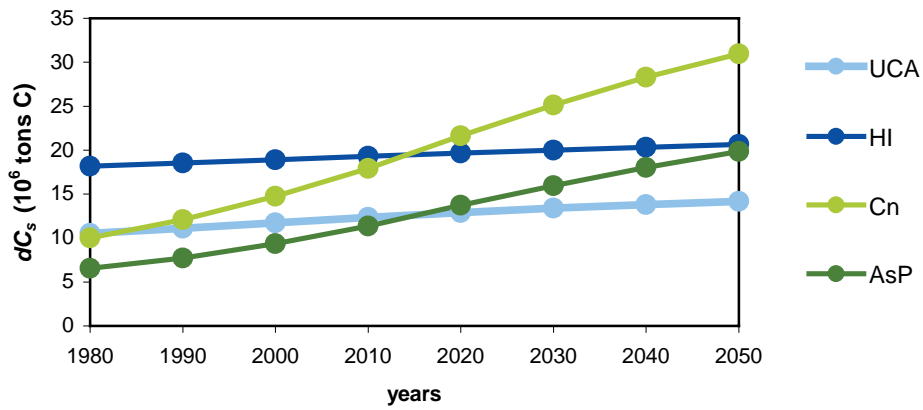


Fig. 4.5. Annual export of organic carbon out of “urbanised” ecosystems into neighbouring territories between 1980-2050.

As to the world dynamics of annual export of carbon by urbanised territories, we observe a monotonous, almost linear growth of this value (see Fig. 4.6). In the course of time, from 1980 until 2050, it will increase by almost three times, from 24 MtC up to 66 MtC. It is natural therefore that it should lead to a significant redistribution of horizontal carbon flows.

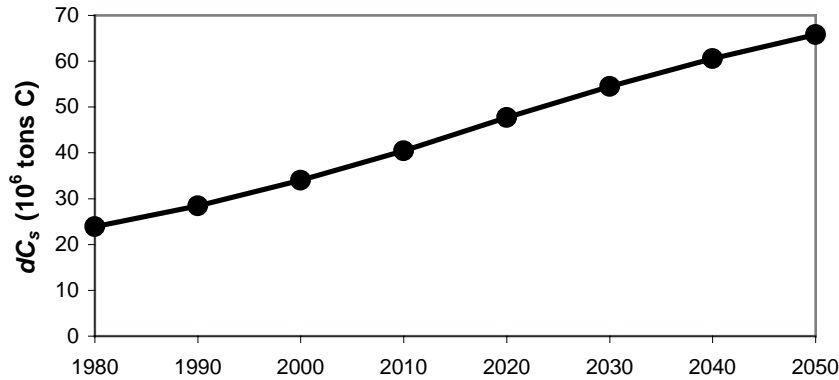


Fig. 4.6. World annual export of organic carbon out of “urbanised” ecosystems into neighbouring territories between 1980-2050.

This effect is qualitatively similar to the transportation of carbon by rivers, but it is quantitatively lower by one order of magnitude (for instance, the annual export of carbon by rivers into the ocean is 196 – 537 Mt, Svirezhev, 1997).

Finally, using Eq. (5), we estimate the total atmospheric carbon balance of urbanised territory for each region (Fig. 4.7). Immediately, we obtain some paradoxical results, when the *urbanised territories of the ET, UCA* (after the year 2010), and especially *HI regions play the role of carbon sinks*. We emphasise that this conclusion concerns only natural, non-anthropogenic carbon, and that an “overflow” of carbon from the atmosphere is not accumulated within a given “urbanised” ecosystem but is transported to other territories.

Moreover, even the other urbanised territories that play the role of sources (Cn, AsP, Afr and Ar regions), sooner or later manifest a tendency to decrease the misbalance of carbon between two processes: its emission into the atmosphere and its export into the neighbouring territories. It is obvious that the misbalance is equal to $dC_{tot}(t)$, i.e., the total balance. The single exception is the LAC region, where the misbalance is already decreasing, beginning from 1980. In the Arabian region, the decrease of the misbalance will be observed after 2015, when stagnation in the dynamics of the total balance, observed at the present time, will have ended.

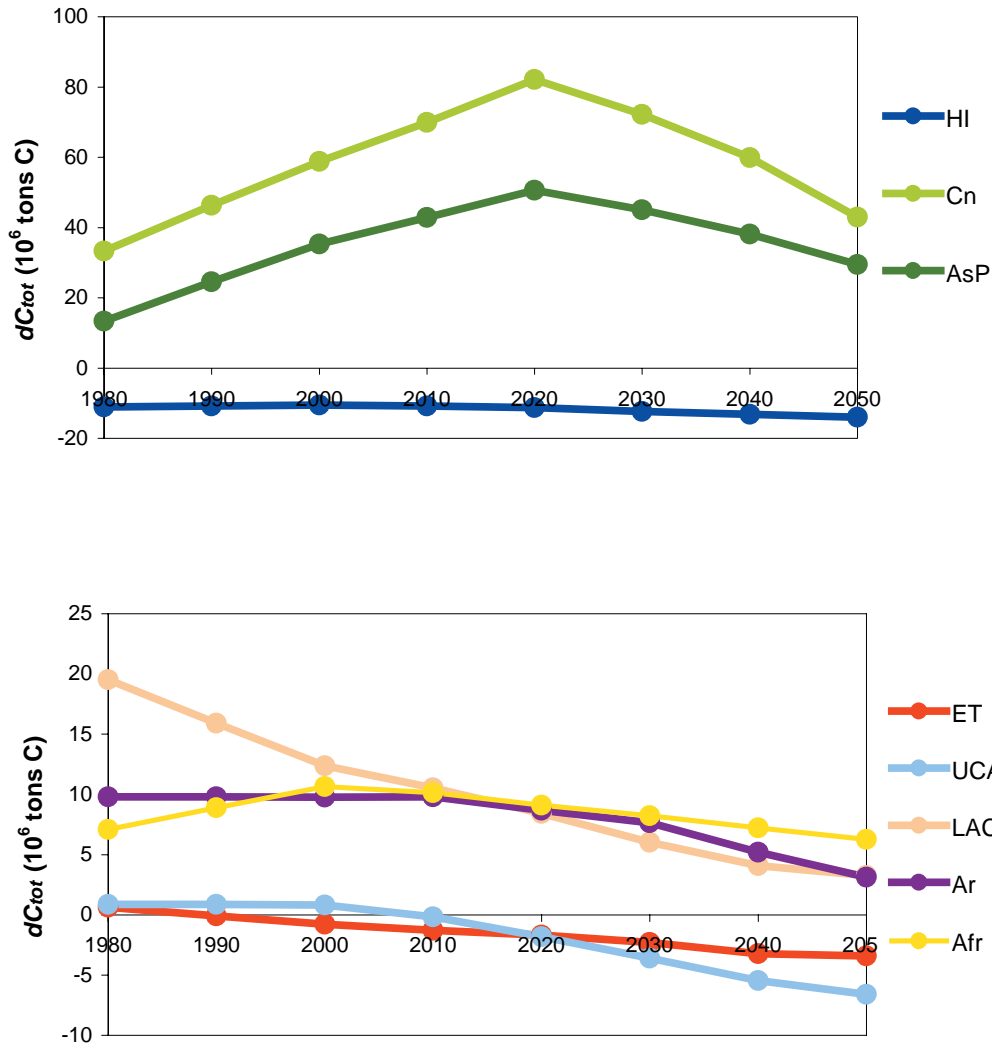


Fig. 4.7. Total annual balance of natural carbon for regional urbanised territories in 1980–2050.

In the Afr region, stagnation is observed since 2000, and it will also be completed by 2015. In the Cn and AsP regions, the period of the fast growth of misbalance that is now observed, after a very short period of stagnation, will be replaced by an equally fast process of misbalance decrease after 2030. In the ET (after the year 1990), HI (after the year 2000) and UCA (after the year 2010), we observe the opposite picture, with the misbalance increasing.

Such types of dynamics are explained by the total balance being the sum of two processes, as mentioned above. The first is the loss of carbon as a result of land conversion and its emission in the form of CO_2 into the atmosphere, when the total balance of carbon is shifted to a “source” side. It

is obvious that when the growth of urbanised territories in a given region is faster, the shift towards a “source” side is greater. This is most distinctly seen in the AsP, Cn and Afr regions at the initial stage of their “urbanistic” evolution.

The second process is a “through-pumping” of the atmosphere carbon through an “urbanised” ecosystem into neighbouring natural ecosystems. It is natural that the process shifts the total balance to a “sink” side, i.e. where the green area is larger, the shift towards a “sink” side is greater.

If the process of urbanisation is stagnant or regressive, then the export of organic carbon to neighbouring natural territories prevails, and the urbanised territory is transformed into a carbon sink, as seen in the HI, UCA and ET regions. On the contrary, if the process of urbanisation is progressive, then carbon emissions into the atmosphere dominate, and the urbanised territory is transformed into a carbon source, as is seen in the Cn and AsP regions.

World dynamics of the interaction of these processes is shown in Fig. 4.8. One can see that the world urbanised territories work as a source of carbon, where its power increases till the year 2020, when the maximal amount of carbon, 160 MtC per year, is emitted into the atmosphere as a result of urbanisation.

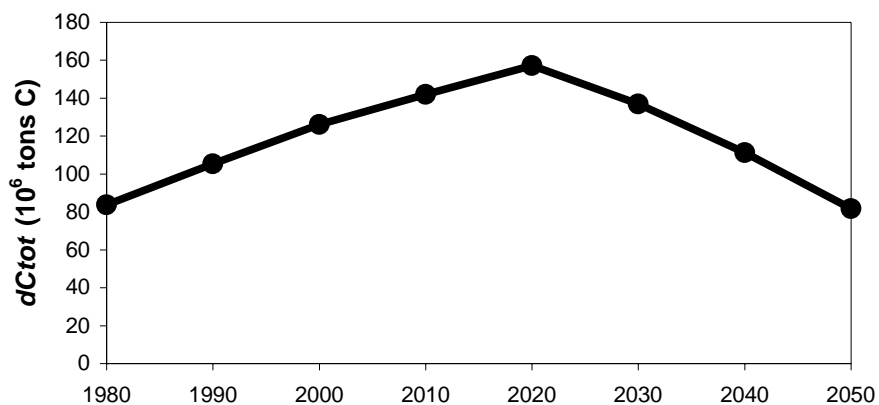


Fig. 4.8. World dynamics of the total annual balance of natural carbon for urbanised territories in 1980–2050.

Today, the influence of urban territories on the specific mechanisms behind the transformations of the GCC is not significant, since they occupy relatively

small areas. However, city territories grow fast and if contemporary trends continue, then the following examples could be interesting.

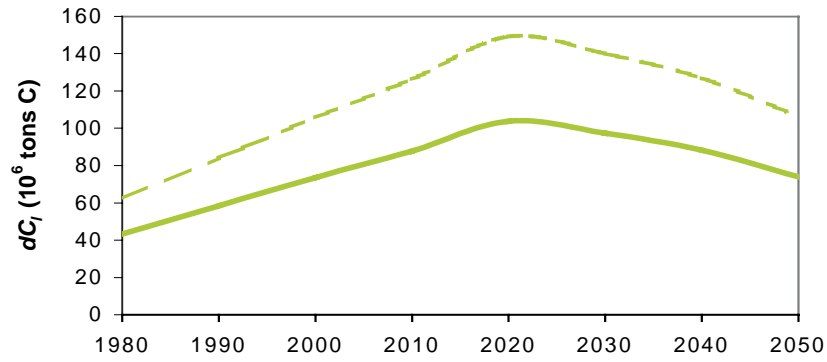
For instance, while at present only 1% of the Asian region is covered by urbanised territories, over the next 60 years it will become half urbanised. For Africa, where only 0.15% of the total territory is currently urbanised, the same level is reached after 90 years.

Fortunately, in accordance with our estimations, the process of urbanisation is inhibited between 2020-2030, and by the middle of the century, the growth of urbanised areas would have almost stopped. Hence, the total emission of natural carbon at that stage will be stabilised at the level of the 1980s (80 MtC per year).

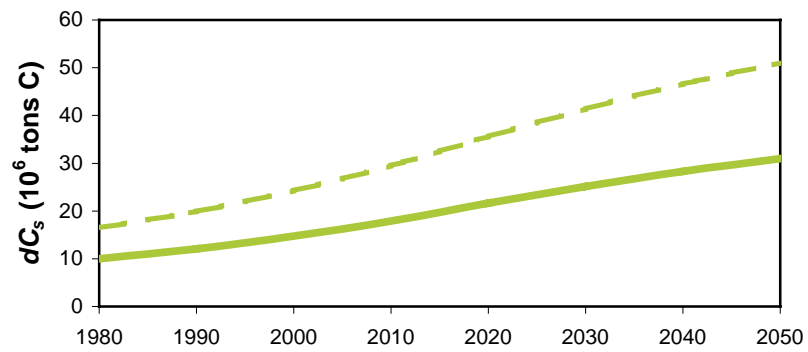
4.7. Effect of non-random cities' distribution on components of the total carbon balance.

We have not yet used the second model of (non-random) cities' distribution. Its use reduces to replacing in Eqs. (3)-(5) the values of NPP^* and $B^* + D^*$ from Table 4.5 by the values of NPP_u^* and $B_u^* + D_u^*$ from Table 4.7. Since, as shown above, the significant deviation from a random model was only observed for the Cn and ET regions, we shall calculate the comparative dynamics of: (a) carbon losses due to land conversion accompanying the process of urbanisation, $dC_l(t)$; (b) the export of carbon, $dC_s(t)$; and (c) their interaction, determining the total carbon balance in the exchange between the atmosphere and the urbanised territory, $dC_{tot}(t)$, only for these regions (see Figs. 4.9 and 4.10). Note that since the ET region is characterised by a significant shift only for the sum of living biomass and humus storages, while the NPP-value is nearly constant, the dynamics of $dC_s(t)$ are therefore the same for both models of cities' distribution, hence the second model may be omitted.

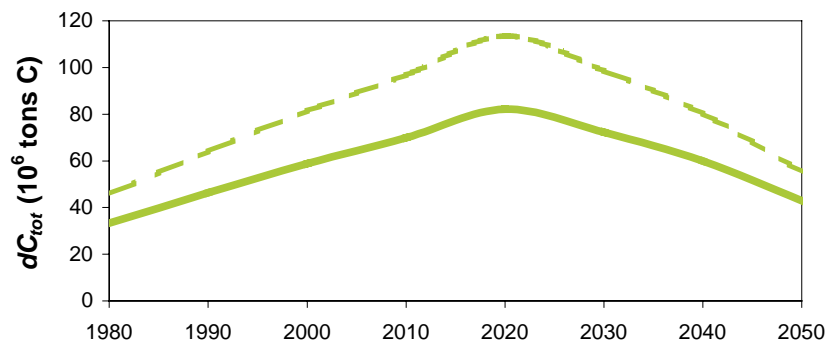
As seen from Eqs. (3)-(5), the annual emission and export of carbon is proportional to the values of the sum of living biomass and humus, and the NPP, respectively. Therefore, any increase in these values with necessity leads to an increase of the corresponding flows.



a)

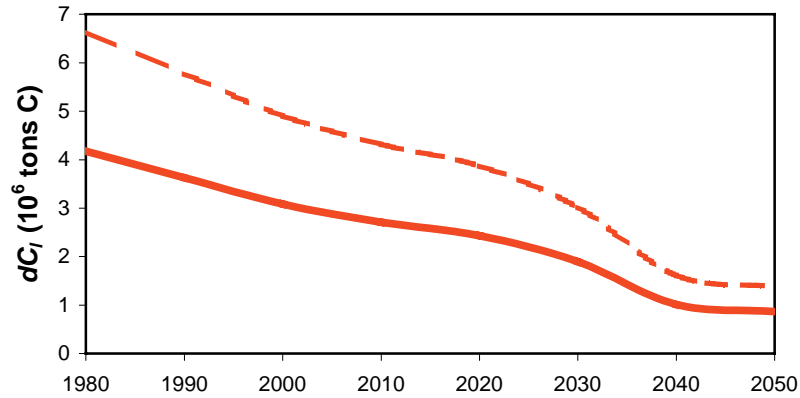


b)

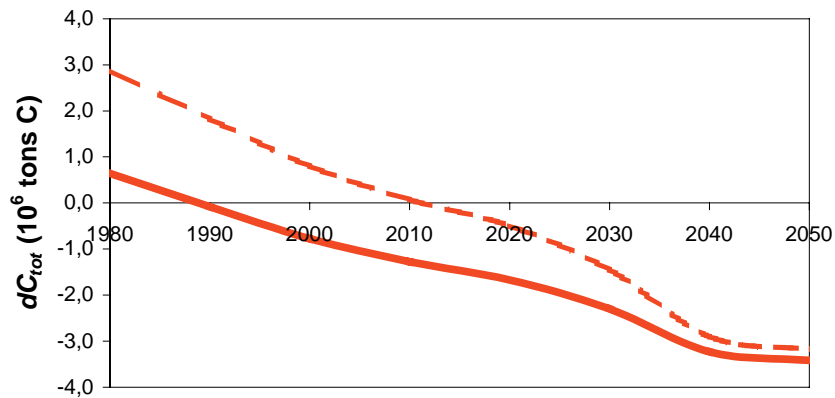


c)

Fig. 4.9. Comparison of the dynamics of carbon flows for the Cn region between 1980-2050: (a) the annual carbon emission as a result of urbanisation; (b) the export of carbon into neighbouring territories; (c) the total carbon balance. Solid line corresponds to *Model I* (random distribution), dotted line to *Model II* (non-random distribution).



a)



b)

Fig. 4.10. Comparison of the dynamics of carbon flows for the ET region between 1980-2050: (a) the annual carbon emission as a result of urbanisation; (b) the total carbon balance. Solid line corresponds to *Model I* (random distribution), dotted line to *Model II* (non-random distribution).

Since direct proportionality takes place, the relative increase in flows is therefore equal to the ratios $(B_u^* + D_u^*) / (B^* + D^*)$ and $(NPP)_u^* / (NPP)^*$. These ratios are equal to 1.44 and 1.65 for the Cn region, and 1.59 and 1.06 for the ET region. Therefore, we can say that in the case of non-random cities' distribution, the emissions from the urbanised territories of the Cn and ET regions increases by 44% and 59%, and the export by 65% and 6%, correspondingly. This is shown in Figs. 4.9a,b and 4.10a. As to the total balance, here there is not such a simple dependence. While the general tendency of a shift towards a "source" side is observed (see Figs. 4.9c and 4.10c), it however manifests itself differently.

If in the Cn region the shift to a “source” side is simply the result of an increase in the source power, then in the ET region, the moment when the “source” functional type of urban territory is switched to the “sink” one is shifted to the future from 1990 to 2010.

At last, it is necessary to say a few words about the world dynamics of carbon flows. In the case of non-random cities’ distribution, the emission from the urbanised territories of the whole world increases by 20%, and the export by 18%. Maximum emission rates will be attained in 2020, and are equal to 269 mtC. The total carbon balance is shown in Fig.4.11. One can see that the world urbanised territories are working as a “source” of carbon for both models of cities’ distribution.

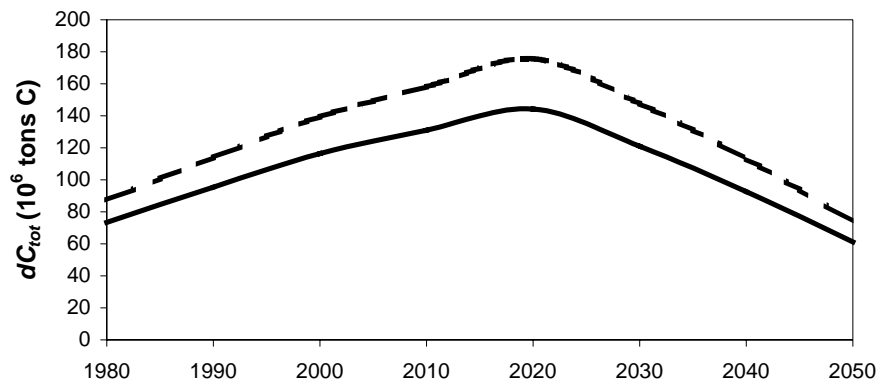


Fig. 4.11. Comparison of the world dynamics of the total carbon balance. Solid line corresponds to *Model I* (random distribution), dotted line – to *Model II* (non-random distribution).

However, in the case of non-random distribution, the power of the source is greater in comparison with the random distribution by 19% at the beginning and end of the time interval, and by 22% in 2020, when both values attain their maximum, which for the non-random distribution is 176 MtC.

Finally, we can state that the non-random distribution (*Model II*) amplifies all estimations. Therefore, if we wish to obtain maximal estimations, we must use *Model II* (we shall indeed do this in the next section, where the Γ -model is applied).

4.8. Losses of carbon as a result of urbanisation, export of carbon into neighbouring territories, and the total carbon balance in urbanised areas. II. Γ -model.

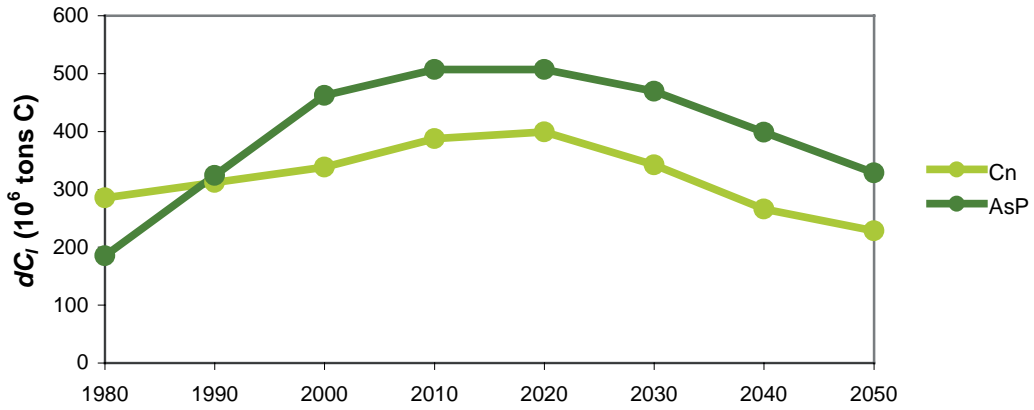
In this section, we will estimate the dynamics of all three flows (emission, export and the total balance) by using data describing the dynamics of an urbanized area obtained by means of the Γ -model (Part 3, Table 3.6) and applying the model of non-random cities distribution (*Model II*). The latter means that we have to replace the values of NPP^* and $(B^* + D^*)$ from Table 4.5 (in Eqs. (3) - (5)) by the values of NPP_u^* and $B_u^* + D_u^*$ from Table 4.7. Results of these calculations are represented in Table 4.9 and Figs. 4.12, 4.13, and 4.14, where the annual carbon losses due to land conversion accompanying the process of urbanisation, $dC_l(t)$, the annual export of carbon, $dC_s(t)$, and a result of their interaction, determining the total carbon balance in the exchange between the atmosphere and urbanised territory, $dC_{tot}(t)$, are represented.

The general impression is that the qualitative dynamic tendencies of these values are similar to those obtained by the regression model. However, there are certain differences. Firstly, the absolute values of the flows in the Γ -model are higher by an order of magnitude than in the regression model. Secondly, the graphs that describe the dynamics of emission, Fig. 4.12, and the total carbon balance, Fig. 4.14, in the case of Γ -model are less smooth than they are for the regression model.

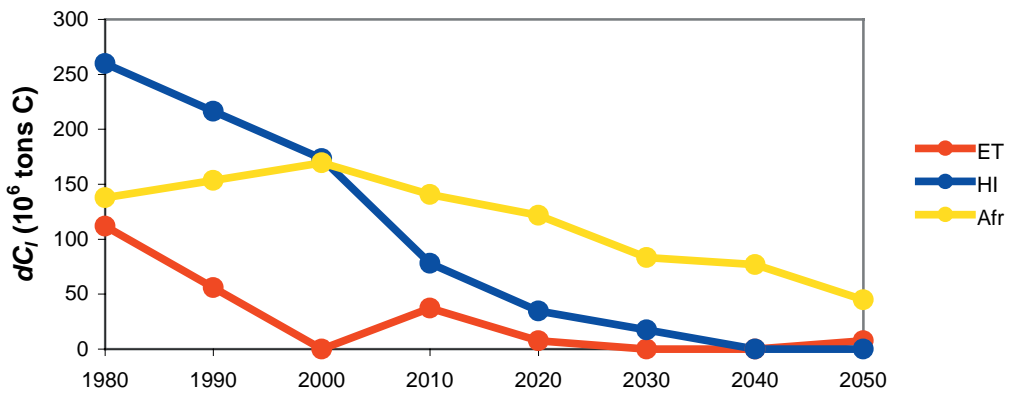
The point is that the values of urban area, obtained by the Γ -model, are functionally independent, that is for different moments of time, they are calculated independently from each other. Their time correlation is manifested only through empirical values (observed or predicted) of the total and urban populations, whereas in the regression model any two values of urban area are connected by the equation of regression.

Table 4.9. Regional carbon balance of urbanised territories (10^6 tonsC per year). Γ -model

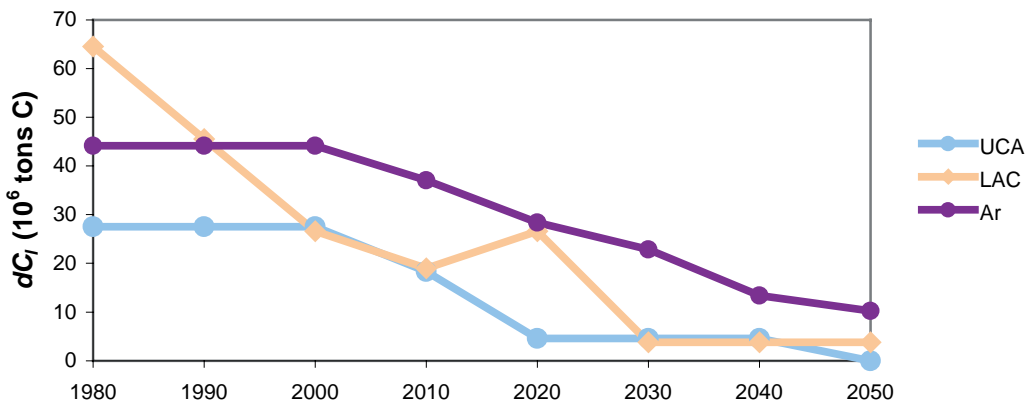
		Year							
Region		1980	1990	2000	2010	2020	2030	2040	2050
Afr	dC_l	138	154	170	141	122	83.2	76.8	44.8
	dC_s	7.93	13.1	18.9	23.7	27.8	30.6	33.2	34.8
	dC_{tot}	130	140	151	117	93.8	52.6	43.6	10.1
Ar	dC_l	44.1	44.1	44.1	37.0	28.4	22.9	13.4	10.2
	dC_s	3.57	5.22	6.87	8.25	9.31	10.2	10.7	11.0
	dC_{tot}	40.6	38.9	37.3	28.8	19.1	12.7	2.73	0.80
Cn	dC_l	285	312	338	388	399	342	266	228
	dC_s	48.8	61.6	75.5	91.5	108	122	133	142
	dC_{tot}	236	250	263	296	291	220	133	85
AsP	dC_l	185	324	462	507	507	469	399	329
	dC_s	32.9	43.9	59.5	76.7	93.9	110	123	135
	dC_{tot}	153	280	403	430	413	360	276	194
LAC	dC_l	64.5	45.6	26.6	19.0	26.6	3.80	3.80	3.80
	dC_s	3.61	4.42	4.88	5.22	5.69	5.75	5.82	5.89
	dC_{tot}	60.9	41.1	21.7	13.8	20.9	1.96	2.02	2.09
ET	dC_l	112	55.9	0.00	37.2	7.45	0.00	0.00	7.45
	dC_s	22.8	24.6	24.6	25.8	26.0	25.8	25.8	26
	dC_{tot}	88.9	31.3	-24.6	11.5	-18.6	-25.8	-25.8	-18.6
HI	dC_l	260	216	173	77.9	34.6	17.3	0.00	0.00
	dC_s	112	120	127	130	131	131	130	129
	dC_{tot}	148	96.2	46.5	-51.7	-96.3	-114	-130	-129
UCA	dC_l	27.5	27.5	27.5	18.4	4.59	4.59	4.59	0.00
	dC_s	17.2	18.6	19.9	20.9	21.1	21.3	21.6	21.3
	dC_{tot}	10.3	8.9	7.57	-2.52	-16.51	-16.74	-17.0	-21.3
World	dC_l	1116	1179	1242	1225	1129	943	764	623
	dC_s	249	292	337	382	423	457	484	505
	dC_{tot}	867	887	905	843	707	486	280	118



a)



b)



c)

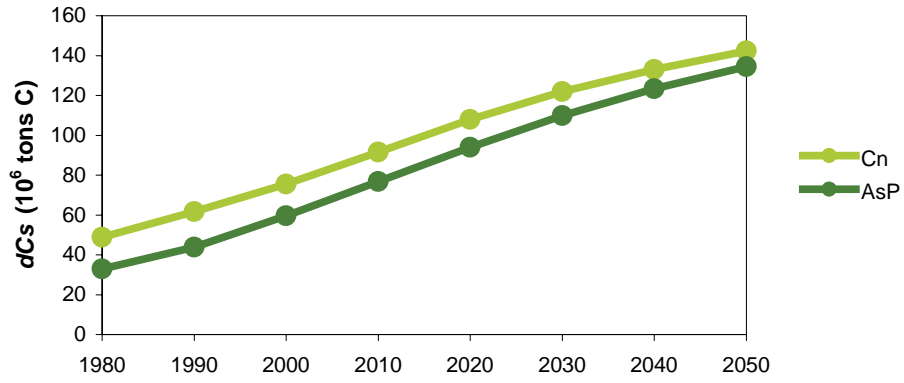
Fig. 4.12. Annual carbon emission as a result of urbanisation in 1980-2050 (Γ -model and non-random cities distribution). Regions: a) Cn and AsP, b) ET, HI and Afr, c) UCA, LAC and Ar.

As we can see in Fig. 4.12, emissions almost monotonously decrease in the Ar, HI, UCA, LAC, and ET regions. This is a result of “saturation” in the process of cities’ growth, that occurred apparently before the 1980’s-1990’s. Although in the two latter regions the monotonicity is violated. As for the LAC region, this violation (a jump during the 2020s) is caused by a sharp acceleration and an equally sharp deceleration in the growth of the total and urban populations between 2010-2030. As for the ET region, the violation of monotonicity is a result of the sharp deceleration of the cities growth between 1990 – 2000 due to the general socio-economic processes connected with the downfall of the USSR.

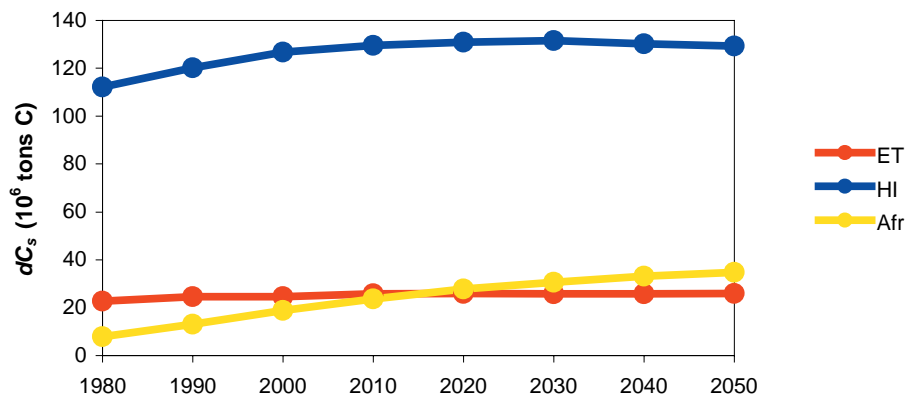
If we now compare both dynamics of emission (described by the regression and Γ -model) in the Afr, Ar, UCA, and HI regions, we see that a short period of increase in the emissions (1980-2010) in the regression model is replaced by a period of stagnation in the Γ -model. Only the Afr region shows emission growth in both models. In other words, the difference between the two models in relation to these regions is as follows: the regression model states that saturation occurs today, or has occurred recently, while the Γ -model states that saturation had already occurred before the 1980s (although, possibly, for different reasons).

The qualitative dynamics of carbon emission in the Cn and AsP regions are similar in both models, the single difference being that in the Γ -model, saturation occurs earlier and is “softer” than in the regression one. There is one more difference: if in the regression model the maximal emission occurs in the Cn region, then in the Γ -model, on the contrary, the maximal emission are from the AsP region.

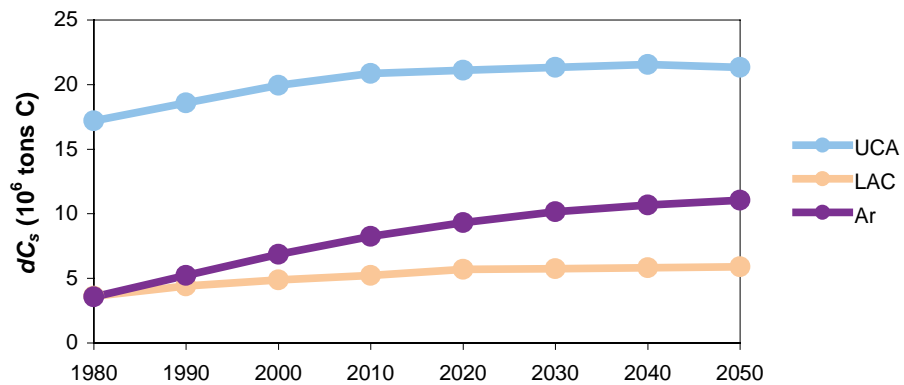
The qualitative difference between the dynamics of export flow between the models is insignificant but is present. For instance, in the regression model, the HI region maintains its leading position in the annual export of carbon only up to the year 2015, while in the Γ -model, this “critical point” is shifted to the year 2040, when the leaders become the Cn and AsP regions (see Fig. 4.13). The other four regions (Afr, ET, LAC and Ar) demonstrate similar dynamics of carbon export in both models. Moreover, in the Γ -model, the amounts of exported carbon are minimal in the same regions.



a)



b)



c)

Fig. 4.13. Annual export of organic carbon out of “urbanised” ecosystems into neighbouring territories between 1980-2050 (Γ -model and non-random cities distribution). Regions: a) Cn and AsP, b) ET, HI and Afr, c) UCA, LAC and Ar.

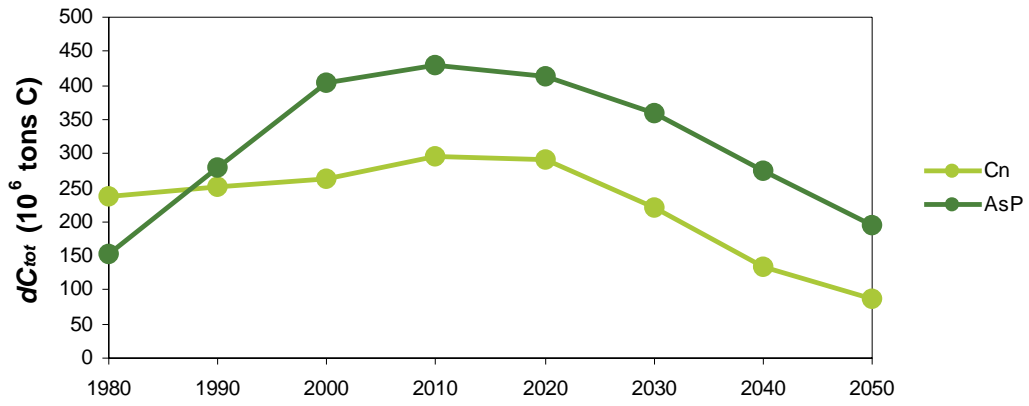
By passing to the dynamics of the total carbon balance of urbanised territories described by the Γ -model (see Fig. 4.14), we can say that the “sink” effect, that is when the urbanised territories of some regions play the role of carbon sinks, is the same as was observed in the regression model results.

The dynamics of the total balance are qualitatively almost similar for both models, nevertheless there are some general differences in the moments of switching between “source” and “sink” states. For instance, in the regression model, the HI region became a “sink” before 1980, and the ET and UCA regions transform into “sinks” in 1990 and 2010.

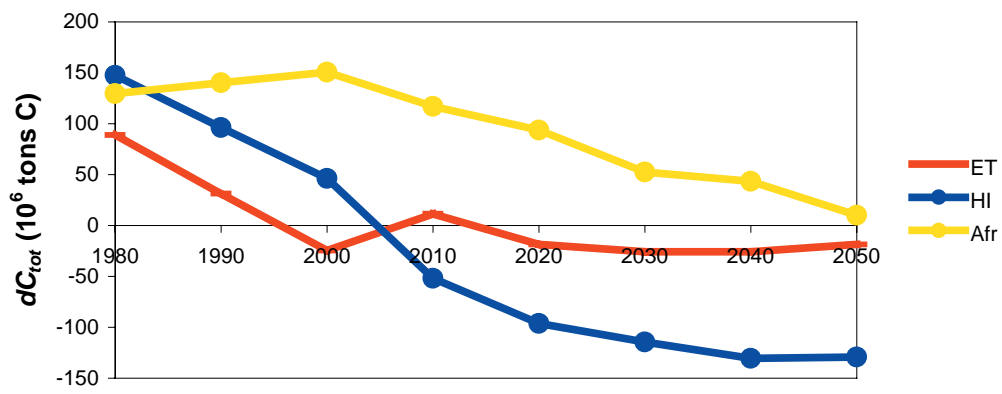
Correspondingly, in the Γ -model, HI and UCA transform into “sinks” in 2005 and, as in the regression model, in 2010, respectively. A special situation appears here with the ET region: because of its specific dynamics, there are two switching points. In 1995 the ET switches from a “sink” to a “source”, then after 2005 it becomes a “sink” again.

The total balance (misbalance) almost monotonously decreases in the LAC, Ar, and Afr regions (in the latter after a very slow ascendance at the end of last century). It is interesting that the misbalance almost vanishes by the year 2050. In the Cn region, the period of fast misbalance growth that is now observed, after a short period of stagnation, will be replaced by an equally fast process of misbalance decrease after 2020. The same decreasing trend is observed also in the AsP region, but only after a long stagnation. In the HI (after the year 2005) and UCA (after the year 2010) we observe the opposite picture with misbalance increasing. Only the ET region manifests a specific picture: the fast increase in misbalance between 1980-1995, then the damped oscillations with stabilisation at the “sink” state, which is very close to a zero misbalance.

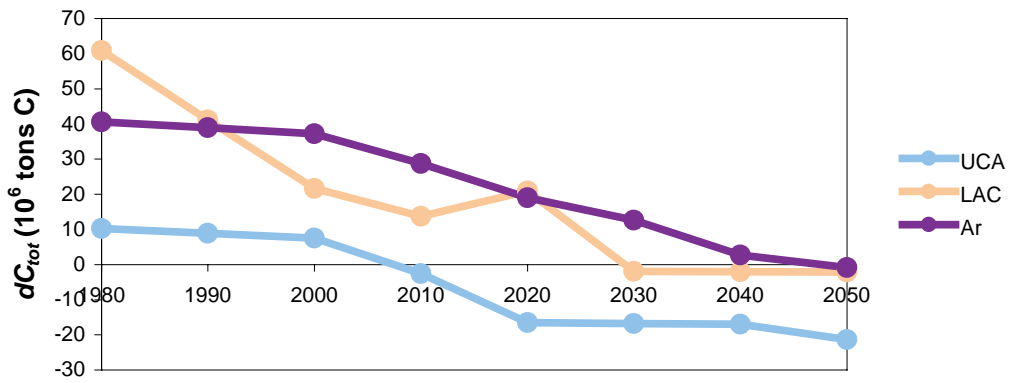
Since the World as a whole is an integrator of all-regional tendencies, then, as we can see in Figs. 4.15-4.17, that the corresponding dynamics of carbon flows appears smoother. What kind of tendencies is therefore observed at the global level?



a)



b)



c)

Fig. 4.14. Total annual balance of natural carbon for regional urbanised territories in 1980 – 2050 (Γ -model and non-random cities distribution). Regions: a) Cn and AsP, b) , ET, HI, and Afr, c) UCA, LAC, and Ar.

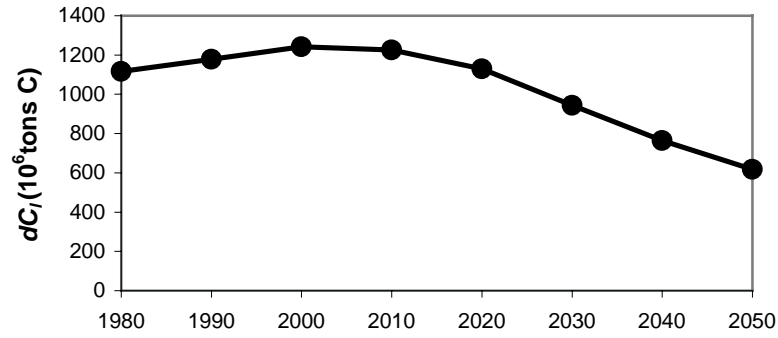


Fig. 4.15. World annual emission of carbon as a result of land conversion during the process of urbanisation between 1980-2050 (Γ -model and non-random cities distribution).

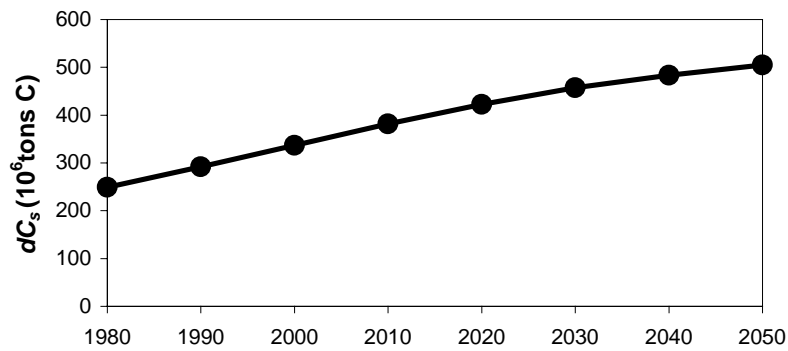


Fig. 4.16. World annual export of organic carbon out of “urbanised” ecosystems into neighboring territories between 1980-2050 (Γ -model and non-random cities distribution).

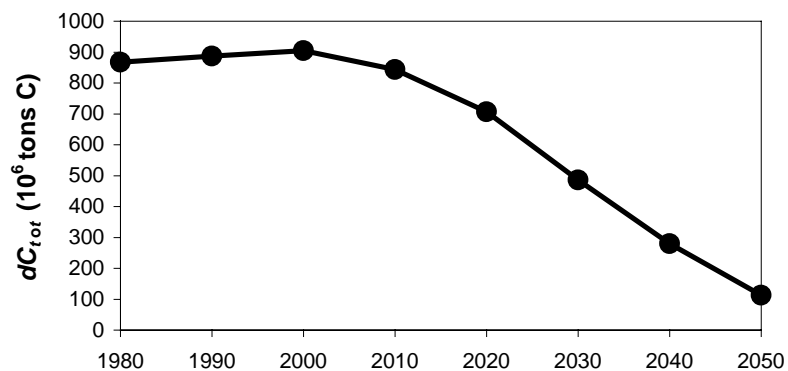


Fig. 4.17. World dynamics of the total carbon of urbanised territories between 1980-2050 (Γ -model and non-random cities distribution).

For the annual emission flow out of the world urbanised territories, we can say that it will slowly increase from 1.12 GtC per year in 1980 up to 1.25 GtC per year in 2005 (1Gt = 10^9 tons), after which an increasingly accelerated decrease starts, such that by the year 2050 emissions will have fallen to 623 MtC. If we compare the emission maximum, 1.25 GtC per year, with the annual emission caused by the process of deforestation, 1.36 GtC per year in 1980 (see Part 2, Table 2.3), then we can say that the role of urbanised territories in the GCC is of a comparable magnitude as the role of deforestation. However, while the latter is commonly a part of the advanced models of the GCC, currently no global model includes the impact of urbanisation on the GCC.

World dynamics of the annual “horizontal” export of carbon out of urbanised territories is very simple: this is an almost linear growth from 249 MtC in 1980 up to 505 MtC in 2050, i.e., during those seventy years export increases two fold (see Fig. 4.16). As already mentioned, the transport power of urbanised territories is comparable to the amount of carbon transported by rivers into the ocean (196-537 MtC per year, Svirezhev et al, 1997).

Finally, the total carbon balance (Fig. 4.17), being almost constant until 2000, then starts decreasing at an almost constant rate. If its maximal value in 2000 is 905 MtC, then by 2050 this value has fallen to 118 MtC, i.e., by almost eight times. By extrapolating this graph into the future, we can say that by the end of the XXI century, the total carbon balance will be equal to zero, and may even be negative!

This means that if at the beginning of the century the world urbanized territories act as “source” of carbon, emitting annually about 1GtC, then the misbalance in the exchange carbon flows between the atmosphere and urbanized territories decreases with time. By the end of the current century, the misbalance will, in fact, fade away or become negative. This means that, in the first case, a system such as urbanized territories passes from a “source” state to a “neutralistic” one, when the exchange flows are fully balanced, and therefore can be excluded from consideration in the GCC. In the second case, when the balance becomes negative, the system begins to take up carbon from the atmosphere, i.e., to become a “sink”. However, it is necessary to note that the formation of “sinks” in urbanised territories is accompanied by the appearance of “sources” in other locations. In general,

this situation is functionally similar to the case when rivers transport organic carbon to other locations, where it is then decomposed and emitted into the atmosphere.

Note that we must keep in mind that in this section, we dealt with maximal estimations.

5 CONCLUSIONS

In order to estimate the role of urbanised territories in the global balance of carbon, we have to calculate the total balance of carbon between the atmosphere and urbanised territories. The balance is the sum of two flows. The first is a consequence of the loss of organic carbon, caused by the decomposition of living biomass and dead organic matter as a result of land conversion and its emission in the form of CO₂ into the atmosphere. The second flow is a “through-pumping” of the atmosphere carbon through “urbanised” ecosystems into neighbouring natural ecosystems along the chain “atmosphere → vegetation → dead organic matter → export.

An urbanised territory can either take up carbon from the atmosphere or emit it, in both cases playing the role of either carbon sink or carbon source. “Urbanistic” land conversion shifts the total balance towards a “sink” state. It is obvious that when the growth of urbanised territories in a given region is faster, then the shift towards a “source” state is greater. This is most distinctly seen in the AsP, Cn and Afr regions at the initial stage of their “urbanistic” evolution. The “through-pumping” of atmospheric carbon through an “urbanised” ecosystem shifts its state to a “sink” one. In this situation, where the green area is larger, the shift towards a “sink” state is greater.

These estimations are based on two models. In the first model, which gives minimal estimates, a regression equation relating city area and population is used, as well as an assumption of random spatial distribution of cities. In the second model, which gives maximal estimates, the so-called Γ -approach is used, based on the assumption that the distribution of populated areas with respect to population density is a Γ -distribution, while assuming a non-random spatial distribution of cities.

The first model (minimal estimation) gives the following results. Carbon emissions monotonously decrease for the LAC and ET regions. This could be a result of the “saturation” in the cities’ growth between 1980-1990s. As for the ET region, the sharp deceleration of city growth was caused by the collapse of the USSR. In the Afr, Ar, UCA, and HI regions, saturation will be attained between the years 2000 – 2010; in the Cn and AsP regions, saturation will be attained later, between the years 2020 – 2030. After these

“turning points”, the emissions from all regions will begin to drop, corresponding in general to the deceleration of urbanisation.

The world annual emissions will attain a maximum of 205 MtC between ca. 2020-2030. Emissions will then slowly decrease, so that by the year 2050, they will equal ca. 150 MtC. The maximum contributions to world emissions are given by two regions: Cn and AsP.

At the first stage (up to the year 2015), the maximum amount of organic carbon is exported by the HI region. However, after this the export rate from the Cn region becomes the highest. Nevertheless, the AsP export, which is growing almost as fast as the Cn rate, does not exceed the HI rate till 2050. Four regions (Afr, ET, LAC and Ar) exhibit almost the same dynamics of carbon export, although the amounts of exported carbon are minimal in these regions.

Regarding the world dynamics of the annual export of carbon by urbanised territories, we observe its monotonous, almost linear growth by almost three times, from 24 MtC up to 66 MtC. This effect is qualitatively similar to the transportation of carbon by rivers, but is quantitatively lower by one order of magnitude (for instance, the annual export of carbon by rivers into the ocean is 196 – 537 Mt).

When we estimate the total atmospheric carbon balance of the world's urbanised territory, we find that the urbanised territories of the ET, UCA (after the year 2010), and especially the HI regions play the role of carbon sinks. Moreover, even the other urbanised territories that play the role of sources (Cn, AsP, Afr and Ar regions), sooner or later manifest a tendency to decrease the misbalance of carbon between its emission into the atmosphere and its export into the neighbouring territories (the misbalance is equal to the total balance). The single exception is the LAC region, where the misbalance already decreases, beginning from 1980. In the Ar region, the decrease of the misbalance will be observed after 2015, when the stagnation in the dynamics of the total balance, observed at the present time, will have ended. In the Afr region, stagnation is observed since 2000, and it will also be completed by 2015. In the Cn and AsP regions, the period of fast misbalance growth that is now observed, after a very short period of stagnation will be replaced by an equally fast process of misbalance decrease after 2030. In the ET (after the year 1990), HI (after the year 2000) and UCA (after the year 2010), we

observe the opposite picture, with the misbalance increasing. The world urbanised territories work as a source of carbon, where its power increases until the year 2020, at which time the maximal amount of carbon, 160 MtC per year, is emitted into the atmosphere as a result of urbanisation.

Fortunately, in accordance with our estimations, the process of urbanisation is inhibited between 2020-2030, and by the middle of the century, the growth of urbanised areas will almost stop. Hence, the total emission of natural carbon at that stage will stabilise at the level of the 1980s (80 MtC per year).

The second model (maximal estimation) gives the following results. Despite the qualitative dynamic tendencies of these values to be similar to those obtained by the first model, the absolute values of the flows in this model are higher by an order of magnitude.

If we now compare both dynamics of emission in the Afr, Ar, UCA, and HI regions, we see that a short period of increase in the emissions (1980-2010) in the first model is replaced by a period of stagnation in the second model. Only the Afr region shows emission growth in both models. In other words, the difference between the two models in relation to these regions is as follows: the first model states that saturation occurs today, or has occurred recently, while the second states that saturation has already occurred before the 1980s. The qualitative dynamics of carbon emission in the Cn and AsP regions are similar in both models, the single difference being that in the second model, saturation occurs earlier and is “softer” than in the first one. There is one more difference: if in the first model the maximal emission occurs in the Cn region, then in the second model, the maximal emissions are from the AsP region.

The qualitative difference between the dynamics of export flow between the models is insignificant but is nonetheless present. For instance, in the first model, the HI region maintains its leading position in the annual export of carbon only up until the year 2015, while in the second model, this “critical point” is shifted to the year 2040, when the leaders become the Cn and AsP regions. Four other regions (Afr, ET, LAC and Ar) demonstrate similar dynamics of carbon export in both models. Moreover, in the second model, the amounts of exported carbon are minimal in the same regions.

The dynamics of the total balance are qualitatively almost similar for both models, nevertheless there are some general differences in the timing of switching between “source” and “sink” states. In the first model, the HI region became a “sink” before 1980, and the ET and UCA regions transform into “sinks” in 1990 and 2010, respectively. In the second model, HI and UCA transform into “sinks” in 2005 and, as in the first model, 2010, respectively. A special situation appears here with the ET region: because of its specific dynamics, there are two switching points. In 1995 the ET switches from a “sink” to a “source”, then after 2005 it becomes a “sink” again.

The total balance (misbalance) almost monotonously decreases in the LAC, Ar, and Afr regions (in the latter after a very slow ascendance at the end of last century), with the misbalance almost vanishing by the year 2050. In the Cn region, the period of fast misbalance growth that is now observed, after a short period of stagnation, will be replaced by an equally fast process of misbalance decrease after 2020. The same decreasing trend is observed also in the AsP region, but only after a long stagnation. In the HI (after the year 2005) and UCA (after the year 2010) we observe the opposite picture with misbalance increasing. Only the ET region manifests a specific picture: first, the fast increase in misbalance between 1980-1995, followed by the damped oscillations with stabilisation at the “sink” state, which is very close to a zero misbalance.

The world annual emission of carbon as a result of land conversion in the process of urbanisation increased from 1.12 GtC per year in 1980 up to 1.25 GtC per year in 2005 ($1\text{Gt} = 10^9$ tons), after which it will begin to decrease, such that by the year 2050, emissions will have decreased to 623 MtC. If we compare the emission maximum, 1.25 GtC per year, with the annual emission caused by the process of deforestation, 1.36 GtC per year in 1980, then we can say that the role of urbanised territories in the GCC is of a comparable magnitude as the role of deforestation.

World dynamics of the annual “horizontal” export of carbon out of urbanised territories is very simple: this is an almost linear growth from 249 MtC in 1980 up to 505 MtC in 2050, i.e., during those seventy years export increases two fold. The transport power of urbanised territories is therefore comparable to the amount of carbon transported by rivers into the ocean (196-537 MtC per year).

Finally, the total carbon balance, being almost constant until 2000, starts to decrease afterwards at an almost constant rate. If its maximal value in 2000 was 905 MtC, then by 2050 this value has fallen to 118 MtC, i.e., by almost eight times. By extrapolating this graph into the future, we can say that by the end of the XXI century, the total carbon balance will be equal to zero, and may even be negative! This means that if at the beginning of the century the world urbanized territories act as a “source” of carbon, emitting annually about 1 GtC, then the misbalance in the exchange carbon flows between the atmosphere and urbanized territories will decrease with time. By the end of the current century, the misbalance will, in fact, fade away or become negative. This means that, in the first case, a system such as an urbanized territory will pass from being in a “source” state, to a “neutralistic” one, when the exchange flows are fully balanced and therefore can be excluded from consideration in the GCC. In the second case, when the balance becomes negative, the system begins to take up carbon from the atmosphere, i.e., to become a “sink”. However, it is necessary to note that the formation of “sinks” in urbanised territory is accompanied by the appearance of “sources” in other locations. In general, this situation is functionally similar to the case when rivers transport organic carbon to other locations, where it is then decomposed and emitted into the atmosphere.

REFERENCES

- Alberti, M., Waddell, P., 2000. An integrated urban development and ecological simulation model. *Integrated Assessment*, 1: 215-227.
- Allen, P.M., Sanglier M., 1979. A dynamic model of urban growth: II. *J. Social Biological Structures*. 2: 269-278.
- Alonso, W. , 1964. *Location and land use*. Harvard University Press, Cambridge, MA.
- Antrop, M., 2000. Changing patterns in the urbanized countryside of Western Europe. *Landscape Ecology* 15: 257-270.
- Bazilevich, N, I., 1979. Biogeochemistry of the Earth and functional models of exchange processes in natural ecosystems. In: *Modern Concepts and Problem of Biogeochemistry (Proceedings of the Biogeochemical Laboratory, vol. 17)*, Nauka, Moscow: 56-73.
- Bazilevich, N, I., Grebentshikov, O. S., Tishkov, A. A., 1986. *Geographic regularities of ecosystems structure an function*. Nauka, Moscow: 297 pp.
- Birdsey, R.A., 1996. Carbon storage for major forest types and regions in the conterminous US. In: Sampson, R.L., Hair, D. (Eds.), *Forest and Global Change, Vol. 2: Forest Management Opportunities for Mitigating Carbon Emission*. American Forests, Washington, DC: 1-26.
- Bolin, B. Degens, E. T., Duvigneaud, P., Kempe, S., 1979. The global biogeochemical carbon cycle. In: *The Global Carbon Cycle (Eds: Bolin, B. Degens, E. T., Kempe, S., Ketner, H.)*, SCOPE 13, Wiley, Chichester: 1-56.

- Botkin, D. B., Breveridge, C. E., 1997. Cities as environments. *Urban Ecosystems*, 1: 3-19.
- Bramryd, T., 1980. Fluxes and accumulation of organic carbon in urban ecosystems on a global scale. *Urban Ecology. The Second European Symposium. Berlin, 8-12 September*: 3-12.
- Brundtland's World Commission on Environment and Development, 1987. *Our common future*. Oxford, New York.
- Cohen, J., 1995. *How many people can the Earth support?*, New York: W. W. Norton: 532 pp.
- Donald, J., 1999. *Imagining the Modern city*. University of Minnesota Press, Minneapolis.
- Gordon, P., Wong, H. L., 1985. The costs of urban sprawl: some new evidence. *Environment and planning , A* 27: 661-666.
- Gregg, J. W., Jones, C. G., Dawson, T. E., 2003. Urbanisation effects on tree growth in the vicinity of New York City. *Nature*, 424: 183-187.
- HABITAT, 1996. *Global Report of Human Settlements*. Oxford University Press, Oxford: 332pp.
- Hauser, J. A., 1992. Population, ecology and the new economics: Guidelines for a steady-state economy, *Futures*, v. 24, 4: 364-387.

- Heinke, Gary W., 1997. The challenge of urban growth and sustainable development for Asian cities in the 21st century. *Environmental monitoring and assessment* 44: 155-171.
- Houtum, van H., Ernste, H., 2001. Re-imagining spaces of (in)difference: Contextualising and reflecting on the intertwining of cities across borders. *GeoJournal* 54: pp. 101-105.
- IPPC, 2000. Emissions Scenarios. Special Report on Emission Scenarios (SRES), Oxford University Press, Oxford: 691pp.
- Kalnay, E., Ming Cai, 2003. Impact of urbanisation and land–use change on climate. *Nature*. Vol. 423: 528-531.
- Kendall, M. G., Stuart, A., 1958. *The Advanced Theory of Statistics*, v. 1.2. Academic Press, New York.
- Krapivin, V. F., Svirezhev, Yu. M., Tarko, A. M., 1982. Mathematical modelling of the global biosphere processes. Nauka, Moscow: 272.
- Landis, J. D., Zhang, M., 1967. The Second Generation of the California urban Futures Model, Model Logic and Theory. Part I.
- Landsberg, H. E., 1981. *The Urban Climate*. Academic Press, New York.
- Leontieff, W. , 1967. *Input-Output Economics*. Oxford University Press, New York.
- Lindemann, R. I., 1942. The trophic-dynamic aspect of ecology. *Ecology*, 23: 399-418.

- Lo, C. P., Quattrochi, D. A., et al., 1997. Application of high-resolution thermal infrared remote sensing and GIS to assess the urban heat island effect. *Int. J. Remote Sens.* 18 (2): 287-304.
- Lopreato, 1984. *Human Nature and Biocultural Evolution*. Unwin Hyman, London.
- Luck, M., Wu, J., 2002. A gradient analysis of urban landscape pattern: a case study from the Phoenix metropolitan region, Arizona, USA. *Landscape Ecology* 17: 327-339.
- Mackett, R. L., 1992. *Micro Simulation Modeling of Travel demand and Location Processes; Testing and further Development*. Report to the Transport and Road Research laboratory. University College London.
- McDonnell, M. J., Pickett, S. T. A., 1990. Ecosystem structure and function along urban-rural gradients: an unexploited opportunity for ecology. *Ecology*, 71(4): 1232-1237
- McFadden, D., 1978. Discrete-choice models of urban development. In: *Spatial Interaction Theory and Planning Models*, eds. A. Larlqvist et al., North Holland Press, Amsterdam: 73-91.
- Miller, G.T., 1988. *Living in the Environment*, 6th ed. Woodswort, Belmont, CA.
- Miller, R.B. and Small, C., 2003. Cities from space: potential applications of remote sensing in urban environmental research and policy. *Environmental Science and Policy*, 6: 129-137.

- Nowak, D.J., 1994. Atmospheric carbon dioxide reduction by Chicago's urban forest. In: McPherson, E.G., Nowak, D.J., Rowntree, R.A. (Eds.). "Chicago's Urban Forest Ecosystem: Results of the Chicago Urban Forest Climate Project. USDA Forest Service General Technical Report NE-186, Radnor, PA: 83-94.
- Nowak, D. J., Crane, D. E., 2000. The urban forest effect (UFORE) model: quantifying urban forest structure and functions. In: Hansen, M., Burk, T. (Eds.), Proceedings: Integrated Tools for Natural Resources Inventories in the 21st Century. IUFRO Conference, August 1998, Boise, ID. General Technical Report NC-212. US Dept. Agr. Forest Service. North Central Research Station, St. Paul, MN: 714-720.
- Nowak, D. J., Crane, D. E., 2002. Carbon storage and sequestration by urban trees in the USA. *Environmental Pollution*, 116: 381-389.
- Odum, E. P., 1971. *Fundamentals of ecology* (3rd ed.). Saunders College Publishing, Philadelphia-New York-Chicago-Montreal-Toronto-London, 564pp.
- Odum, E. P., 1983. *Basic ecology*. Saunders College Publishing, Philadelphia-New York-Chicago-Montreal-Toronto-London, 376pp.
- O'Meara, M., 1999. *Reinventing Cities for People and the Planet*. Worldwatch, Washington DC.
- Pimentel, D., Hurd, L. E., Bellotti, A. C., 1973. Food Production and energetic crisis. *Science*, 182: 443-449.

- Prentice, I.C., G.D. Farquhar, M.J.R. Fasham, M.L. Goulden, M. Heimann, V.J. Jaramillo, H.S. Khashgi, C. Le Quéré, R.J. Scholes, and D.W.R. Wallace, 2001. The carbon cycle and atmospheric carbon dioxide. In: Climate Change 2001: The Scientific Basis. Contribution of Working Group I to the Third Assessment Report of the Intergovernmental Panel on Climate Change, 1st ed. J.T. Houghton, Y. Ding, D.J. Griggs, M. Noguer, P.J. van der Linden, X. Dai, K. Maskell, and C.A. Johnson (Eds.), Cambridge University Press, Cambridge, 185-225.
- Rees, W.E., 1997. Urban ecosystems: the human dimension. *Urban Ecosystems*, 1: 63-75.
- Schweitzer, F. (ed.), 1997. *Self-Organization of Complex Structures*. Gordon and Breach, Amsterdam, The Netherlands.
- Smil, V., 1991. *General energetics: energy in the biosphere and civilization*. A Wiley Interscience Publication, New York – Chichester – Toronto - Singapur: 369pp.
- Small, C., Cohen, J.E., 1999. Continental physiography, climate and the global distribution of human population. In: *Proceedings of the International Symposium on Digital Earth*. Chinese Academy of Science, Beijing: 965-971.
- Solecki, W. D., Rosenzweig, C., 2001. *Biodiversity and the City: A Case Study of the New York Metropolitan Region*. Unpublished paper, cited in Miller and Small (2003).
- Soloviev, S., 1959. *The history of the Russian state, v. 1. Social and Economic Publishing, Moscow*.

- Space Biology and Medicine, v. II (2), 1994. Life Supporting Systems (part 2).
Genin, A. M., Sulzmann, F. M. (Eds.). Nauka, Moscow and American
Institute of Aeronautics and Astronautics, Washington, DC.
- Stempell, D., 1985. Weltbevölkerung 2000. Urania-Verlag, Leipzig-Jena-
Berlin.
- Stuart, A., Ord, J. K., 1987. Kendall's Advanced Theory of Statistics, 5th ed.,
v. 1, Griffin and Co., London: 604 pp.
- Svirezhev, Yu. M., 2002. Simple spatially distributed model of the global
carbon cycle and its dynamic properties. Ecol. Modelling, 155: 53-69.
- Svirezhev, Yu. M. et al. 1985. Ecological and Demographic Consequences of
a Nuclear War. The USSR Acad. Sci., Computer Center, Moscow:
355pp.
- Svirezhev, Yu. M. et al. 1997. New version of the Moscow Global Biosphere
Model. PIK Core Project BBM/Gaia. Final scientific report. Potsdam-
Institut für Klimafolgenforschung, Potsdam – Moscow: 834pp.
- Tobler, W., 1975. City Sizes, Morphology, and Interaction, Internal Report
WR-75-18, IIASA, Laxenburg, Austria.
- Tobler, W., 1979. Cellular geography. In: Gale S. and Olson G.D. (eds),
Philosophy in Geography. Reidel Publishing Company, Dordrecht, The
Netherlands: 376-386.
- Tobler, W., Deichmann, U., Gottsegen, J., and K. Malloy, 1997. World
Population in a Grid of Spherical Quadrilaterals. Int. J. Population
Geography, 3: 203-225.

- UNESCO, 1973. World Urbanization Perspectives. MAB report series, n° 1. Paris.
- United Nations (UN), 1992. Long-range world population projection. Two centuries of population growth 1950-2050. United Nations, New York.
- United Nations (UN), 1999. Prospects for Urbanization-1999 Revision. United Nations (ST/ESA/SER.A/166), Sales No. E.97.XIII.3.
- United Nations (UN), 2000. Demographic Yearbook. United Nations, New York.
- United Nations (UN), 2001. The state of the World Cities 2001. Centre for Human Settlements, UNCHS: 121pp.
- Vaughn, R., 1987. Urban Spatial Traffic Patterns, Pion, London.
- Waddel, P. A., 2000. A behavioral simulation model for metropolitan policy analysis and planning; residential location and housing market components of UbanSim. Environment and planning B: Planning and Design, 27: 247-263.
- Wegener, M., 1994. Operational urban models; state of the art. Journal of the American Planning Association, 60: 17-30.
- White, R., Engelen G., 1993. Cellular automata and fractal urban form : a cellular modelling approach to the evolution of urban land-use patterns. Environ. Planning, A 25: 1175-1199.
- White, R., Engelen, G., 1997. Cellular automata as the basis of integrated dynamic modelling. Environment and Planning, B 24: 235-246.

Whittaker, R. H., Likens, G. E., 1973. Primary production: the biosphere and man. *Human Ecology*, 1 (1): 357-368.

Wilson, A. G., 1976. Catastrophe theory and urban modelling: An application to modal choice. *Environ. Planning, A* 8: 351-356.

Wilson, A. G., 1981. *Catastrophe Theory and Bifurcation*. University of California Press, Berkeley, California, USA.

Wingo, L., 1961. *Transportation and Urban Land*. Johns Hopkins University Press, Baltimore, MD.

Wu, F., Loucks, O. L., 1995. From balance of nature to hierarchical patch dynamics: a paradigm shift in ecology. *Quarterly Review of Biology*, 70:439-466.

Appendix I. Demography of Urbanisation

A1.1. Introduction.

The leading processes determining urbanisation are demographic ones, i.e., the growth of national and regional populations, and the dynamics of their fractions that populate the urbanised territories. On the one hand, such a variable as the area of an urbanised territory is very sensitive with respect to demographic parameters. On the other, the demographic statistics and prognoses are very uncertain. Therefore, the collection and assessment of reliable demographic data was our primary problem. The situation is made much more complicated by the fact that the necessary data is contained in different sources, the accuracy of which was often very different. Therefore, we were compelled to join two demographic sources: from the first (UN, 2001: World of cities. <http://www.unchs.org/istanbul+5/statereport.htm>) we took the dynamics of the percent of urbanised populations for the six UN regions since 1980 until 2020 and estimated the percentages for the period 2030-2050 by non-linear extrapolation.

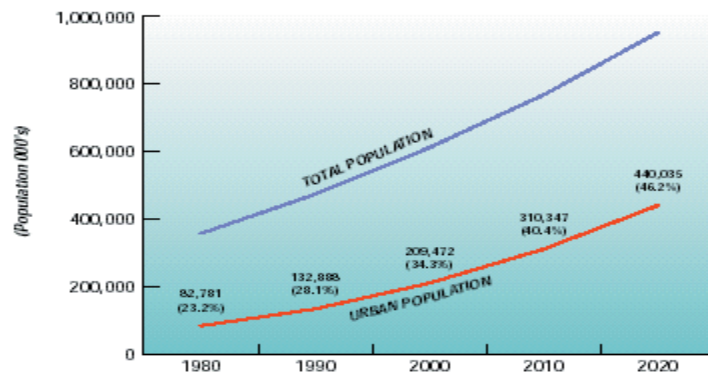
The regional demographic model, developed by Svirezhev et al. (1997), operates within the interval 1980-2050, and the resolution is at the national level. We believe that this model gives accurate prognoses for the dynamics of national populations, and we used these prognoses in our calculations of urban areas.

The selected data from these sources are represented in the next two sections.

A1.2. UN, 2001. World of cities.

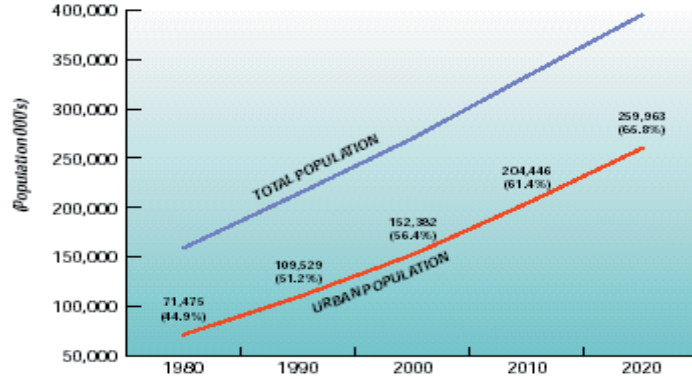
In the following six figures, we compare the dynamics of the total and urban populations for the interval 1980-2020 for the six UN regions.

**Africa Sub Sahara Region
Population: 1980-2020**



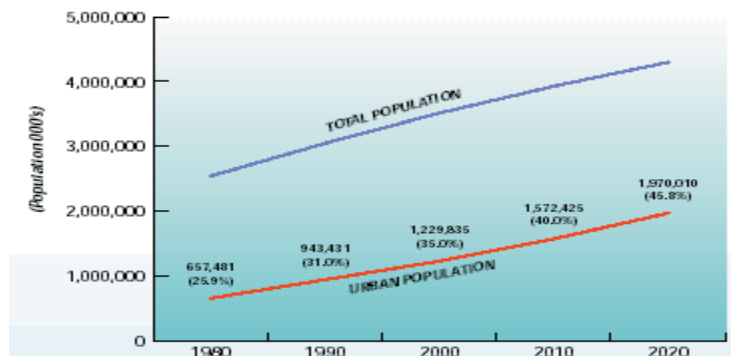
Source: UN, World Urbanization Prospects, 1999

**Arab States Region
Population: 1980-2020**



Source: UN, World Urbanization Prospects, 1999

**Asia and Pacific Region
Population: 1980-2020**



Source: UN, World Urbanization Prospects, 1999

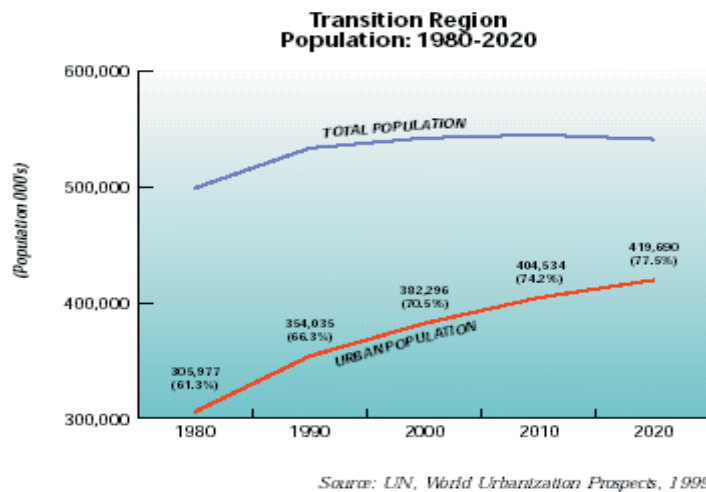
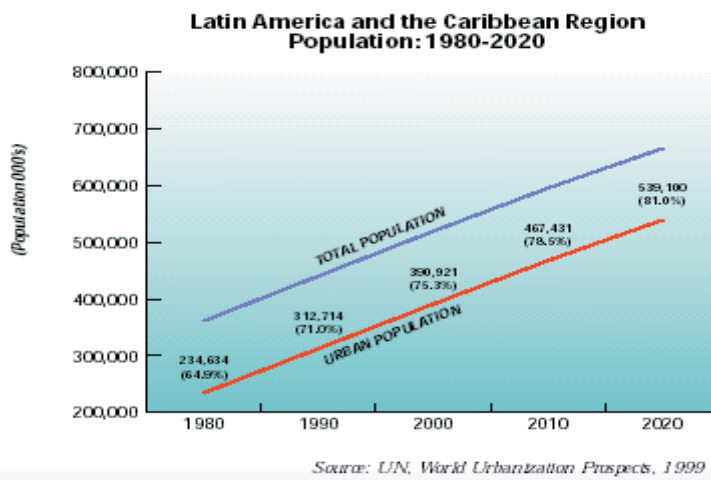
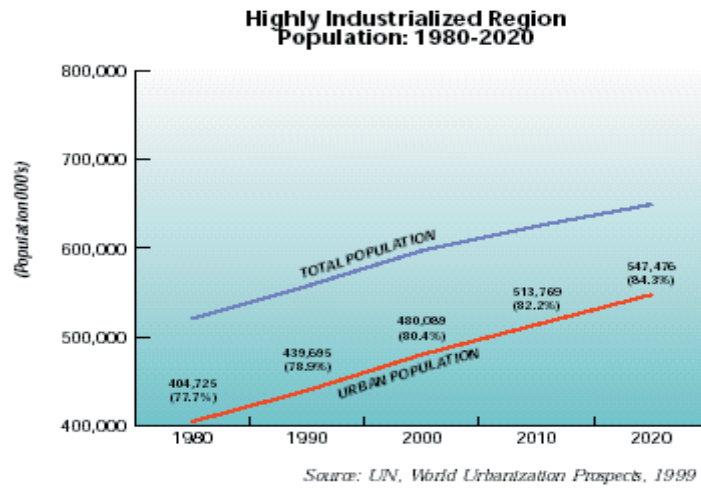


Fig. A1.1. The comparative dynamics of the total and urban populations (1980-2020).

These data are also presented in Table A1.1.

Table A1.1. Total and urban regional population growth projections based on the UN prognoses (in millions of persons).

Year		1980	1990	2000	2010	2020
Region						
Afr	N_{tot}	357	473	12.89	12.78	12.15
	N_u	82.9	133	209	310	440
	k_u (%)	23.2	28.1	34.3	40.4	46.2
Ar	N_{tot}	159	214	270	333	395
	N_u	71.5	110	152	204	260
	k_u (%)	44.9	51.2	56.4	61.4	65.8
AsP	N_{tot}	2 608	3 043	3 514	3 931	4 301
	N_u	675	943	1 230	1 572	1 970
	k_u (%)	25.9	31.0	35.0	40.0	45.8
LAC	N_{tot}	362	440	519	595	666
	N_u	235	313	391	467	539
	k_u (%)	64.9	71.0	75.3	78.5	81.0
ET	N_{tot}	499	534	542	545	542
	N_u	306	354	382	405	420
	k_u (%)	61.3	66.3	70.5	74.2	77.5
HI	N_{tot}	521	557	597	625	649
	N_u	405	440	480	514	547
	k_u (%)	77.7	78.9	80.4	82.2	84.3

A1.3. Multiregional demographic model (Svirezhev et al. 1997).

The multiregional model is a demographic model where migration, sexual and age groupings are not taken into account. At each time step, this model allows us to calculate the total population and population density as being constant throughout an entire region and equal to an average regional value. The model for each region was obtained by modifying the phenomenological model proposed by S. Kapitza (Kapitza S.P. Phenomenological theory of the increase of the world population. *Uspechi phisicheskich nauk*, v. 166, 1, 1996. (in Russian)).

Let t be the current moment of time, and n be the number of regions. If $P_k(t)$ is the total number of persons populating the k^{th} region, where $k = 1, \dots, n$, then Kapitza's model for this region is written as:

$$\frac{dP_k}{dt} = \frac{\tau_k (P_{+\infty k} - P_{-\infty k})}{\pi [(t - T_k)^2 + \tau_k^2]}, \quad P_{+\infty k} = P_k(\infty), \quad P_{-\infty k} = P_k(-\infty), \quad k = 1, \dots, n \quad (1)$$

where the parameters $\tau_k, T_k, P_{+\infty}, P_{-\infty}$ are the characteristic period of demographic transition, the moment of this transition and the total population when $t \rightarrow \infty$ and $t \rightarrow -\infty$. These parameters are estimated by real statistical data. We also assume that $P_{-\infty k} = 0$. As it follows from Eq. (1), the absolute rate of population growth, $dP_k(t)/dt \sim 1/t^2$ when $t \rightarrow \infty$. However, as real demographic statistics have shown, such a type of proportionality takes place for the relative rate of population growth, i.e., $dP_k(t)/P_k(t)dt \sim 1/t^2$ when $t \rightarrow \infty$. If we take this into consideration, then we have to modify Kapitza's equation, so that

$$\frac{dP_k}{dt} = \frac{\tau_k (\ln P_{+\infty k} - \ln P_{-\infty k})}{\pi [(t - T_k)^2 + \tau_k^2]} \cdot P_k(t), \quad P_{+\infty k} = P_k(\infty), \quad P_{-\infty k} = P_k(-\infty), \quad k = 1, \dots, n \quad (2)$$

In this model, the parameter $P_{-\infty k}$ is not equal to zero, and must therefore be estimated together with the other parameters.

Equation (2) has an analytical solution written as:

$$P_k(t) = P_{+\infty k} \cdot \left(\frac{P_{-\infty k}}{P_{+\infty k}} \right)^{a_k(t)}, \quad k = 1, \dots, n, \quad \text{where} \quad a_k(t) = \frac{1}{2} - \frac{1}{\pi} \operatorname{arctg} \left(\frac{t - T_k}{\tau_k} \right). \quad (3)$$

Formula (3) is applied in the modelling of population growth for both countries and regions (groups of countries) and the entire World. In order to calibrate the model, the UN demographic statistics were used.

The final version of the demographic model includes about 200 countries (regions) and consequently about 200 regional models. The model parameters were estimated for every region independently by the Method of Least Squares. These estimates were corrected in the process of fitting the model trajectory to the real trajectory, obtained from real demographic data for time before 1991.

Results of the modelling (demographic prognoses) and the real statistical data are presented in the next section in a tabular format.

A1.4. Data of the national demographic statistics and the modelling results.

Table A1.2. Total populations (in 10³ persons) of the countries and regions for the years 1980-2050.

	Area, 10 ³ km ²	1980	1990	2000	2010	2020	2030	2040	2050
ET (Economy in Transition)									
Armenia	29.8	3103	3352	4518	6822	9206	10669	11531	12078
Azerbaijan	86.6	6157	7020	8036	9063	10059	10969	11770	12462
Belarus	207.6	9627	10212	10623	10927	11156	11334	11477	11594
Bulgaria	110.9	8862	8991	9035	9055	9068	9076	9081	9085
Czech Republic	78.9	10327	10363	10366	10370	10373	10374	10375	10376
Estonia	45.1	1477	1571	1658	1724	1777	1820	1855	1884
Ex-Yugoslavia	256.0	22304	23818	25009	25917	26639	27224	27706	28109
Georgia	69.7	5042	5418	5641	5830	5979	6100	6199	6283
Hungary	93.0	10711	10365	10668	10669	10670	10670	10670	10670
Kazakhstan	2717.3	14955	16670	18125	19634	21097	22506	23857	25149
Kyrgyzstan	199.9	3617	4362	4640	4751	4806	4838	4859	4874
Latvia	64.5	2512	2671	2802	2905	2987	3053	3108	3153
Lithuania	65.2	3413	3711	3907	4099	4263	4406	4531	4642
Moldova	33.7	3982	4362	4749	5092	5417	5724	6014	6288
Mongolia	1564.6	1669	2182	2723	3239	3702	4106	4453	4751
Poland	312.7	35578	38119	39786	41055	42037	42817	43450	43975
Romania	237.5	22201	23207	23306	23541	23699	23812	23898	23964
Russia	17075.4	137956	147913	155192	161234	166183	170308	173800	176792
Slovakia	49.0	4984	5298	5444	5548	5618	5668	5706	5735
Tajikistan	143.1	3982	5287	6071	6309	6416	6477	6516	6543
Turkmenistan	488.1	2897	3657	4448	4810	4984	5083	5147	5190
Ukraine	603.7	49647	51637	52349	52673	52860	52981	53066	53129
Uzbekistan	447.4	15936	20420	23700	24950	25550	25896	26119	26274
Total	24979.7	380940	410603	432795	450217	464545	475911	485188	493000

	Area, 10 ³ km ²	1980	1990	2000	2010	2020	2030	2040	2050
LAC (Latin America and Caribbean)									
Argentina	2766.9	27036	32297	36674	39451	41160	42274	43046	43608
Bolivia	1098.6	5570	6727	7269	7792	8193	8509	8764	8973
Brazil	8512.0	122320	153765	173691	193813	211132	226088	239074	250421
Chile	756.9	11104	13019	14833	16367	17607	18596	19389	20032
Colombia	1138.9	25794	32584	39131	44246	47960	50661	52674	54217
Costa Rica	51.0	2213	2457	2541	2581	2604	2619	2630	2638
Cuba	110.9	9732	10544	11117	11549	11887	12158	12380	12565
Dominican R.	48.7	5947	6986	7753	8337	8795	9163	9464	9714
Ecuador	283.6	7921	10508	12588	14670	16581	18315	19881	21294
Fr. Guiana	91.0	62	95	179	266	321	354	376	391
Guatemala	108.9	7262	9336	11271	12913	14265	15369	16276	17028
Guyana	215.0	883	764	1173	1249	1300	1336	1363	1383
Haiti	27.7	5799	6411	6615	6708	6761	6795	6818	6836
Honduras	112.1	3691	5262	5685	6321	6823	7228	7559	7835
Jamaica	11.0	2188	2512	2640	2780	2890	2979	3052	3112
Mexico	1972.5	69752	88266	105017	119279	131230	141221	149614	156720
Nicaragua	129.5	2733	3605	4558	5544	6534	7505	8444	9341
Panama	78.2	1927	2423	2879	3252	3543	3769	3946	4087
Paraguay	406.8	3168	4658	6028	6942	7532	7929	8212	8422
Peru	1285.2	17625	21899	23467	24290	24757	25056	25263	25415
Salvador	21.0	4797	5993	6781	7273	7595	7819	7983	8107
Suriname	163.3	388	407	430	451	472	493	514	534
Uruguay	176.2	2924	3001	3161	3333	3529	3731	3921	4086
Venezuela	912.1	15620	19745	22307	23909	24982	25742	26306	26739
Total	20478	356456	443263	507786	563318	608454	645709	676949	703498

	Area, 10 ³ km ²	1980	1990	2000	2010	2020	2030	2040	2050
UCA (USA, Canada, Australia, New Zealand)									
Australia	7686.8	14488	16649	19175	21509	23558	25277	26693	27857
Canada	9976.1	23960	26521	29075	31521	33878	36138	38298	40357
New Zealand	269.0	3100	3367	3564	3730	3872	3995	4101	4195
United States	9372.6	227658	250465	272422	291484	307601	321021	332169	341470
Total	27304.6	269206	297002	324236	348244	368910	386431	401261	413879

	Area, 10 ³ km ²	1980	1990	2000	2010	2020	2030	2040	2050
HI (Highly Industrialised)									
Austria	83.8	7505	7718	8161	8201	8213	8219	8223	8225
Belgium	30.5	9855	9845	9924	9938	9946	9953	9957	9961
Denmark	43.1	5123	5140	5214	5239	5256	5269	5278	5285
Finland	337.0	4780	4986	5181	5364	5540	5708	5869	6022
France	547.0	53714	56735	59375	62137	64895	67647	70390	73121
Germany	357.0	78286	79365	81407	81452	81467	81474	81478	81480
Greece	131.9	9643	10089	10631	10972	11236	11445	11615	11755
Italy	301.2	57070	57661	57893	58101	58235	58329	58398	58451
Netherlands	41.5	14150	14952	15848	16679	17474	18233	18958	19649
Norway	324.2	4086	4241	4370	4479	4571	4650	4719	4779
Portugal	92.1	9884	10533	10221	10237	10245	10251	10255	10257
Spain	504.8	37542	38959	39268	39414	39495	39546	39582	39607
Sweden	450.0	8311	8559	8888	9267	9660	10032	10360	10637
Switzerland	41.3	6327	6712	7345	7533	7600	7633	7653	7666
Turkey	780.6	44468	57705	71979	88034	103893	118645	131886	143555
U.K.	244.1	55945	57411	58787	59132	59269	59340	59385	59414
Total	4310.1	406686	430611	454494	476178	496995	516374	534006	549864

	Area, 10 ³ km ²	1980	1990	2000	2010	2020	2030	2040	2050
Cn^{*)} (China)	9 597	994.9	1 130	1 258	1 372	1 474	1 566	1 648	1 721

*) Population in million persons

	Area, 10 ³ km ²	1980	1990	2000	2010	2020	2030	2040	2050
AsP (Asia and Pacific)									
Afghanistan	647.5	15940	15166	16493	17267	17750	18076	18311	18487
Bangladesh	144.0	88164	117930	147760	170441	186417	197776	206109	212425
Cambodia	181.0	6747	6988	18832	18927	18953	18966	18973	18978
India	3287.6	684460	850090	1044657	1253598	1463214	1662917	1846865	2012945
Indonesia	1919.4	147933	191216	238696	276257	302206	320107	332886	342360
Iran	1648.0	38126	55698	79903	105053	126592	143683	157033	167543
Japan	377.8	116782	123836	127863	130777	132895	134503	135766	136783
Lao PDR	236.8	3721	4023	4117	4157	4180	4194	4204	4212
Malaysia	329.8	14068	17062	20113	22890	25449	27789	29924	31870
Burma	676.6	35289	41261	46303	50367	53720	56522	58892	60921
Nepal	140.8	14288	19149	25566	32183	37832	42288	45744	48445
North Korea	121.2	17892	21927	25499	28472	30893	32862	34477	35816
Pakistan	803.9	86899	113388	142746	171894	198883	222893	243841	261986
Papua New G.	462.0	3154	3651	3849	3948	4005	4042	4068	4088
Philippines	300.0	49211	66659	83946	97048	106259	112806	117608	121250

	Area, 10 ³ km ²	1980	1990	2000	2010	2020	2030	2040	2050
South Korea	98.4	38455	42724	45616	47650	49144	50284	51180	51901
Sri Lanka	66.0	14815	17030	19032	20838	22446	23872	25138	26263
Thailand	514.0	47063	56468	64052	69961	74587	78258	81220	83650
Viet Nam	329.6	53740	68492	85179	100683	113557	123793	131877	138318
Total	12284.4	1476747	1832756	2240224	2622412	2968981	3275631	3544116	3778241

	Area 10 ³ km ²	1980	1990	2000	2010	2020	2030	2040	2050
Ar (Arabian Countries)									
Algeria	2381.7	18919	25694	32159	37265	41091	43963	46163	47887
Egypt	1001.4	41963	56202	73871	91389	106325	118286	127730	135232
Iraq	434.9	13072	18761	25729	32766	39002	44218	48502	52019
Israel	20.8	3879	4660	5488	6036	6460	6797	7071	7297
Kuwait	91.9	1353	2079	2662	3072	3363	3577	3740	3867
Lebanon	10.4	2658	3337	3520	3559	3576	3586	3592	3596
Libya	1759.5	2978	4206	5396	6401	7213	7861	8384	8810
Morocco	446.6	20296	26246	27914	28740	29190	29470	29662	29801
Oman	212.5	891	1345	1880	2472	3082	3684	4260	4802
Saudi Arabia	2150.0	8960	16506	18493	19301	19734	20001	20183	20315
Sudan	2505.8	18371	25137	31739	36880	40578	43249	45230	46744
Syria	185.2	8977	12467	16425	20363	24025	27300	30174	32679
Yemen	528.0	7670	9739	12779	16646	20824	24786	28262	31204
Total	11728.7	149987	206379	258053	304889	344461	376778	402953	424253

	Area 10 ³ km ²	1980	1990	2000	2010	2020	2030	2040	2050
Afr (Africa)									
Angola	1246.7	7078	8833	10711	12462	14003	15317	16425	17359
Benin	112.6	3530	4840	4889	4956	4991	5013	5027	5038
Botswana	600.4	797	1275	1446	1510	1542	1561	1574	1582
Burkina Faso	274.0	9191	9191	9191	9191	9191	9191	9191	9191
Burundi	27.8	4241	5652	6550	7687	8812	9906	10961	11968
Cameroon	475.4	8444	11109	13868	15922	17315	18274	18961	19473
C. A. R.	623.0	2294	5143	2492	2510	2520	2526	2531	2534
Chad	1284.0	4455	5063	5574	5980	6313	6590	6824	7025
Congo	342.0	1537	2304	2964	3306	3492	3607	3684	3738
Ethiopia	1221.9	31468	51305	63884	68360	70501	71741	72546	73110
Gabon	267.7	548	1068	1112	1123	1127	1130	1132	1133

	Area 10 ³ km ²	1980	1990	2000	2010	2020	2030	2040	2050
Gambia	11.3	603	819	1038	1222	1363	1469	1552	1616
Ghana	238.5	11679	15215	18423	20955	22890	24377	25537	26461
Gui.-Bissau	36.1	573	997	1118	1150	1165	1173	1179	1182
Ivory Coast	322.5	7934	10259	11933	13193	14160	14918	15526	16023
Kenya	582.6	16466	25369	35703	44580	51352	56416	60259	63241
Liberia	111.4	1967	2643	3342	3994	4573	5075	5508	5880
Madagascar	587.0	8742	11796	15309	18327	20606	22285	23540	24501
Malawi	118.5	6162	9261	13893	19180	24109	28251	31609	34318
Mali	1240.0	6940	9177	11331	12940	14071	14876	15468	15919
Mauritius	1.9	959	1141	1357	1568	1747	1889	2001	2089
Mozambique	801.6	10473	14532	15524	15937	16147	16273	16358	16418
Namibia	824.3	1009	1445	2143	2945	3664	4239	4686	5033
Niger	1267.0	5318	7686	9968	11464	12402	13022	13455	13774
Nigeria	923.8	77082	118775	152698	171455	182287	189167	193881	197300
Rwanda	26.3	4797	7600	10064	11382	12119	12578	12887	13110
Senegal	196.2	5661	7739	10113	12284	14043	15414	16482	17326
Sierra Leone	72.0	3474	4281	4780	5070	5252	5375	5463	5529
Somalia	637.7	4637	8512	9937	10560	10897	11106	11248	11351
South Africa	1221.0	29285	32956	34000	34477	34748	34922	35043	35132
Tanzania	945.1	17934	26038	33695	39098	42700	45177	46957	48288
Togo	56.8	2625	3563	4622	5623	6465	7142	7681	8115
Uganda	236.0	13201	17586	21988	25958	29338	32149	34477	36415
W. Sahara	266.0	76	76	76	76	76	76	76	76
Zaire	2345.4	28291	35273	41213	46041	49920	53045	55591	57692
Zambia	752.6	5766	8111	10188	11670	12688	13405	13931	14329
Zimbabwe	390.6	7396	10463	12886	14478	15525	16248	16771	17165
Total	20687.8	352633	497096	610025	688635	744112	784923	816022	840434

Appendix II. The Global City Database.

A2.1. Description.

We analyse the demographic statistics for 1248 cities distributed around the World, implementing the following procedure for each region. Data dealing with the population and area of cities for the 1990s are collected from different sources (see the references at the end of this appendix - from At, 2001 to Za, 1994). These data are ordered with respect to the corresponding urban populations, ensuring no noticeable gaps occur in this ordination.

We classify the data by region, then by country and finally by arranging the cities in alphabetical order.

The basic unit of the database is the city with its characteristics.

The database table consists of the following fields:

1. Region. The classification, widely used by the United Nations, divides countries into the following six regions: Sub-Saharan Africa (Afr), Arab States (Ar), Latin America and Caribbean (LAC), Asia and Pacific (AsP), Economies in Transition (ET) and Highly Industrialised countries (HI) (UN, 2001. The world of cities).

Nevertheless, based on the results from the regression analysis (see Chapter II), the regions are further subdivided in the following manner. We determined the regression between city area to urban population for the six UN regions. However, in two regions, AsP and HI, we find that the sampling points form two separate clouds in each region. In the AsP region, these clouds are formed by Chinese and the other cities, respectively. In the HI region, Australian, New Zealand, US and Canadian cities form one cloud, while the other is formed by European cities. Separate regression curves correspond to these clouds. This shows that the UN regional subdivision, that mainly takes into account political and economic factors and does not consider the culture-specific urban life style, is not applicable in some cases. For instance, in accordance with the UN classification, Japan belongs to the HI region, although the Japanese life style is closer to that of the Asian and Pacific countries. For this reason, we include

Japan in the AsP region. Similarly, Israel's ancient cities follow the Arabian tradition, and are therefore included in the Ar region.

As for China, it is a country where city growth is strongly planned. Therefore, in the new AsP region, Japan is included and China is excluded, the latter forming a new region, Cn. The subdivision of the HI region corresponds to the classic concept of the "Old" and "New" World. As a result, the HI region will contain only European countries, while the USA, Canada, Australia and New Zealand will form another new region, UCA.

The final map of the 8 regions is shown in Fig. 3.6, Part 3.

2. Country. The countries were selected within each region. Normally we use the modern name for a country, with the exception of former Yugoslavia.

3. City.

4. Source. The references are of 2 types: (a) Printed sources, such as statistical yearbooks, being the most reliable, and (b) Internet sources.

5. Area (in 10^3 km²). We included urbanised area in the database, which is considerably different from metropolitan area. The latter typically includes large tracts of non-urbanised (non-developed) land.

6. Density (in 10^3 persons/km²). In accordance with the definition provided by the US Census Bureau (www.demographia.com), an urbanised area is a densely populated area (built-up area) with a population density of more than 1,000 inhabitants per square mile (or 386 persons per square kilometre) with a population of more than 50 000¹).

However, we do not take this into account, since some cities are spread over the large territories, for example some Chinese and Finish cities, and have low population densities due to their construction and historical background.

7. Population (millions persons). The data were taken for the year 1990 or as close as possible to that year.

¹ Certainly these threshold values differ between different countries, and especially between different regions (see, for instance, Table 2.5, Part 2, and Table 3.2, Part 3).

Additional: The representability of the data is defined as the ratio of the sampling urban population to the total urban population in a corresponding region. The value varies from 10-11% in the ET and Ar regions to 37% in HI countries.

A2.2. Data.

In this section, the statistical data, taken from national demographic reports and other sources, are presented in a tabular format.

Region	Country	City	area (10 ³ km ²)	density (10 ³ pers./km ²)	population (millions)
Afr	Angola	Luanda	0.564	5317	3.000
Afr	Benin	Cotonou	0.088	6128	0.537
Afr	Benin	Porto Novo	0.050	3583	0.179
Afr	Burkina Faso	Bobo-Dioulasso	0.067	4020	0.269
Afr	Burkina Faso	Ouagadougou	0.170	3728	0.634
Afr	Burundi	Bujumbura	0.100	2780	0.278
Afr	Cameroun	Douala	0.144	8333	1.200
Afr	Central African Republic	Bangui	0.163	2778	0.452
Afr	Chad	N'Djamena	0.087	6124	0.531
Afr	Cote d'Ivoire	Abidjan	0.369	5222	1.929
Afr	Cote d'Ivoire	Bouake	0.135	2447	0.330
Afr	Dem. Rep. of Congo	Kinshasa	0.591	7450	4.400
Afr	Ethiopia	Addis Ababa	0.408	2564	1.047
Afr	Ethiopia	Arbaminch	0.006	5844	0.037
Afr	Ethiopia	Awassa	0.020	3226	0.063
Afr	Ethiopia	Diredawa	0.029	5626	0.165
Afr	Ethiopia	Mekelle	0.013	8285	0.108
Afr	Ghana	Accra	0.411	2319	0.954
Afr	Ghana	Tamale	0.023	6716	0.151
Afr	Guinee	Conakry	0.200	6197	1.239
Afr	Kenya	Mombasa	0.234	1629	0.382
Afr	Kenya	Nairobi	0.170	7918	1.346
Afr	Mali	Bamako	0.267	3298	0.880
Afr	Mauritania	Nouakchott	0.072	7660	0.550
Afr	Mozambique	Beira	0.193	1554	0.299
Afr	Mozambique	Maputo	0.300	2943	0.883
Afr	Namibia	Windhoek	0.069	2048	0.142

Region	Country	City	area	density	population
			(10 ³ km ²)	(10 ³ pers./km ²)	(millions)
Afr	Niger	Niamey	0.224	2259	0.506
Afr	Nigeria	Ibadan	0.063	22938	1.445
Afr	Nigeria	Onitsha	0.025	23952	0.599
Afr	Rwanda	Kigali	0.047	5851	0.275
Afr	Senegal	Dakar	0.072	22284	1.600
Afr	Sierra Leone	Freetown	0.082	4795	0.395
Afr	South Africa	Benoni	0.073	1418	0.104
Afr	South Africa	Boksburg	0.049	2459	0.120
Afr	South Africa	Brakpan	0.060	829	0.050
Afr	South Africa	Cape Town	0.185	12704	2.350
Afr	South Africa	Durban	0.073	9804	0.716
Afr	South Africa	Germiston	0.038	3526	0.134
Afr	South Africa	Johannesburg	0.300	2375	0.713
Afr	South Africa	Pietermaritzburg	0.268	584	0.156
Afr	South Africa	Port Elizabeth	0.338	897	0.303
Afr	South Africa	Pretoria	0.343	4079	1.400
Afr	South Africa	Roodepoort	0.059	2756	0.163
Afr	South Africa	Soweto	0.065	9179	0.597
Afr	South Africa	Springs	0.083	878	0.073
Afr	South Africa	Stellenbosch	0.107	405	0.043
Afr	South Africa	Welkom	0.142	481	0.068
Afr	Tanzania	Dar es Salaam	0.200	8650	1.730
Afr	Tanzania	Mbeya	0.045	3396	0.153
Afr	Togo	Lome	0.288	2783	0.802
Afr	Uganda	Jinja	0.028	2329	0.065
Afr	Uganda	Kampala	0.181	4420	0.800
Afr	Uganda	Mbale	0.017	3234	0.054
Afr	Zimbabwe	Harare	0.218	6784	1.479

Region	Country	City	area	density	population
			(10 ³ km ²)	(10 ³ pers./km ²)	(millions)
Ar	Egypt	Alexandria	0.314	9311	2.927
Ar	Egypt	Cairo	0.214	28332	6.069
Ar	Egypt	Port-Said	0.072	5566	0.401
Ar	Egypt	Suez	0.307	1068	0.328
Ar	Lebanon	Beirut	0.067	22388	1.500
Ar	Syria	Damaskus	0.042	32893	1.394
Ar	Israel	Jerusalem District	0.627	922	0.578
Ar	Israel	Petah Tiqwa S.D.	0.284	1316	0.374
Ar	Israel	Ramla S.D.	0.312	395	0.123
Ar	Jordan	Amman	0.520	2654	1.380
Ar	Morocco	Casablanca	1.615	1959	3.163
Ar	Morocco	Rabat	1.275	1096	1.397
Ar	Morocco	Tangier	0.360	1189	0.428
Ar	Saudi Arabia	Riyadh	0.620	2419	1.500
Ar	Sudan	Khartoum	0.249	3319	0.827
Ar	United Arab Emirates	Dubai	0.604	984	0.594
Ar	Yemen	Sana'a	0.363	2439	0.886

Region	Country	City	area	density	population
			(10 ³ km ²)	(10 ³ pers./km ²)	(millions)
Cn	China	Beihai	0.275	727	0.200
Cn	China	Beijing	4.568	1531	6.995
Cn	China	Changchun	1.116	1891	2.110
Cn	China	Changsha	0.367	3616	1.327
Cn	China	Chengdu	1.382	2032	2.808
Cn	China	Chongqing	1.534	1945	2.984
Cn	China	Dalian	2.415	992	2.396
Cn	China	Fuzhou	1.043	1239	1.292
Cn	China	Guangzhou	1.444	2479	3.579
Cn	China	Guiyang	2.436	629	1.532

Region	Country	City	area	density	population
			(10 ³ km ²)	(10 ³ pers./km ²)	(millions)
Cn	China	Haikou	0.218	1697	0.370
Cn	China	Hangzhou	0.430	3114	1.339
Cn	China	Harbin	1.637	1727	2.827
Cn	China	Hefei	0.458	2188	1.002
Cn	China	Huhehot	2.054	431	0.886
Cn	China	Jinan	2.119	1096	2.323
Cn	China	Kunming	2.081	733	1.525
Cn	China	Lanzhou	1.632	923	1.507
Cn	China	Lianyungang	0.830	628	0.521
Cn	China	Nanchang	0.617	2194	1.354
Cn	China	Nanjing	0.947	2638	2.498
Cn	China	Nanning	1.834	583	1.070
Cn	China	Nantong	0.121	3777	0.457
Cn	China	Ningbo	1.003	1082	1.085
Cn	China	Qingdao	1.103	1866	2.058
Cn	China	Qinhuangdao	0.363	1380	0.501
Cn	China	Shanghai	0.749	10461	7.835
Cn	China	Shantou	0.246	3480	0.856
Cn	China	Shengzhen	0.328	1204	0.395
Cn	China	Shenyang	3.495	1298	4.538
Cn	China	Shijiazhuang	0.307	4296	1.319
Cn	China	Taiyuan	1.460	1345	1.964
Cn	China	Tianjin	4.276	1350	5.771
Cn	China	Weihai	0.408	630	0.257
Cn	China	Wenzhou	0.187	3005	0.562
Cn	China	Wuhan	1.627	2305	3.751
Cn	China	Xiamen	0.555	1086	0.603
Cn	China	Xian	1.066	2586	2.757
Cn	China	Xining	0.350	1857	0.650
Cn	China	Yantai	0.835	964	0.805
Cn	China	Zhanjiang	1.460	726	1.060
Cn	China	Zhengzhou	1.010	1689	1.706

Region	Country	City	area	density	population
			(10 ³ km ²)	(10 ³ pers./km ²)	(millions)
Cn	China	Zhuhai	0.654	560	0.366
Cn	China	Hong Kong	0.103	52570	5.400

Region	Country	City	area	density	population
			(10 ³ km ²)	(10 ³ pers./km ²)	(millions)
AsP	Bangladesh	Chittagong	0.210	11445	2.400
AsP	Bangladesh	Dhaka	0.046	32500	1.495
AsP	Bangladesh	Matlab	0.184	1159	0.213
AsP	Bangladesh	Tangail	0.032	4819	0.155
AsP	Fiji	Suva	0.035	4060	0.141
AsP	India	Agarthala	0.015	1771	0.027
AsP	India	Agra	0.062	17979	1.111
AsP	India	Ahmedabad	0.093	37808	3.515
AsP	India	Aizawl	0.110	2364	0.260
AsP	India	Amritsar	0.115	21776	2.503
AsP	India	Bangalore	0.159	32684	5.200
AsP	India	Bhiwandi	0.026	21655	0.572
AsP	India	Bhopal	0.285	3721	1.060
AsP	India	Bhubaneshwar	0.125	3299	0.412
AsP	India	Bikaner	0.166	10097	1.674
AsP	India	Bodh Gaya	0.010	2700	0.027
AsP	India	Calcutta	0.104	42195	4.388
AsP	India	Chamba	0.004	4388	0.019
AsP	India	Chandigarh	0.114	7018	0.800
AsP	India	Chennai (Madras)	0.174	33908	5.900
AsP	India	Dehradun	0.030	17333	0.520
AsP	India	Delhi	1.483	8092	12.000
AsP	India	Gandhinagar	0.057	2316	0.132
AsP	India	Gangtok	0.010	24479	0.245
AsP	India	Goa	0.385	3494	1.344
AsP	India	Gulbarga	0.032	10280	0.330

Region	Country	City	area	density	population
			(10 ³ km ²)	(10 ³ pers./km ²)	(millions)
AsP	India	Hubli-Dharbad	0.109	6207	0.678
AsP	India	Hyderabad	0.217	23041	5.000
AsP	India	Imphal	0.030	13527	0.400
AsP	India	Indore	0.165	9923	1.639
AsP	India	Itanagar	0.010	1078	0.011
AsP	India	Jaipur	0.200	24950	5.000
AsP	India	Kanyakumari	0.026	772	0.020
AsP	India	Kochi	0.109	14616	1.600
AsP	India	Kullu	0.007	2395	0.016
AsP	India	Lucknow	0.310	7310	2.267
AsP	India	Manali	0.005	820	0.004
AsP	India	Mathura	0.009	48586	0.455
AsP	India	Mumbai (Bombay)	0.603	17024	10.265
AsP	India	Mysore	0.103	30824	3.165
AsP	India	Nagarjunakonda	0.023	652	0.015
AsP	India	Nagpur	0.217	7470	1.622
AsP	India	Nainital	0.012	3410	0.040
AsP	India	Nashik	0.220	4895	1.077
AsP	India	Panchmarhi	0.024	667	0.016
AsP	India	Patna	0.107	11473	1.229
AsP	India	Puri	0.010	12324	0.125
AsP	India	Rameswaram	0.052	965	0.050
AsP	India	Rishikesh	0.011	8929	0.100
AsP	India	Sambhajinagar (Aurangabad)	0.139	4924	0.682
AsP	India	Shimla	0.018	6833	0.123
AsP	India	Srinagar	0.105	6905	0.725
AsP	India	Surat	0.153	9917	1.519
AsP	India	Thiruvananthapuram	0.142	3701	0.524
AsP	India	Trichur	0.013	21678	0.274
AsP	India	Tumkur	0.019	7721	0.147
AsP	India	Udaipur	0.064	4095	0.263

Region	Country	City	area	density	population
			(10 ³ km ²)	(10 ³ pers./km ²)	(millions)
AsP	India	Vadodara	0.108	16627	1.800
AsP	India	Varanasi	0.074	8120	0.600
AsP	Indonesia	Banjarmasin	0.079	6159	0.487
AsP	Indonesia	Jakarta	0.652	12577	8.200
AsP	Indonesia	Medan	0.421	4299	1.810
AsP	Indonesia	Semarang	0.254	4244	1.076
AsP	Indonesia	Surabaya	0.330	7298	2.411
AsP	Iran	Tehran	0.600	11333	6.800
AsP	Japan	Aichi	0.714	6073	4.337
AsP	Japan	Akita	0.082	4792	0.391
AsP	Japan	Aomori	0.139	4643	0.643
AsP	Japan	Chiba	0.476	7019	3.344
AsP	Japan	Ehime	0.128	5140	0.659
AsP	Japan	Fukui	0.055	5316	0.294
AsP	Japan	Fukuoka	0.478	6247	2.988
AsP	Japan	Fukushima	0.141	4972	0.699
AsP	Japan	Gifu	0.138	5390	0.746
AsP	Japan	Gumma	0.157	4669	0.733
AsP	Japan	Hiroshima	0.269	6127	1.650
AsP	Japan	Hokkaido	0.705	5380	3.790
AsP	Japan	Hyogo	0.479	7906	3.786
AsP	Japan	Ibaraki	0.163	4895	0.796
AsP	Japan	Ishikawa	0.089	5998	0.535
AsP	Japan	Iwate	0.076	5177	0.395
AsP	Japan	Kagawa	0.069	4804	0.331
AsP	Japan	Kagoshima	0.117	5636	0.660
AsP	Japan	Kanagawa	0.835	7930	6.623
AsP	Japan	Kochi	0.051	6383	0.323
AsP	Japan	Kumatoto	0.119	5638	0.672
AsP	Japan	Kyoto	0.232	8873	2.055
AsP	Japan	Mie	0.143	4653	0.664
AsP	Japan	Miyagi	0.185	5962	1.103

Region	Country	City	area	density	population
			(10 ³ km ²)	(10 ³ pers./km ²)	(millions)
AsP	Japan	Miyazaki	0.092	4989	0.459
AsP	Japan	Nagano	0.139	4770	0.664
AsP	Japan	Nagasaki	0.102	6513	0.663
AsP	Japan	Nara	0.108	6382	0.688
AsP	Japan	Niigata	0.192	5495	1.055
AsP	Japan	Oita	0.100	5065	0.505
AsP	Japan	Okayama	0.145	4483	0.650
AsP	Japan	Okinawa	0.085	7872	0.666
AsP	Japan	Osaka	0.824	9862	8.128
AsP	Japan	Saga	0.046	5237	0.243
AsP	Japan	Saitama	0.554	7596	4.205
AsP	Japan	Shiga	0.059	5683	0.337
AsP	Japan	Shimane	0.042	4460	0.186
AsP	Japan	Shizuoka	0.332	5552	1.842
AsP	Japan	Tochigi	0.137	4788	0.654
AsP	Japan	Tokushima	0.045	5112	0.229
AsP	Japan	Tokyo	0.995	11544	11.483
AsP	Japan	Tottori	0.033	4954	0.162
AsP	Japan	Toyama	0.089	4780	0.424
AsP	Japan	Wakayama	0.086	5330	0.460
AsP	Japan	Yamagata	0.095	4863	0.463
AsP	Japan	Yamaguchi	0.186	3786	0.705
AsP	Japan	Yamanashi	0.047	5534	0.259
AsP	Laos	Vientiane	0.029	5394	0.156
AsP	Malaysia	Kuala Lumpur	0.243	5103	1.240
AsP	Myanmar	Yangon	0.199	12355	2.459
AsP	Nepal	Bharatpur	0.055	1136	0.063
AsP	Nepal	Biratnagar	0.060	2307	0.138
AsP	Nepal	Kathmandu	0.048	9891	0.472
AsP	Nepal	Pokhara	0.053	2093	0.110
AsP	Pakistan	Islamabad Federal Area	0.906	376	0.340
AsP	Papua New Guinea	Port Moresby	0.240	815	0.196

Region	Country	City	area	density	population
			(10 ³ km ²)	(10 ³ pers./km ²)	(millions)
AsP	Philippines	Angeles	0.060	3930	0.237
AsP	Philippines	Bacolod	0.156	2332	0.364
AsP	Philippines	Bago	0.402	308	0.124
AsP	Philippines	Baguio	0.049	3742	0.183
AsP	Philippines	Bais	0.317	189	0.060
AsP	Philippines	Batangas	0.283	654	0.185
AsP	Philippines	Butuan	0.526	433	0.228
AsP	Philippines	Cabanatuan	0.193	898	0.173
AsP	Philippines	Cadiz	0.517	232	0.120
AsP	Philippines	Cagayan de Oro	0.413	824	0.340
AsP	Philippines	Calbayog	0.903	127	0.115
AsP	Philippines	Caloocan	0.056	13638	0.761
AsP	Philippines	Canlaon	0.161	230	0.037
AsP	Philippines	Cavite	0.012	7797	0.092
AsP	Philippines	Cebu	0.281	2172	0.610
AsP	Philippines	Cotabato	0.176	722	0.127
AsP	Philippines	Dagupan	0.037	3280	0.122
AsP	Philippines	Danao	0.107	680	0.073
AsP	Philippines	Dapitan	0.215	274	0.059
AsP	Philippines	Davao	2.211	384	0.850
AsP	Philippines	Dipolog	0.220	364	0.080
AsP	Philippines	Dumaguete	0.056	1434	0.080
AsP	Philippines	General Santos	0.423	591	0.250
AsP	Philippines	Gingoog	0.405	205	0.083
AsP	Philippines	Iligan	0.731	311	0.227
AsP	Philippines	Iloilo	0.056	5536	0.310
AsP	Philippines	Iriga	0.120	619	0.074
AsP	Philippines	La Carlota	0.137	408	0.056
AsP	Philippines	Laoag	0.108	781	0.084
AsP	Philippines	Lapu-Lapu	0.058	2513	0.146
AsP	Philippines	Legaspi	0.154	787	0.121
AsP	Philippines	Lipa	0.209	764	0.160

Region	Country	City	area	density	population
			(10 ³ km ²)	(10 ³ pers./km ²)	(millions)
AsP	Philippines	Lucena	0.069	2204	0.151
AsP	Philippines	Mandaue	0.012	15385	0.180
AsP	Philippines	Manila	0.038	41749	1.599
AsP	Philippines	Marawi	0.023	4071	0.092
AsP	Philippines	Naga	0.078	1484	0.115
AsP	Philippines	Olongapo	0.103	1868	0.193
AsP	Philippines	Ormos	0.464	278	0.129
AsP	Philippines	Oroquieta	0.195	272	0.053
AsP	Philippines	Ozamis	0.144	638	0.092
AsP	Philippines	Pagadian	0.379	280	0.106
AsP	Philippines	Palayan	0.036	562	0.020
AsP	Philippines	Pasay	0.014	26403	0.367
AsP	Philippines	Puerto Princesa	2.107	44	0.092
AsP	Philippines	Quezon City	0.166	10030	1.667
AsP	Philippines	Roxas	0.102	1010	0.103
AsP	Philippines	San Carlos (Neg. Occ.)	0.451	235	0.106
AsP	Philippines	San Carlos (Pangasinan)	0.166	745	0.124
AsP	Philippines	San Jose	0.181	488	0.088
AsP	Philippines	San Pablo	0.214	752	0.161
AsP	Philippines	Silay	0.215	428	0.092
AsP	Philippines	Surigao	0.245	408	0.100
AsP	Philippines	Tacloban	0.101	1368	0.138
AsP	Philippines	Tagaytay	0.074	324	0.024
AsP	Philippines	Tagbilaran	0.030	1848	0.056
AsP	Philippines	Tangub	0.119	361	0.043
AsP	Philippines	Toledo	0.175	688	0.120
AsP	Philippines	Trece Martires	0.039	409	0.016
AsP	Philippines	Zamboanga	1.415	312	0.442
AsP	Singapore	Singapore	0.299	8574	2.560
AsP	South Korea	Inchon	0.965	2567	2.476
AsP	South Korea	Kwangju	0.501	2696	1.352

Region	Country	City	area	density	population
			(10 ³ km ²)	(10 ³ pers./km ²)	(millions)
AsP	South Korea	Pusan	0.760	4822	3.664
AsP	South Korea	Seoul	0.606	16335	9.891
AsP	South Korea	Taegu	0.886	2800	2.480
AsP	South Korea	Taejon	0.540	2532	1.367
AsP	Sri Lanka	Colombo	0.235	5532	1.300
AsP	Taiwan	Taipei	0.275	9474	2.605
AsP	Thailand	Bangkok (Krung Thep)	1.565	3584	5.609
AsP	Vietnam	Hanoi	0.921	2288	2.106

Region	Country	City	area	density	population
			(10 ³ km ²)	(10 ³ pers./km ²)	(millions)
ET	Armenia	Yerevan	0.230	4991	1.148
ET	Bulgaria	Sofia	0.198	6002	1.190
ET	Czech Republic	Brno-mesto	0.230	1707	0.393
ET	Czech Republic	Breclav	1.189	106	0.126
ET	Czech Republic	Ceske Budejovice	1.625	107	0.174
ET	Czech Republic	Cesky Krumlov	1.615	36	0.058
ET	Czech Republic	Cheb	0.933	94	0.088
ET	Czech Republic	Karlovy Vary	1.628	76	0.123
ET	Czech Republic	Karvina	0.347	830	0.288
ET	Czech Republic	Kolin	0.819	112	0.092
ET	Czech Republic	Ostrava-mesto	0.214	1549	0.332
ET	Czech Republic	Plzen-mesto	0.125	1400	0.175
ET	Czech Republic	Hlavni mesto Praha	0.496	2450	1.215
ET	Czech Republic	Tabor	1.303	80	0.104
ET	Czech Republic	Znojmo	1.637	69	0.113
ET	Estonia	Tallinn	0.158	2828	0.448
ET	Georgia	Tbilisi	0.204	6364	1.295
ET	Hungary	Budapest	0.525	3844	2.018
ET	Hungary	Pomaz	0.049	260	0.013
ET	Kazakhstan	Almaty	0.290	3894	1.129

Region	Country	City	area	density	population
			(10 ³ km ²)	(10 ³ pers./km ²)	(millions)
ET	Kyrgyzstan	Bishkek	0.167	3784	0.631
ET	Lithuania	Vilnius	0.162	4144	0.670
ET	Moldova	Chisinau	0.131	5038	0.662
ET	Poland	Warsaw	0.495	3320	1.643
ET	Romania	Tirgoviste	0.099	1014	0.100
ET	Russian Federation	Kostroma	0.131	2168	0.284
ET	Russian Federation	Moscow	1.071	8054	8.625
ET	Russian Federation	Nizhny Novgorod	0.364	3789	1.379
ET	Russian Federation	Novgorod	0.135	1782	0.241
ET	Russian Federation	Ryazan	0.234	2292	0.537
ET	Russian Federation	Saratov	0.371	2449	0.909
ET	Russian Federation	St. Petersburg	0.606	8102	4.910
ET	Russian Federation	Volgograd	0.565	1749	0.988
ET	Slovak Republic	Banska Bystrica	2.075	86	0.179
ET	Slovak Republic	Hlavni mesto Bratislava	0.368	1208	0.444
ET	Slovak Republic	Kosice-mesto	0.243	981	0.238
ET	Slovak Republic	Trencin	1.310	138	0.181
ET	Slovak Republic	Zilina	1.097	167	0.183
ET	Ukraine	Kyiv	0.800	3298	2.639
ET	Ukraine	Sevastopol	0.900	452	0.407
ET	Yugoslavia, SR Bosna i Hercegovina	Sarajevo-Centar	0.035	2079	0.073
ET	Yugoslavia, SR Bosna i Hercegovina	Sarajevo-Novii grad	0.047	1714	0.081
ET	Yugoslavia, SR Bosna i Hercegovina	Novo Sarajevo	0.047	2004	0.094
ET	Yugoslavia, SR Bosna i Hercegovina	Sarajevo-Stari grad	0.123	457	0.056
ET	Yugoslavia, SR Hercegovina	Tuzla	0.307	396	0.122
ET	Yugoslavia, SR Hrvatska	Zagreb-Centar	0.021	2665	0.056
ET	Yugoslavia, SR Hrvatska	Zagreb-Crnomerec	0.021	2455	0.052
ET	Yugoslavia, SR Hrvatska	Zagreb-Dubrava	0.052	1572	0.082
ET	Yugoslavia, SR Hrvatska	Zagreb-Maksimir	0.053	1188	0.063

Region	Country	City	area	density	population
			(10 ³ km ²)	(10 ³ pers./km ²)	(millions)
ET	Yugoslavia, SR Hrvatska	Zagreb-Pescenica	0.029	1793	0.052
ET	Yugoslavia, SR Hrvatska	Zagreb-Susedgrad	0.047	1077	0.051
ET	Yugoslavia, SR Hrvatska	Zagreb-Tresnjevka	0.014	8205	0.115
ET	Yugoslavia, SR Hrvatska	Zagreb-Trnje	0.007	6819	0.048
ET	Yugoslavia, SR Makedonija	Skoplje-Centar	0.018	5201	0.094
ET	Yugoslavia, SR Slovenija	Ljubljana-Bezigrad	0.046	1209	0.056
ET	Yugoslavia, SR Slovenija	Ljubljana-Center	0.005	6457	0.032
ET	Yugoslavia, SR Slovenija	Izola	0.028	447	0.013
ET	Yugoslavia, SR Srbija	Beograd-Cukarica	0.155	852	0.132
ET	Yugoslavia, SR Srbija	Novi Beograd	0.041	4233	0.174
ET	Yugoslavia, SR Srbija	Beograd-Rakovica	0.029	3002	0.087
ET	Yugoslavia, SR Srbija	Beograd-Savski Venac	0.016	3336	0.053
ET	Yugoslavia, SR Srbija	Beograd-Stari Grad	0.007	10538	0.074
ET	Yugoslavia, SR Srbija	Beograd-Vozdovac	0.150	1062	0.159
ET	Yugoslavia, SR Srbija	Beograd-Vracar	0.003	26287	0.079
ET	Yugoslavia, SR Srbija	Beograd-Zvezdara	0.031	4153	0.129
ET	Yugoslavia, SR Hrvatska	Zagreb-Medvescak	0.018	2812	0.051

Region	Country	City	area	density	population
			(10 ³ km ²)	(10 ³ pers./km ²)	(millions)
UCA	Australia	Melbourne	1.148	2634	3.023
UCA	Australia	Sydney	0.006	4854	0.030
UCA	Canada	Calgary	0.358	2093	0.750
UCA	Canada	Edmonton	0.333	1803	0.600
UCA	Canada	Hamilton	0.294	1868	0.550
UCA	Canada	Montreal	0.870	2999	2.610
UCA	Canada	Ottawa	0.320	2281	0.730
UCA	Canada	Quebec	0.333	1593	0.530
UCA	Canada	Toronto	1.434	2679	3.840
UCA	Canada	Vancouver	0.896	2020	1.810

Region	Country	City	area	density	population
			(10 ³ km ²)	(10 ³ pers./km ²)	(millions)
UCA	Canada	Winnipeg	0.294	2038	0.600
UCA	New Zealand	Wellington	0.175	1861	0.326
UCA	U.S.A.	Akron	0.161	1384	0.22302
UCA	U.S.A.	Albuquerque	0.338	1137	0.38474
UCA	U.S.A.	Arlington	0.066	2578	0.171
UCA	U.S.A.	Atlanta	0.337	1168	0.394
UCA	U.S.A.	Austin	0.558	835	0.466
UCA	U.S.A.	Bakersfield	0.235	744	0.175
UCA	U.S.A.	Baltimore	0.205	3594	0.736
UCA	U.S.A.	Boston	0.124	4635	0.574
UCA	U.S.A.	Buffalo	0.104	3157	0.328
UCA	U.S.A.	Charlotte	0.446	887	0.396
UCA	U.S.A.	Cincinnati	0.198	1842	0.364
UCA	U.S.A.	Cleveland	0.197	2565	0.506
UCA	U.S.A.	Colorado Springs	0.469	599	0.281
UCA	U.S.A.	Columbus	0.489	1295	0.633
UCA	U.S.A.	Dallas	0.877	1149	1.007
UCA	U.S.A.	Denver	0.392	1192	0.468
UCA	U.S.A.	Detroit	0.355	2895	1.028
UCA	U.S.A.	El Paso	0.628	820	0.515
UCA	U.S.A.	Fort Wayne	0.161	1078	0.173
UCA	U.S.A.	Fort Worth	0.720	622	0.448
UCA	U.S.A.	Fremont	0.197	879	0.173
UCA	U.S.A.	Fresno	0.254	1396	0.354
UCA	U.S.A.	Garland	0.147	1232	0.181
UCA	U.S.A.	Glendale	0.078	2298	0.180
UCA	U.S.A.	Honolulu	0.083	4411	0.365
UCA	U.S.A.	Indianapolis	0.926	790	0.731
UCA	U.S.A.	Jersey City	0.039	5922	0.229
UCA	U.S.A.	Kansas	0.797	546	0.435
UCA	U.S.A.	Little Rock	0.263	667	0.176
UCA	U.S.A.	Long Beach	0.128	3355	0.429
UCA	U.S.A.	Los Angeles	1.201	2901	3.485

Region	Country	City	area	density	population
			(10 ³ km ²)	(10 ³ pers./km ²)	(millions)
UCA	U.S.A.	Memphis	0.655	931	0.610
UCA	U.S.A.	Mesa	0.278	1036	0.288
UCA	U.S.A.	Miami	0.091	3934	0.359
UCA	U.S.A.	Milwaukee	0.246	2553	0.628
UCA	U.S.A.	Minneapolis	0.141	2621	0.368
UCA	U.S.A.	New Orleans	0.462	1075	0.497
UCA	U.S.A.	New York	0.791	9260	7.323
UCA	U.S.A.	Oakland	0.144	2592	0.372
UCA	U.S.A.	Philadelphia	0.346	4585	1.586
UCA	U.S.A.	Phoenix	1.075	915	0.983
UCA	U.S.A.	Pittsburgh	0.142	2599	0.370
UCA	U.S.A.	Portland	0.319	1370	0.437
UCA	U.S.A.	Sacramento	0.247	1498	0.369
UCA	U.S.A.	San Antonio	0.852	1098	0.936
UCA	U.S.A.	San Diego	0.829	1339	1.111
UCA	U.S.A.	San Francisco	0.120	6056	0.724
UCA	U.S.A.	San Jose	0.439	1784	0.782
UCA	U.S.A.	Santa Ana	0.069	4234	0.294
UCA	U.S.A.	Seattle	0.215	2404	0.516
UCA	U.S.A.	Spokane	0.143	1238	0.177
UCA	U.S.A.	St. Louis	0.158	2503	0.397
UCA	U.S.A.	St. Paul	0.137	1991	0.272
UCA	U.S.A.	Tacoma	0.048	3681	0.177
UCA	U.S.A.	Tampa	0.276	1013	0.280
UCA	U.S.A.	Toledo	0.206	1614	0.333
UCA	U.S.A.	Tucson	0.400	1013	0.405
UCA	U.S.A.	Tulsa	0.470	782	0.367
UCA	U.S.A.	Virginia Beach	0.636	618	0.393
UCA	U.S.A.	Washington	0.157	3861	0.607
UCA	U.S.A.	Wichita	0.295	1032	0.304
UCA	U.S.A.	Yonkers	0.047	4012	0.188

Region	Country	City	area	density	population
			(10 ³ km ²)	(10 ³ pers./km ²)	(millions)
HI	Austria	Amstetten	0.052	421	0.022
HI	Austria	Ansfelden	0.031	466	0.015
HI	Austria	Attnang-Puchheim	0.012	661	0.008
HI	Austria	Bad Aussee	0.082	62	0.005
HI	Austria	Bad Ischl	0.163	85	0.014
HI	Austria	Bad Sankt Leonhard im Lavanttal	0.112	45	0.005
HI	Austria	Bad Vöslau	0.039	285	0.011
HI	Austria	Baden	0.027	873	0.023
HI	Austria	Bärnbach	0.017	301	0.005
HI	Austria	Berndorf	0.018	471	0.008
HI	Austria	Bischofshofen	0.050	204	0.010
HI	Austria	Bludenz	0.030	446	0.013
HI	Austria	Braunau am Inn	0.025	655	0.016
HI	Austria	Bregenz	0.030	918	0.027
HI	Austria	Bruck an der Leitha	0.024	307	0.007
HI	Austria	Bruck an der Mur	0.038	366	0.014
HI	Austria	Deutschlandsberg	0.024	318	0.008
HI	Austria	Deutsch-Wagram	0.031	200	0.006
HI	Austria	Dornbirn	0.121	337	0.041
HI	Austria	Eisenerz	0.125	62	0.008
HI	Austria	Eisenstadt	0.043	241	0.010
HI	Austria	Enns	0.033	306	0.010
HI	Austria	Feldkirch	0.034	778	0.027
HI	Austria	Feldkirchen in Kärnten	0.077	167	0.013
HI	Austria	Ferlach	0.117	64	0.007
HI	Austria	Freistadt	0.013	537	0.007
HI	Austria	Friesach	0.121	47	0.006
HI	Austria	Fürstenfeld	0.015	397	0.006
HI	Austria	Gänserndorf	0.031	213	0.007
HI	Austria	Gerasdorf bei Wien	0.035	189	0.007
HI	Austria	Gleisdorf	0.005	1098	0.005
HI	Austria	Gloggnitz	0.020	307	0.006
HI	Austria	Gmünd	0.025	240	0.006

Region	Country	City	area	density	population
			(10 ³ km ²)	(10 ³ pers./km ²)	(millions)
HI	Austria	Gmunden	0.064	207	0.013
HI	Austria	Graz	0.128	1864	0.238
HI	Austria	Groß-Enzersdorf	0.084	80	0.007
HI	Austria	Haag	0.055	94	0.005
HI	Austria	Hainburg an der Donau	0.025	230	0.006
HI	Austria	Hall in Tirol	0.006	2232	0.012
HI	Austria	Hallein	0.027	641	0.017
HI	Austria	Hartberg	0.022	287	0.006
HI	Austria	Hermagor-Pressegger See	0.204	36	0.007
HI	Austria	Herzogenburg	0.046	162	0.007
HI	Austria	Hohenems	0.029	464	0.014
HI	Austria	Hollabrunn	0.152	69	0.010
HI	Austria	Horn	0.039	160	0.006
HI	Austria	Imst	0.113	66	0.008
HI	Austria	Innsbruck	0.105	1126	0.118
HI	Austria	Judenburg	0.013	801	0.011
HI	Austria	Kapfenberg	0.061	382	0.023
HI	Austria	Kindberg	0.041	146	0.006
HI	Austria	Kitzbühel	0.058	140	0.008
HI	Austria	Klagenfurt	0.120	745	0.089
HI	Austria	Klosterneuburg	0.076	321	0.024
HI	Austria	Knittelfeld	0.005	2842	0.013
HI	Austria	Köflach	0.020	553	0.011
HI	Austria	Korneuburg	0.010	1001	0.010
HI	Austria	Krems an der Donau	0.052	441	0.023
HI	Austria	Kufstein	0.039	342	0.013
HI	Austria	Laa an der Thaya	0.073	86	0.006
HI	Austria	Landeck	0.016	467	0.007
HI	Austria	Langenlois	0.067	95	0.006
HI	Austria	Leibnitz	0.006	1101	0.007
HI	Austria	Leoben	0.108	268	0.029
HI	Austria	Leonding	0.024	882	0.021
HI	Austria	Lienz	0.016	744	0.012

Region	Country	City	area	density	population
			(10 ³ km ²)	(10 ³ pers./km ²)	(millions)
HI	Austria	Liezen	0.056	125	0.007
HI	Austria	Linz	0.096	2116	0.203
HI	Austria	Marchtrenk	0.023	450	0.010
HI	Austria	Mattersburg	0.028	205	0.006
HI	Austria	Melk	0.026	200	0.005
HI	Austria	Mistelbach	0.131	78	0.010
HI	Austria	Mödling	0.010	2039	0.020
HI	Austria	Mürzzuschlag	0.019	519	0.010
HI	Austria	Neulengbach	0.052	119	0.006
HI	Austria	Neunkirchen	0.020	504	0.010
HI	Austria	Oberwart	0.036	173	0.006
HI	Austria	Perg	0.026	225	0.006
HI	Austria	Pinkafeld	0.027	183	0.005
HI	Austria	Poysdorf	0.097	56	0.005
HI	Austria	Purkersdorf	0.030	212	0.006
HI	Austria	Radenthein	0.089	77	0.007
HI	Austria	Ried im Innkreis	0.007	1663	0.011
HI	Austria	Rottenmann	0.113	48	0.005
HI	Austria	Saalfelden am Steinernen Meer	0.119	106	0.013
HI	Austria	Salzburg	0.066	2193	0.144
HI	Austria	Sankt Andrä	0.113	93	0.011
HI	Austria	Sankt Johann im Pongau	0.078	114	0.009
HI	Austria	Sankt Pölten	0.109	461	0.050
HI	Austria	Sankt Valentin	0.046	193	0.009
HI	Austria	Sankt Veit an der Glan	0.051	237	0.012
HI	Austria	Schärding	0.004	1335	0.005
HI	Austria	Schrems	0.061	97	0.006
HI	Austria	Schwaz	0.020	586	0.012
HI	Austria	Schwechat	0.045	328	0.015
HI	Austria	Seekirchen am Wallersee	0.050	165	0.008
HI	Austria	Spittal an der Drau	0.048	317	0.015
HI	Austria	Steyr	0.027	1481	0.039

Region	Country	City	area	density	population
			(10 ³ km ²)	(10 ³ pers./km ²)	(millions)
HI	Austria	Stockerau	0.037	364	0.014
HI	Austria	Ternitz	0.065	236	0.015
HI	Austria	Traiskirchen	0.029	477	0.014
HI	Austria	Traismauer	0.043	119	0.005
HI	Austria	Traun	0.015	1441	0.022
HI	Austria	Trofaiach	0.005	1700	0.009
HI	Austria	Tulln an der Donau	0.072	167	0.012
HI	Austria	Villach	0.135	405	0.055
HI	Austria	Vöcklabruck	0.016	721	0.011
HI	Austria	Voitsberg	0.029	363	0.010
HI	Austria	Völkermarkt	0.137	81	0.011
HI	Austria	Waidhofen an der Thaya	0.046	121	0.006
HI	Austria	Waidhofen an der Ybbs	0.132	87	0.011
HI	Austria	Weiz	0.005	1671	0.008
HI	Austria	Wels	0.046	1145	0.053
HI	Austria	Wien	0.415	3711	1.540
HI	Austria	Wiener Neustadt	0.061	576	0.035
HI	Austria	Wilhelmsburg	0.047	141	0.007
HI	Austria	Wolfsberg	0.278	87	0.024
HI	Austria	Wolkersdorf im Weinviertel	0.044	128	0.006
HI	Austria	Wörgl	0.020	510	0.010
HI	Austria	Ybbs an der Donau	0.024	242	0.006
HI	Austria	Zell am See	0.055	159	0.009
HI	Austria	Zeltweg	0.009	938	0.008
HI	Austria	Zistersdorf	0.089	62	0.006
HI	Austria	Zwettl-Niederösterreich	0.256	45	0.011
HI	Belgium	Alost	0.138	551	0.076
HI	Belgium	Anvers	0.510	922	0.470
HI	Belgium	Bruges	0.291	404	0.117
HI	Belgium	Brussels	0.023	5976	0.137
HI	Belgium	Charleroi	0.269	769	0.207
HI	Belgium	Courtrai	0.111	683	0.076

Region	Country	City	area	density	population
			(10 ³ km ²)	(10 ³ pers./km ²)	(millions)
HI	Belgium	Gand	0.448	515	0.231
HI	Belgium	Hasselt	0.164	402	0.066
HI	Belgium	Liege	0.266	741	0.197
HI	Belgium	Louvain	0.231	369	0.085
HI	Belgium	Malines	0.131	578	0.076
HI	Belgium	Mons	0.212	433	0.092
HI	Belgium	Mouscron	0.076	707	0.054
HI	Belgium	Namur	0.448	231	0.103
HI	Belgium	Ostende	0.146	470	0.069
HI	Belgium	Roulers	0.104	506	0.053
HI	Belgium	Saint-Nicolas	0.150	453	0.068
HI	Belgium	Tournai	0.292	232	0.068
HI	Belgium	Verviers	0.429	125	0.054
HI	Denmark	Albertslund	0.023	1277	0.029
HI	Denmark	Allerod	0.067	317	0.021
HI	Denmark	Ballerup	0.034	1326	0.045
HI	Denmark	Birkerod	0.034	616	0.021
HI	Denmark	Brondby	0.021	1648	0.034
HI	Denmark	Dragor	0.018	677	0.012
HI	Denmark	Farum	0.023	739	0.017
HI	Denmark	Fredensborg-Humlebaek	0.072	260	0.019
HI	Denmark	Frederiksberg	0.009	9762	0.086
HI	Denmark	Gentofte	0.026	2557	0.065
HI	Denmark	Gladsakse	0.025	2435	0.061
HI	Denmark	Glostrup	0.013	1484	0.020
HI	Denmark	Greve	0.060	753	0.045
HI	Denmark	Herlev	0.012	2219	0.027
HI	Denmark	Hvidovre	0.022	2225	0.049
HI	Denmark	Hoje Tastrup	0.080	558	0.044
HI	Denmark	Horsholm	0.031	739	0.023
HI	Denmark	Ishoj	0.025	831	0.021
HI	Denmark	Karlebo	0.040	472	0.019
HI	Denmark	Kobenhavn	0.088	5289	0.467

Region	Country	City	area	density	population
			(10 ³ km ²)	(10 ³ pers./km ²)	(millions)
HI	Denmark	Ledoje-Smorum	0.031	296	0.009
HI	Denmark	Lyngby-Tarbaek	0.039	1268	0.049
HI	Denmark	Rodovre	0.012	2917	0.035
HI	Denmark	Sollerod	0.040	773	0.031
HI	Denmark	Solrod	0.040	472	0.019
HI	Denmark	Tarnby	0.063	634	0.040
HI	Denmark	Vallensbaek	0.009	1279	0.012
HI	Denmark	Vaerlose	0.034	512	0.017
HI	Finland	Alajärvi	0.739	13	0.009
HI	Finland	Alavus (- Alavo)	0.790	13	0.011
HI	Finland	Anjalankoski	0.726	26	0.019
HI	Finland	Äänekoski	0.301	39	0.012
HI	Finland	Ähtäri - Etseri	0.804	10	0.008
HI	Finland	Espoo - Esbo	0.312	545	0.170
HI	Finland	Forssa	0.249	79	0.020
HI	Finland	Haapajärvi	0.781	11	0.008
HI	Finland	Hämeelinna - Tavastehus	0.167	259	0.043
HI	Finland	Hamina - Fredrikshamn	0.019	542	0.010
HI	Finland	Hanko - Hangoe	0.115	100	0.011
HI	Finland	Heinola	0.049	336	0.016
HI	Finland	Helsinki - Helsingfors	0.185	2659	0.491
HI	Finland	Hyvinkää - Hyvinge	0.323	124	0.040
HI	Finland	Iisalmi - Idensalmi	0.763	31	0.024
HI	Finland	Imatra	0.155	219	0.034
HI	Finland	Jämsä	0.670	19	0.013
HI	Finland	Jämsänkoski	0.401	20	0.008
HI	Finland	Järvenpää - Träskända	0.038	822	0.031
HI	Finland	Joensuu	0.082	576	0.047
HI	Finland	Jyväskylä	0.097	685	0.066
HI	Finland	Kajaani - Kajana	1.158	31	0.036
HI	Finland	Kannus	0.408	15	0.006
HI	Finland	Karjaa - Karis	0.197	44	0.009
HI	Finland	Karkkila - Högfors	0.243	36	0.009

Region	Country	City	area	density	population
			(10 ³ km ²)	(10 ³ pers./km ²)	(millions)
HI	Finland	Kaskinen - Kaskö	0.010	177	0.002
HI	Finland	Kauhava	0.483	18	0.009
HI	Finland	Kauniainen - Grankulla	0.006	1338	0.008
HI	Finland	Kemi	0.091	282	0.026
HI	Finland	Kemijärvi	3.568	3	0.012
HI	Finland	Kerava - Kervo	0.031	882	0.027
HI	Finland	Keuruu	1.261	10	0.013
HI	Finland	Kokkola - Karleby	0.328	106	0.035
HI	Finland	Kotka	0.268	212	0.057
HI	Finland	Kouvola	0.044	722	0.032
HI	Finland	Kristiinankaupunki - Kristinestad	0.679	13	0.009
HI	Finland	Kuhmo	4.821	3	0.013
HI	Finland	Kuopio	0.779	103	0.080
HI	Finland	Kurikka	0.463	25	0.011
HI	Finland	Kuusankoski	0.114	191	0.022
HI	Finland	Lahti - Lahtis	0.135	690	0.093
HI	Finland	Lappeenranta - Villmanstrand	0.760	72	0.055
HI	Finland	Lapua - Lappo	0.738	20	0.015
HI	Finland	Lieksa	3.425	5	0.018
HI	Finland	Lohja - Lojo	0.016	962	0.015
HI	Finland	Loviisa - Lovisa	0.045	191	0.008
HI	Finland	Maarianhamina - Mariehamn	0.012	872	0.010
HI	Finland	Mänttä	0.064	120	0.008
HI	Finland	Mikkeli - St. Michel	0.089	359	0.032
HI	Finland	Nokia	0.289	89	0.026
HI	Finland	Nurmes	1.606	7	0.011
HI	Finland	Orivesi	0.545	17	0.009
HI	Finland	Oulainen	0.589	14	0.008
HI	Finland	Oulu - Uleaborg	0.328	306	0.100
HI	Finland	Outokumpu	0.445	21	0.009
HI	Finland	Pieksämäki	0.036	391	0.014
HI	Finland	Pietarsaari - Jakobstad	0.087	228	0.020

Region	Country	City	area	density	population
			(10 ³ km ²)	(10 ³ pers./km ²)	(millions)
HI	Finland	Porvoo - Borga	0.019	1062	0.020
HI	Finland	Raahe - Brahestad	0.269	69	0.019
HI	Finland	Raisio - Reso	0.049	422	0.021
HI	Finland	Rauma - Raumo	0.051	590	0.030
HI	Finland	Riihimäki	0.121	206	0.025
HI	Finland	Rovaniemi	0.094	350	0.033
HI	Finland	Saarijärvi	0.888	12	0.011
HI	Finland	Savonlinna - Nyslott	0.821	35	0.029
HI	Finland	Seinäjoki	0.129	213	0.028
HI	Finland	Suolahti	0.058	107	0.006
HI	Finland	Suonenjoki	0.720	12	0.009
HI	Finland	Tammisaari - Ekenäs	0.278	41	0.011
HI	Finland	Tampere - Tammerfors	0.523	328	0.172
HI	Finland	Toijala	0.051	161	0.008
HI	Finland	Tornio - Tornea	1.182	19	0.023
HI	Finland	Turku - Abo	0.243	655	0.159
HI	Finland	Uusikaarlepyy - Nykarleby	0.722	11	0.008
HI	Finland	Vaasa - Vasa	0.183	291	0.053
HI	Finland	Valkeakoski	0.273	81	0.022
HI	Finland	Vantaa - Vanda	0.241	632	0.152
HI	Finland	Varkaus	0.087	283	0.025
HI	Finland	Virrat - Virdois	1.163	8	0.009
HI	Finland	Ylivieska	0.566	23	0.013
HI	France	Agen	0.176	386	0.068
HI	France	Ajaccio	0.089	659	0.059
HI	France	Albi	0.099	650	0.064
HI	France	Ales	0.200	385	0.077
HI	France	Amiens	0.112	1390	0.156
HI	France	Angers	0.195	1068	0.208
HI	France	Angouleme	0.164	629	0.103
HI	France	Annecy	0.141	901	0.127
HI	France	Armentieres (partie française)	0.093	621	0.058

Region	Country	City	area	density	population
			(10 ³ km ²)	(10 ³ pers./km ²)	(millions)
HI	France	Arles	0.799	68	0.054
HI	France	Arras	0.081	985	0.080
HI	France	Avignon	0.286	634	0.181
HI	France	Bastia	0.051	1019	0.052
HI	France	Bayonne	0.211	778	0.164
HI	France	Beauvais	0.070	823	0.058
HI	France	Belfort	0.081	966	0.078
HI	France	Besancon	0.097	1263	0.123
HI	France	Bethune	0.384	681	0.262
HI	France	Beziers	0.125	610	0.076
HI	France	Blois	0.111	589	0.065
HI	France	Bordeaux	0.821	848	0.696
HI	France	Boulogne-sur-Mer	0.081	1128	0.091
HI	France	Bourg-en-Bresse	0.102	545	0.056
HI	France	Bourges	0.141	674	0.095
HI	France	Brest	0.199	1010	0.201
HI	France	Brive-la-Gaillarde	0.123	524	0.064
HI	France	Caen	0.121	1583	0.191
HI	France	Calais	0.136	746	0.102
HI	France	Cayenne	0.070	757	0.053
HI	France	Chalon-sur-Saone	0.088	880	0.078
HI	France	Chalons-sur-Marne	0.075	821	0.061
HI	France	Chambery	0.135	767	0.103
HI	France	Charleville-Mezieres	0.071	945	0.067
HI	France	Chartres	0.066	1306	0.086
HI	France	Chateauroux	0.172	389	0.067
HI	France	Cherbourg	0.069	1343	0.092
HI	France	Cholet	0.088	630	0.055
HI	France	Clermont-Ferrand	0.181	1407	0.254
HI	France	Compiègne	0.122	549	0.067
HI	France	Creil	0.095	1018	0.097
HI	France	Dijon	0.149	1549	0.230
HI	France	Douai	0.202	988	0.200

Region	Country	City	area	density	population
			(10 ³ km ²)	(10 ³ pers./km ²)	(millions)
HI	France	Dunkerque	0.183	1042	0.191
HI	France	Elbeuf	0.062	869	0.054
HI	France	Epinal	0.118	528	0.062
HI	France	Evreux	0.059	989	0.058
HI	France	Forbach (partie française)	0.090	1093	0.099
HI	France	Fort-de-France	0.109	1233	0.134
HI	France	Frejus	0.219	338	0.074
HI	France	Geneve - Annemasse	0.117	842	0.099
HI	France	Grasse - Cannes - Antibes	0.341	983	0.336
HI	France	Grenoble	0.304	1331	0.405
HI	France	Hagondange-Briey	0.174	645	0.112
HI	France	La Rochelle	0.082	1226	0.100
HI	France	Laval	0.066	857	0.057
HI	France	Le Havre	0.145	1751	0.254
HI	France	Le Mans	0.187	1011	0.189
HI	France	Lens	0.268	1205	0.323
HI	France	Lille (partie française)	0.391	2456	0.959
HI	France	Limoges	0.199	853	0.170
HI	France	Lorient	0.089	1293	0.115
HI	France	Lyon	0.818	1544	1.262
HI	France	Marseille - Aix-en-Provence	0.940	1309	1.231
HI	France	Martigues	0.115	632	0.072
HI	France	Maubeuge (partie française)	0.118	872	0.103
HI	France	Meaux	0.056	1119	0.063
HI	France	Melun	0.060	1794	0.108
HI	France	Menton - Monaco (française)	0.074	899	0.066
HI	France	Metz	0.147	1315	0.193
HI	France	Montargis	0.113	466	0.053
HI	France	Montauban	0.140	379	0.053
HI	France	Montbeliard	0.140	838	0.118
HI	France	Montlucon	0.118	534	0.063

Region	Country	City	area	density	population
			(10 ³ km ²)	(10 ³ pers./km ²)	(millions)
HI	France	Montpellier	0.106	2335	0.248
HI	France	Mulhouse	0.194	1156	0.224
HI	France	Nancy	0.268	1230	0.329
HI	France	Nantes	0.459	1080	0.496
HI	France	Nevers	0.106	556	0.059
HI	France	Nice	0.243	2127	0.517
HI	France	Nimes	0.202	687	0.139
HI	France	Niort	0.101	651	0.066
HI	France	Orleans	0.289	840	0.243
HI	France	Paris	2.377	3920	9.319
HI	France	Pau	0.172	843	0.145
HI	France	Perigueux	0.136	465	0.063
HI	France	Perpignan	0.133	1185	0.158
HI	France	Pointe-a-Pitre-Les- Abymes	0.175	710	0.124
HI	France	Poitiers	0.149	720	0.108
HI	France	Quimper	0.094	704	0.066
HI	France	Reims	0.080	2588	0.206
HI	France	Rennes	0.171	1430	0.245
HI	France	Roanne	0.123	628	0.077
HI	France	Rouen	0.247	1539	0.380
HI	France	Saint-Brieuc	0.118	712	0.084
HI	France	Saint-Chamond	0.134	609	0.082
HI	France	Saint-Denis	0.143	854	0.122
HI	France	Saint-Etienne	0.212	1479	0.313
HI	France	Saint-Nazaire	0.281	468	0.132
HI	France	Saint-Omer	0.093	586	0.055
HI	France	Saint-Paul	0.241	297	0.072
HI	France	Saint-Pierre	0.096	613	0.059
HI	France	Saint-Quentin	0.042	1695	0.071
HI	France	Sete	0.066	972	0.064
HI	France	Strasbourg (partie française)	0.171	2272	0.388
HI	France	Tarbes	0.079	1015	0.081

Region	Country	City	area	density	population
			(10 ³ km ²)	(10 ³ pers./km ²)	(millions)
HI	France	Thionville	0.138	963	0.132
HI	France	Thonon-les-Bains	0.101	546	0.055
HI	France	Toulon	0.464	942	0.438
HI	France	Toulouse	0.618	1052	0.650
HI	France	Tours	0.382	738	0.282
HI	France	Troyes	0.105	1167	0.123
HI	France	Valence	0.110	978	0.108
HI	France	Valenciennes (partie française)	0.448	755	0.338
HI	France	Vichy	0.114	540	0.062
HI	France	Villefranche-sur-Saone	0.079	697	0.055
HI	Germany	Aachen	0.161	1542	0.248
HI	Germany	Amberg	0.050	872	0.04
HI	Germany	Ansbach	0.100	399	0.040
HI	Germany	Aschaffenburg	0.063	1057	0.066
HI	Germany	Augsburg	0.147	1765	0.260
HI	Germany	Baden-Baden	0.140	376	0.053
HI	Germany	Bamberg	0.055	1275	0.070
HI	Germany	Bayreuth	0.067	1092	0.073
HI	Germany	Berlin	0.891	3897	3.472
HI	Germany	Bielefeld	0.258	1258	0.324
HI	Germany	Bochum	0.145	2753	0.400
HI	Germany	Bonn	0.141	2064	0.291
HI	Germany	Bottrop	0.101	1199	0.121
HI	Germany	Brandenburg an der Havel	0.208	413	0.086
HI	Germany	Braunschweig	0.192	1315	0.253
HI	Germany	Bremen	0.327	1682	0.549
HI	Germany	Bremerhaven	0.078	1679	0.130
HI	Germany	Chemnitz	0.143	1865	0.267
HI	Germany	Coburg	0.048	918	0.044
HI	Germany	Cottbus	0.150	820	0.123
HI	Germany	Darmstadt	0.122	1137	0.139
HI	Germany	Delmenhorst	0.062	1254	0.078

Region	Country	City	area	density	population
			(10 ³ km ²)	(10 ³ pers./km ²)	(millions)
HI	Germany	Dessau	0.148	622	0.092
HI	Germany	Dortmund	0.280	2137	0.599
HI	Germany	Dresden	0.226	2078	0.469
HI	Germany	Duisburg	0.233	2299	0.535
HI	Germany	Düsseldorf	0.217	2632	0.571
HI	Germany	Emden	0.113	458	0.052
HI	Germany	Erfurt	0.269	785	0.211
HI	Germany	Erlangen	0.077	1318	0.101
HI	Germany	Essen	0.210	2923	0.615
HI	Germany	Flensburg	0.056	1546	0.087
HI	Germany	Frankenthal (Pfalz)	0.044	1105	0.048
HI	Germany	Frankfurt (Oder)	0.148	547	0.081
HI	Germany	Frankfurt am Main	0.248	2618	0.650
HI	Germany	Freiburg im Breisgau	0.153	1302	0.199
HI	Germany	Fürth	0.063	1712	0.108
HI	Germany	Gelsenkirchen	0.105	2777	0.291
HI	Germany	Gera	0.152	813	0.124
HI	Germany	Görlitz	0.044	1499	0.066
HI	Germany	Greifswald	0.050	1211	0.061
HI	Germany	Hagen	0.160	1322	0.212
HI	Germany	Halle / Saale	0.134	2147	0.287
HI	Germany	Hamburg	0.755	2261	1.708
HI	Germany	Hamm	0.226	811	0.183
HI	Germany	Hannover	0.204	2563	0.523
HI	Germany	Heidelberg	0.109	1275	0.139
HI	Germany	Heilbronn	0.100	1217	0.122
HI	Germany	Herne	0.051	3499	0.180
HI	Germany	Hof	0.058	908	0.053
HI	Germany	Hoyerswerda	0.081	742	0.060
HI	Germany	Ingolstadt	0.133	840	0.112
HI	Germany	Jena	0.114	885	0.101
HI	Germany	Kaiserslautern	0.140	730	0.102
HI	Germany	Karlsruhe	0.174	1589	0.276

Region	Country	City	area	density	population
			(10 ³ km ²)	(10 ³ pers./km ²)	(millions)
HI	Germany	Kassel	0.107	1888	0.202
HI	Germany	Kaufbeuren	0.040	1068	0.043
HI	Germany	Kempten (Allgäu)	0.063	974	0.062
HI	Germany	Kiel	0.117	2106	0.246
HI	Germany	Koblenz	0.105	1039	0.109
HI	Germany	Köln	0.405	2384	0.966
HI	Germany	Krefeld	0.138	1815	0.250
HI	Germany	Landau in der Pfalz	0.083	480	0.040
HI	Germany	Landshut	0.066	901	0.059
HI	Germany	Leipzig	0.153	3075	0.471
HI	Germany	Leverkusen	0.079	2058	0.162
HI	Germany	Lübeck	0.214	1013	0.217
HI	Germany	Ludwigshafen am Rhein	0.078	2155	0.167
HI	Germany	Magdeburg	0.193	1361	0.262
HI	Germany	Mainz	0.098	1880	0.184
HI	Germany	Mannheim	0.145	2147	0.311
HI	Germany	Memmingen	0.070	578	0.041
HI	Germany	Mönchengladbach	0.170	1565	0.267
HI	Germany	Mülheim an der Ruhr	0.091	1934	0.177
HI	Germany	München	0.311	3982	1.237
HI	Germany	Münster	0.303	875	0.265
HI	Germany	Neubrandenburg	0.086	940	0.081
HI	Germany	Neumünster	0.072	1146	0.082
HI	Germany	Neustadt an der Weinstraße	0.117	459	0.054
HI	Germany	Nürnberg	0.186	2650	0.492
HI	Germany	Oberhausen	0.077	2913	0.224
HI	Germany	Offenbach am Main	0.045	2599	0.116
HI	Germany	Oldenburg	0.103	1470	0.151
HI	Germany	Osnabrück	0.120	1408	0.169
HI	Germany	Passau	0.070	730	0.051
HI	Germany	Pforzheim	0.098	1214	0.119
HI	Germany	Pirmasens	0.061	788	0.048
HI	Germany	Plauen	0.068	1000	0.068

Region	Country	City	area	density	population
			(10 ³ km ²)	(10 ³ pers./km ²)	(millions)
HI	Germany	Potsdam	0.109	1249	0.137
HI	Germany	Regensburg	0.081	1557	0.126
HI	Germany	Remscheid	0.075	1639	0.122
HI	Germany	Rosenheim	0.037	1583	0.059
HI	Germany	Rostock	0.181	1260	0.228
HI	Germany	Saarbrücken	0.411	872	0.358
HI	Germany	Salzgitter	0.224	526	0.118
HI	Germany	Schwabach	0.041	925	0.038
HI	Germany	Schweinfurt	0.036	1559	0.056
HI	Germany	Schwerin	0.130	881	0.115
HI	Germany	Solingen	0.090	1853	0.166
HI	Germany	Speyer	0.043	1166	0.050
HI	Germany	Stralsund	0.039	1706	0.066
HI	Germany	Straubing	0.068	654	0.044
HI	Germany	Stuttgart	0.207	2824	0.585
HI	Germany	Suhl	0.103	522	0.054
HI	Germany	Trier	0.117	849	0.099
HI	Germany	Ulm	0.119	975	0.116
HI	Germany	Weiden in der OberPfalz	0.069	631	0.043
HI	Germany	Weimar	0.084	737	0.062
HI	Germany	Wiesbaden	0.204	1310	0.267
HI	Germany	Wilhelmshaven	0.103	877	0.091
HI	Germany	Wismar	0.042	1212	0.050
HI	Germany	Wolfsburg	0.204	619	0.126
HI	Germany	Worms	0.109	736	0.080
HI	Germany	Wuppertal	0.168	2268	0.382
HI	Germany	Würzburg	0.088	1452	0.127
HI	Germany	Zweibrücken	0.071	512	0.036
HI	Germany	Zwickau	0.060	1713	0.103
HI	Greece	Athens	0.427	2074	0.886
HI	Italy	Milan	0.182	7500	1.365
HI	Italy	Rome	1.507	1958	2.950
HI	Italy	Trieste	0.212	1119	0.237

Region	Country	City	area	density	population
			(10 ³ km ²)	(10 ³ pers./km ²)	(millions)
HI	Netherlands	Amsterdam	0.636	1644	1.045
HI	Netherlands	Arnhem	0.375	802	0.301
HI	Netherlands	Breda	0.175	909	0.159
HI	Netherlands	Dordrecht/Zwijndrecht	0.135	1532	0.206
HI	Netherlands	Eindhoven	0.450	853	0.384
HI	Netherlands	Enschede/Hengelo	0.252	997	0.251
HI	Netherlands	Geleen/Sittard	0.245	732	0.180
HI	Netherlands	Groningen	0.196	1057	0.207
HI	Netherlands	Haarlem	0.110	1938	0.214
HI	Netherlands	The Hague / Den Haag	0.213	3223	0.685
HI	Netherlands	Heerlen/Kerkrade	0.212	1263	0.267
HI	Netherlands	's-Hertogenbosch	0.238	825	0.196
HI	Netherlands	Hilversum	0.083	1234	0.102
HI	Netherlands	Leiden	0.084	2226	0.187
HI	Netherlands	Maastricht	0.161	1005	0.162
HI	Netherlands	Nijmegen	0.274	884	0.243
HI	Netherlands	Rotterdam	0.422	2473	1.044
HI	Netherlands	Tilburg	0.274	834	0.229
HI	Netherlands	Utrecht	0.440	1206	0.530
HI	Netherlands	Velsen/Beverwijk	0.091	1396	0.127
HI	Netherlands	Zaanstreek	0.094	1507	0.142
HI	Norway	Alta	0.008	1172	0.01
HI	Norway	Arendal	0.024	1045	0.025
HI	Norway	Askim	0.007	1596	0.011
HI	Norway	Askoy	0.014	988	0.013
HI	Norway	Bergen	0.085	2210	0.187
HI	Norway	Bodo	0.013	2334	0.030
HI	Norway	Drammen	0.046	1279	0.059
HI	Norway	Drobak	0.007	1309	0.009
HI	Norway	Egersund	0.006	1231	0.007
HI	Norway	Elverum	0.012	929	0.011
HI	Norway	Gjovik	0.012	1304	0.016
HI	Norway	Grimstad	0.009	889	0.008

Region	Country	City	area	density	population
			(10 ³ km ²)	(10 ³ pers./km ²)	(millions)
HI	Norway	Halden	0.013	1612	0.020
HI	Norway	Hamar	0.016	1691	0.028
HI	Norway	Harstad	0.011	1489	0.016
HI	Norway	Haugesund	0.021	1526	0.033
HI	Norway	Honefoss	0.009	1138	0.011
HI	Norway	Horten	0.008	2031	0.016
HI	Norway	Jessheim	0.006	1031	0.006
HI	Norway	Kongsberg	0.012	1274	0.015
HI	Norway	Kongsvinger	0.008	1438	0.011
HI	Norway	Kristiansand	0.029	1871	0.054
HI	Norway	Kristiansund	0.008	2249	0.017
HI	Norway	Larvik	0.013	1584	0.021
HI	Norway	Leirvik	0.008	1276	0.010
HI	Norway	Lillehammer	0.011	1509	0.017
HI	Norway	Mandal	0.006	1403	0.009
HI	Norway	Mo i Rana	0.011	1739	0.019
HI	Norway	Molde	0.009	1896	0.017
HI	Norway	Mosjoen	0.006	1592	0.009
HI	Norway	Moss	0.016	1847	0.029
HI	Norway	Namsos	0.007	1298	0.008
HI	Norway	Narvik	0.006	2168	0.014
HI	Norway	Nesoddtangen	0.006	1439	0.009
HI	Norway	Notodden	0.007	1151	0.008
HI	Norway	Oslo	0.266	2578	0.686
HI	Norway	Sandefjord	0.024	1341	0.033
HI	Norway	Ski	0.006	1704	0.011
HI	Norway	Steinkjer	0.008	1220	0.010
HI	Norway	Stjordalshalsen	0.006	1591	0.009
HI	Norway	Tonsberg	0.029	1313	0.038
HI	Norway	Tromso	0.021	1993	0.042
HI	Norway	Trondheim	0.058	2254	0.131
HI	Portugal	Lisbon	0.087	6161	0.536
HI	Spain	Madrid	0.605	8661	5.240

Region	Country	City	area	density	population
			(10 ³ km ²)	(10 ³ pers./km ²)	(millions)
HI	Sweden	Stockholm	0.188	3588	0.674
HI	Switzerland	Basel	0.024	7464	0.178
HI	Switzerland	Bern	0.052	2641	0.136
HI	Switzerland	Biel / Bienne	0.021	2448	0.052
HI	Switzerland	Chur	0.028	1171	0.033
HI	Switzerland	Fribourg	0.009	3914	0.036
HI	Switzerland	Geneve	0.016	10755	0.171
HI	Switzerland	Köniz	0.051	731	0.037
HI	Switzerland	La Chaux-de-Fonds	0.056	662	0.037
HI	Switzerland	Lausanne	0.041	3094	0.128
HI	Switzerland	Luzern	0.016	3861	0.061
HI	Switzerland	Neuchatel	0.018	1856	0.034
HI	Switzerland	Schaffhausen	0.031	1103	0.034
HI	Switzerland	St. Gallen	0.039	1909	0.075
HI	Switzerland	Thun	0.022	1769	0.038
HI	Switzerland	Winterthur	0.068	1281	0.087
HI	Switzerland	Zürich	0.088	4171	0.365
HI	United Kingdom	Aberdeen	0.184	1145	0.211
HI	United Kingdom	Ashford	0.581	165	0.096
HI	United Kingdom	Aylesbury Vale	0.904	163	0.147
HI	United Kingdom	Barnsley	0.329	674	0.222
HI	United Kingdom	Barrow-in-Furness	0.077	932	0.072
HI	United Kingdom	Basildon	0.111	1414	0.157
HI	United Kingdom	Bath	0.029	2921	0.085
HI	United Kingdom	Belfast	0.130	2284	0.297
HI	United Kingdom	Berwick-upon-Tweed	0.975	27	0.026
HI	United Kingdom	Beverley	0.404	285	0.115
HI	United Kingdom	Birmingham	0.264	3759	0.993
HI	United Kingdom	Blackburn	0.137	991	0.136
HI	United Kingdom	Blackpool	0.035	4089	0.143
HI	United Kingdom	Blyth Valley	0.070	1136	0.080
HI	United Kingdom	Bolton	0.140	1893	0.265
HI	United Kingdom	Boston	0.360	146	0.052

Region	Country	City	area	density	population
			(10 ³ km ²)	(10 ³ pers./km ²)	(millions)
HI	United Kingdom	Bournemouth	0.046	3354	0.154
HI	United Kingdom	Bracknell	0.109	960	0.105
HI	United Kingdom	Bradford	0.370	1264	0.468
HI	United Kingdom	Brentwood	0.149	463	0.069
HI	United Kingdom	Brighton	0.058	2467	0.143
HI	United Kingdom	Bristol	0.110	3387	0.373
HI	United Kingdom	Bromsgrove	0.220	404	0.089
HI	United Kingdom	Burnley	0.118	770	0.091
HI	United Kingdom	Bury	0.099	1782	0.176
HI	United Kingdom	Cambridge	0.041	2415	0.099
HI	United Kingdom	Cannock Chase	0.079	1124	0.089
HI	United Kingdom	Canterbury	0.311	423	0.132
HI	United Kingdom	Cardiff	0.120	2374	0.285
HI	United Kingdom	Carlisle	1.030	100	0.103
HI	United Kingdom	Carmarthen	1.180	48	0.057
HI	United Kingdom	Carrickfergus	0.085	358	0.030
HI	United Kingdom	Castle Morpeth	0.619	81	0.050
HI	United Kingdom	Chelmsford	0.342	442	0.151
HI	United Kingdom	Cheltenham	0.035	2457	0.086
HI	United Kingdom	Chester	0.448	255	0.114
HI	United Kingdom	Chesterfield	0.066	1518	0.100
HI	United Kingdom	Chichester	0.787	135	0.106
HI	United Kingdom	Chorley	0.205	472	0.097
HI	United Kingdom	Christchurch	0.050	796	0.040
HI	United Kingdom	Clackmannan	0.160	295	0.047
HI	United Kingdom	Cleethorpes	0.164	416	0.068
HI	United Kingdom	Clydebank	0.035	1349	0.047
HI	United Kingdom	Colchester	0.334	455	0.152
HI	United Kingdom	Corby	0.080	644	0.052
HI	United Kingdom	Coventry	0.097	3135	0.304
HI	United Kingdom	Crawley	0.036	2347	0.085
HI	United Kingdom	Crewe and Nantwich	0.431	232	0.100
HI	United Kingdom	Cumbernauld and Kilsyth	0.103	610	0.063

Region	Country	City	area	density	population
			(10 ³ km ²)	(10 ³ pers./km ²)	(millions)
HI	United Kingdom	Darlington	0.198	505	0.100
HI	United Kingdom	Dartford	0.070	1120	0.078
HI	United Kingdom	Daventry	0.666	97	0.064
HI	United Kingdom	Derby	0.078	2777	0.217
HI	United Kingdom	Doncaster	0.582	504	0.293
HI	United Kingdom	Dover	0.312	343	0.107
HI	United Kingdom	Dudley	0.098	3116	0.305
HI	United Kingdom	Dundee	0.235	734	0.173
HI	United Kingdom	Dunfermline	0.302	430	0.130
HI	United Kingdom	Durham	0.190	453	0.086
HI	United Kingdom	Eastbourne	0.044	1882	0.083
HI	United Kingdom	Eastleigh	0.080	1278	0.102
HI	United Kingdom	Edinburgh	0.261	1660	0.433
HI	United Kingdom	Ellesmere Port and Neston	0.082	967	0.079
HI	United Kingdom	Epsom and Ewell	0.034	2012	0.068
HI	United Kingdom	Exeter	0.044	2325	0.102
HI	United Kingdom	Falkirk	0.291	492	0.143
HI	United Kingdom	Fareham	0.074	1370	0.101
HI	United Kingdom	Gateshead	0.143	1439	0.206
HI	United Kingdom	Gillingham	0.032	2956	0.095
HI	United Kingdom	Glasgow	0.198	3513	0.696
HI	United Kingdom	Gloucester	0.033	2742	0.091
HI	United Kingdom	Gosport	0.025	3060	0.077
HI	United Kingdom	Great Grimsby	0.028	3221	0.090
HI	United Kingdom	Great Yarmouth	0.173	520	0.090
HI	United Kingdom	Guildford	0.271	454	0.123
HI	United Kingdom	Halton	0.074	1686	0.125
HI	United Kingdom	Hamilton	0.131	819	0.107
HI	United Kingdom	Harlow	0.026	2742	0.071
HI	United Kingdom	Harrogate	1.334	111	0.148
HI	United Kingdom	Hartlepool	0.094	944	0.089
HI	United Kingdom	Hastings	0.030	2757	0.083
HI	United Kingdom	Havant	0.056	2077	0.116

Region	Country	City	area	density	population
			(10 ³ km ²)	(10 ³ pers./km ²)	(millions)
HI	United Kingdom	Hereford	0.020	2470	0.049
HI	United Kingdom	Hinckley and Bosworth	0.297	329	0.098
HI	United Kingdom	Hove	0.024	3796	0.091
HI	United Kingdom	Huntingdon	0.924	161	0.149
HI	United Kingdom	Ipswich	0.040	2843	0.114
HI	United Kingdom	Isle of Wight	0.381	343	0.131
HI	United Kingdom	Kettering	0.234	321	0.075
HI	United Kingdom	Kilmarnock and Loudoun	0.373	217	0.081
HI	United Kingdom	Kingston upon Hull	0.071	3452	0.245
HI	United Kingdom	Kirkcaldy	0.248	592	0.147
HI	United Kingdom	Kirklees	0.410	916	0.376
HI	United Kingdom	Knowsley	0.097	1624	0.158
HI	United Kingdom	Lancaster	0.577	227	0.131
HI	United Kingdom	Langbaurgh	0.240	602	0.145
HI	United Kingdom	Leeds	0.562	1266	0.712
HI	United Kingdom	Leicester	0.073	3832	0.280
HI	United Kingdom	Lewes	0.292	313	0.091
HI	United Kingdom	Lichfield	0.330	282	0.093
HI	United Kingdom	Lincoln	0.036	2247	0.081
HI	United Kingdom	Liverpool	0.113	4123	0.466
HI	United Kingdom	Lisburn	0.436	223	0.097
HI	United Kingdom	Llanelli	0.233	321	0.075
HI	United Kingdom	London (Greater L.)	1.579	4279	6.756
HI	United Kingdom	Luton	0.043	3951	0.170
HI	United Kingdom	Macclesfield	0.523	290	0.152
HI	United Kingdom	Maidstone	0.394	349	0.137
HI	United Kingdom	Maldon	0.358	149	0.053
HI	United Kingdom	Malvern Hills	0.902	98	0.088
HI	United Kingdom	Manchester	0.116	3824	0.444
HI	United Kingdom	Mansfield	0.077	1309	0.101
HI	United Kingdom	Merthyr Tydfil	0.111	528	0.059
HI	United Kingdom	Middlesbrough	0.054	2643	0.143
HI	United Kingdom	Milton Keynes	0.310	588	0.182

Region	Country	City	area	density	population
			(10 ³ km ²)	(10 ³ pers./km ²)	(millions)
HI	United Kingdom	Monmouth	0.833	97	0.081
HI	United Kingdom	Newark	0.662	156	0.104
HI	United Kingdom	Newbury	0.705	197	0.139
HI	United Kingdom	Newcastle-under-Lyme	0.211	560	0.118
HI	United Kingdom	Newcastle upon Tyne	0.112	2479	0.278
HI	United Kingdom	Newport	0.190	675	0.128
HI	United Kingdom	Newry and Mourne	0.886	100	0.089
HI	United Kingdom	Newtownabbey	0.151	483	0.073
HI	United Kingdom	Northampton	0.081	2272	0.184
HI	United Kingdom	North Tyneside	0.084	2294	0.193
HI	United Kingdom	Norwich	0.039	3010	0.117
HI	United Kingdom	Nottingham	0.074	3696	0.274
HI	United Kingdom	Nuneaton and Bedworth	0.079	1477	0.117
HI	United Kingdom	Oldham	0.141	1565	0.221
HI	United Kingdom	Oxford	0.036	3236	0.117
HI	United Kingdom	Peterborough	0.334	460	0.154
HI	United Kingdom	Plymouth	0.079	3228	0.255
HI	United Kingdom	Portsmouth	0.037	4973	0.184
HI	United Kingdom	Port Talbot	0.152	321	0.049
HI	United Kingdom	Poole	0.064	2055	0.132
HI	United Kingdom	Preston	0.142	904	0.128
HI	United Kingdom	Reading	0.040	3250	0.130
HI	United Kingdom	Redditch	0.054	1446	0.078
HI	United Kingdom	Reigate and Banstead	0.129	891	0.115
HI	United Kingdom	Renfrew	0.307	653	0.201
HI	United Kingdom	Rhondda	0.100	768	0.077
HI	United Kingdom	Rochdale	0.160	1298	0.208
HI	United Kingdom	Rochester-upon-Medway	0.160	924	0.148
HI	United Kingdom	Rotherham	0.283	896	0.254
HI	United Kingdom	Rugby	0.356	241	0.086
HI	United Kingdom	Runnymede	0.078	904	0.071
HI	United Kingdom	Salford	0.097	2419	0.235
HI	United Kingdom	Salisbury	1.005	100	0.101

Region	Country	City	area	density	population
			(10 ³ km ²)	(10 ³ pers./km ²)	(millions)
HI	United Kingdom	Sandwell	0.086	3436	0.296
HI	United Kingdom	Scarborough	0.817	130	0.106
HI	United Kingdom	Scunthorpe	0.034	1753	0.060
HI	United Kingdom	Sefton	0.151	1984	0.300
HI	United Kingdom	Selby	0.725	129	0.094
HI	United Kingdom	Sheffield	0.368	1431	0.527
HI	United Kingdom	Shrewsbury and Atcham	0.603	151	0.091
HI	United Kingdom	Slough	0.028	3607	0.101
HI	United Kingdom	Solihull	0.180	1136	0.204
HI	United Kingdom	Southampton	0.049	4033	0.198
HI	United Kingdom	Southend-on-Sea	0.042	3952	0.166
HI	United Kingdom	South Tyneside	0.064	2434	0.156
HI	United Kingdom	Stafford	0.599	199	0.119
HI	United Kingdom	Stevenage	0.025	2960	0.074
HI	United Kingdom	St Helens	0.133	1420	0.189
HI	United Kingdom	Stockport	0.126	2312	0.291
HI	United Kingdom	Stockton-on-Tees	0.195	907	0.177
HI	United Kingdom	Stoke-on-Trent	0.093	2658	0.247
HI	United Kingdom	Stratford-on-Avon	0.977	108	0.106
HI	United Kingdom	Sunderland	0.138	2146	0.296
HI	United Kingdom	Swansea	0.246	758	0.186
HI	United Kingdom	Tamworth	0.031	2226	0.069
HI	United Kingdom	Taunton Deane	0.458	207	0.095
HI	United Kingdom	Tewkesbury	0.450	196	0.088
HI	United Kingdom	Thanet	0.103	1275	0.131
HI	United Kingdom	The Wrekin	0.291	468	0.136
HI	United Kingdom	Three Rivers	0.088	913	0.080
HI	United Kingdom	Tonbridge and Malling	0.240	418	0.100
HI	United Kingdom	Torbay	0.063	1906	0.120
HI	United Kingdom	York	0.029	3490	0.101
HI	United Kingdom	Wakefield	0.333	944	0.314
HI	United Kingdom	Walsall	0.106	2487	0.264
HI	United Kingdom	Warrington	0.176	1068	0.188

Region	Country	City	area	density	population
			(10 ³ km ²)	(10 ³ pers./km ²)	(millions)
HI	United Kingdom	Warwick	0.283	407	0.115
HI	United Kingdom	Watford	0.021	3605	0.076
HI	United Kingdom	Wellingborough	0.163	410	0.067
HI	United Kingdom	Weymouth and Portland	0.042	1540	0.065
HI	United Kingdom	Wigan	0.199	1556	0.310
HI	United Kingdom	Winchester	0.659	145	0.096
HI	United Kingdom	Windsor and Maidenhead	0.198	632	0.125
HI	United Kingdom	Wirral	0.158	2128	0.336
HI	United Kingdom	Woking	0.064	1339	0.086
HI	United Kingdom	Wolverhampton	0.069	3622	0.250
HI	United Kingdom	Worcester	0.032	2566	0.082
HI	United Kingdom	Worthing	0.033	2991	0.099
HI	United Kingdom	Wrexham Maelor	0.366	319	0.117

Region	Country	City	area	density	population
			(10 ³ km ²)	(10 ³ pers./km ²)	(millions)
LAC	Argentina	Buenos Aires	0.200	14540	2.908
LAC	Benezuela	Caracas	0.230	17791	4.092
LAC	Bolivia	Cochabamba	0.068	6256	0.425
LAC	Bolivia	El Alto	0.105	4201	0.442
LAC	Bolivia	La Paz	0.116	9817	1.139
LAC	Bolivia	Santa Cruz de la Sierra	0.102	7303	0.742
LAC	Brazil	Curitiba	0.489	4287	2.097
LAC	Brazil	Recife	0.214	12531	2.682
LAC	Brazil	Rio de Janeiro	1.255	4425	5.555
LAC	Brazil	Sao Paulo	1.509	6382	9.630
LAC	Chile	Santiago	2.206	2144	4.730
LAC	Colombia	Bogota	0.482	11035	5.3144
LAC	Colombia	Medellin	0.708	3766	2.666
LAC	Cuba	Camaguey	0.155	1906	0.296
LAC	Cuba	Cienfuegos	0.044	2982	0.131
LAC	Cuba	Havana	0.727	2993	2.176

Region	Country	City	area	density	population
			(10 ³ km ²)	(10 ³ pers./km ²)	(millions)
LAC	Cuba	Pinar del Rio	0.028	4606	0.129
LAC	Dominican Republic	Santo Domingo	0.162	13580	2.200
LAC	Ecuador	Guayaquil	0.178	9962	1.773
LAC	Ecuador	Quito	0.179	9048	1.615
LAC	El Salvador	San Salvador	0.352	3811	1.343
LAC	El Salvador	Santa Ana	0.018	7872	0.142
LAC	Guatemala	Guatemala city	0.259	6840	1.774
LAC	Guyana	George Town	0.019	7864	0.150
LAC	Jamaica	Kingston	0.022	26697	0.582
LAC	Mexico	Guadalajara	0.190	10526	2.000
LAC	Mexico	Mexico City	1.554	12870	20.000
LAC	Paraguay	Asuncion	0.067	14148	0.9493
LAC	Peru	Cajamarca	0.126	732	0.092
LAC	Peru	Lima	0.092	28491	2.627
LAC	Peru	Trujillo	0.070	8078	0.562
LAC	Uruguay	Montevideo	0.191	6776	1.291

A2.3. Statistical references.

Algeria. Statistical Yearbook of Algeria. Edition 1991. Office National des Statistiques, Alger, 387 pp. (in Arab., Fr. and Eng.).

Austria. Bevölkerung und Fläche der Gemeinden mit mindestens 5.000 Einwohnern 1991 und 2001. In: Statistische Jahrbuch Österreichs 2002, Statistik Austria, Wien, 2001, 608 S. See also parallel:
<http://www.statistik.at/jahrbuch/pdf/k02.pdf>

Belarus. Statistical Yearbook of the Republic of Belarus 1997. L.L. Rybchik (Ed.), Ministry of Statistics and Analysis, Minsk, 609 pp. (in Rus. and Eng.). & The Republic of Belarus in Figures, 1990-2001, Population. On:
<http://www.president.gov.by/Minstat/en/indicators/population.htm> &
Statistical Yearbook of the Republic of Belarus 2002. Ministry of Statistics and Analysis, Minsk, 600 pp. (in Rus. and Eng.). Date of publishing: Sept, 2002. See also:
<http://www.president.gov.by/Minstat/en/publications/main.html>

Belgium. Annuaire Statistique de la Belgique 1991. Institut National de Statistique, Ministère des Affaires Economiques, Bruxelles, 792 pp.

Bulgaria. Population on 31.12.1999 & 01.03.2001 (in Bulg.). On:
<http://www.nsi.bg/statistika/Statistics.htm>

Canada. Canada Urbanized Areas: Estimated Population & Land Area: 1996.
On: <http://www.demographia.com/db-canua.htm>

- China.** Statistical Yearbook of China 1991. State Statistical Bureau, China Statistical Publishing House, Zhongguo, Tongji, Nianjian, 858 pp. (in Chin. and Eng.).
- Croatia.** Županije, Površina, Stanovništvo, Gradovi, Općine i Naselja (Teritorijalni Ustroj Prema Stanju 31. Ožujka 2001). In: Statistical Yearbook of the Republic of Croatia 2001, Croatian Bureau of Statistic, Zagreb (in Croat. and Eng.). On: <http://www.dzs.hr/ljetopis2001/02Podat.htm>
- Former Czechoslovakia.** Statistická Ročenka České a Slovenské Federativní Republiky 1991. SEVT, Praha, 745 str. (in Czech).
- Denmark.** Statistik årbog 1991 Statistical Yearbook. Danmarks Statistik, København, 575 pp. (in Dan. and Eng.).
- Egypt.** Statistical Year Book 1990-1995 Arab Republic Of Egypt. Central Agency for Public Mobilization and Statistics (CAPMAS), Nasr City, July 1996, 364 pp.
- Finland.** Statistical Yearbook of Finland 1991. Central Statistical Office of Finland, Helsinki, 598 pp. (in Fin., Swe. and Eng.).
- France.** Annuaire Statistique de la France 1991-92. Résultats de 1991. Institut National de la Statistique et des Études Économiques (INSEE), Paris, 1991, XXIV+824+30* pp.
- Germany.** Statistisches Jahrbuch 1992 für die BRD. Statistisches Bundesamt, Wiesbaden, 764 S. & Kreiszahlen – Ausgewählte Regionaldaten für Deutschland – Ausgabe 1997, Nieder-sächsisches Landesamt für Statistik, 1998, 192 S.

- Greece.** Statistical Yearbook of Greece 1990-1991. National Statistical Service of Greece, Athens, 1994, 567 pp. (in Gr. and Eng.).
- Hungary.** Hungarian Statistical Yearbook 1990. Hungarian Central Statistical Office, Budapest, 1991, 323 pp.
- Israel.** Statistical Abstract of Israel 1991. Central Bureau of Statistics, Jerusalem, 106+761 pp. (abstract + tables: in Ivrit and Eng.).
- Iran.** A Statistical Reflection of the Islamic Republic of Iran. Eighth Issue. Statistical Centre of Iran, Therān, 1991. (The data included in this publication are English translation of some selected information incorporated in the Statistical Yearbook of Iran, which is exclusively published in Farsi).
- Japan.** Japan Statistical Yearbook 1991. Statistics Bureau, Management and Coordination Agency, Japan Statistical Association, Tokyo, 842 pp. (in Japanese and Eng.).
- Kuwait.** Al-Sabah, A.Y.A., 1990. The concentration of population in Kuwait. In: Journal of the Gulf and Arabian Peninsula studies, Kuwait, pp. 320-370. &Annual Statistical Abstract 1997. Edition 34. State of Kuwait, Ministry of Planning, Statistics and Information Sector, 430 pp. (in Arab. and Eng.).
- Morocco.** Morocco in Figures 1993. Direction de la Statistique, Rabat, 147 pp.
- Netherlands.** Statistical Yearbook 1991 of the Netherlands. Central Bureau of Statistics, The Hague, 512 pp.
- Norway.** Urban settlements with 8000 inhabitants or more, Population and area. In: Statistical Yearbook of Norway 2001, Vol. 120, Statistics Norway, Oslo. On: <http://www.ssb.no/www-open/english/yearbook/tab/t-020110-052.html>

Pakistan. Pakistan Statistical Yearbook 1991. Federal Bureau of Statistics, Karachi, 712 pp.

Philippines. 1992 Philippine Statistical Yearbook. National Statistical Coordination Board, Metro Manila, XII+14 pp. + 19 chap.

Switzerland. Kantone und Städte der Schweiz, Statistische Übersichten 2002. Bundesamt für Statistik, Neuchâtel. On:
<http://www.statistik.admin.ch/service-stat/ks2002extrait.pdf>

Ukraine. Statystychnyi Shchorichnyk Ukrainy za 1995 Rik, Statistical Yearbook of Ukraine 1995. V.V. Samchenko (Ed.), Ministry of Statistics of Ukraine, "Technika" Publ., Kyiv, 1996, 576 pp. (in Ukrainian, Preface and Contents in Eng.).

United Kingdom. Regional Trends 26, 1991 Edition. Government Statistical Service, London, 207 pp.

United States. Population of the 100 Largest Urban Places: 1990. U.S. Bureau of the Census, 1998. On:
<http://www.census.gov/population/documentation/twps0027/tab22.txt>

Vietnam. Vietnam Statistical Yearbook 1992. General Statistical Office, Statistical Publishing House, 1993, 267 pp. (in Vietnamese and Eng.).

Yugoslavia. Statistički Godišnjak Jugoslavije 1990. Godina 37. Savezni Zavod za Statistiku, Beograd, 784 str. (in Serbo-Croatian), & Statistical Yearbook of the Socialist Federal Republic of Yugoslavia 1990. 37th issue. Federal Statistical Office, Beograd, 1991, 204 pp. (Note: translated are only Explanations on methodology and the part containing statistical tables relating to Yugoslavia as a whole).

Zaire. South African Statistics 1994. Central Statistical Service, Pretoria, 1 vol.
(various paging, in Afrikaans and Eng.).

PIK Report-Reference:

- No. 1 3. Deutsche Klimatagung, Potsdam 11.-14. April 1994
Tagungsband der Vorträge und Poster (April 1994)
- No. 2 Extremer Nordsommer '92
Meteorologische Ausprägung, Wirkungen auf naturnahe und vom Menschen beeinflusste Ökosysteme, gesellschaftliche Perzeption und situationsbezogene politisch-administrative bzw. individuelle Maßnahmen (Vol. 1 - Vol. 4)
H.-J. Schellnhuber, W. Enke, M. Flechsig (Mai 1994)
- No. 3 Using Plant Functional Types in a Global Vegetation Model
W. Cramer (September 1994)
- No. 4 Interannual variability of Central European climate parameters and their relation to the large-scale circulation
P. C. Werner (Oktober 1994)
- No. 5 Coupling Global Models of Vegetation Structure and Ecosystem Processes - An Example from Arctic and Boreal Ecosystems
M. Plöchl, W. Cramer (Oktober 1994)
- No. 6 The use of a European forest model in North America: A study of ecosystem response to climate gradients
H. Bugmann, A. Solomon (Mai 1995)
- No. 7 A comparison of forest gap models: Model structure and behaviour
H. Bugmann, Y. Xiaodong, M. T. Sykes, Ph. Martin, M. Lindner, P. V. Desanker, S. G. Cumming (Mai 1995)
- No. 8 Simulating forest dynamics in complex topography using gridded climatic data
H. Bugmann, A. Fischlin (Mai 1995)
- No. 9 Application of two forest succession models at sites in Northeast Germany
P. Lasch, M. Lindner (Juni 1995)
- No. 10 Application of a forest succession model to a continentality gradient through Central Europe
M. Lindner, P. Lasch, W. Cramer (Juni 1995)
- No. 11 Possible Impacts of global warming on tundra and boreal forest ecosystems - Comparison of some biogeochemical models
M. Plöchl, W. Cramer (Juni 1995)
- No. 12 Wirkung von Klimaveränderungen auf Waldökosysteme
P. Lasch, M. Lindner (August 1995)
- No. 13 MOSES - Modellierung und Simulation ökologischer Systeme - Eine Sprachbeschreibung mit Anwendungsbeispielen
V. Wenzel, M. Kücken, M. Flechsig (Dezember 1995)
- No. 14 TOYS - Materials to the Brandenburg biosphere model / GAIA
Part 1 - Simple models of the "Climate + Biosphere" system
Yu. Svirezhev (ed.), A. Block, W. v. Bloh, V. Brovkin, A. Ganopolski, V. Petoukhov, V. Razzhevaikin (Januar 1996)
- No. 15 Änderung von Hochwassercharakteristiken im Zusammenhang mit Klimaänderungen - Stand der Forschung
A. Bronstert (April 1996)
- No. 16 Entwicklung eines Instruments zur Unterstützung der klimapolitischen Entscheidungsfindung
M. Leimbach (Mai 1996)
- No. 17 Hochwasser in Deutschland unter Aspekten globaler Veränderungen - Bericht über das DFG-Rundgespräch am 9. Oktober 1995 in Potsdam
A. Bronstert (ed.) (Juni 1996)
- No. 18 Integrated modelling of hydrology and water quality in mesoscale watersheds
V. Krysanova, D.-I. Müller-Wohlfeil, A. Becker (Juli 1996)
- No. 19 Identification of vulnerable subregions in the Elbe drainage basin under global change impact
V. Krysanova, D.-I. Müller-Wohlfeil, W. Cramer, A. Becker (Juli 1996)
- No. 20 Simulation of soil moisture patterns using a topography-based model at different scales
D.-I. Müller-Wohlfeil, W. Lahmer, W. Cramer, V. Krysanova (Juli 1996)
- No. 21 International relations and global climate change
D. Sprinz, U. Luterbacher (1st ed. July, 2nd ed. December 1996)
- No. 22 Modelling the possible impact of climate change on broad-scale vegetation structure - examples from Northern Europe
W. Cramer (August 1996)

- No. 23 A method to estimate the statistical security for cluster separation
F.-W. Gerstengarbe, P.C. Werner (Oktober 1996)
- No. 24 Improving the behaviour of forest gap models along drought gradients
H. Bugmann, W. Cramer (Januar 1997)
- No. 25 The development of climate scenarios
P.C. Werner, F.-W. Gerstengarbe (Januar 1997)
- No. 26 On the Influence of Southern Hemisphere Winds on North Atlantic Deep Water Flow
S. Rahmstorf, M. H. England (Januar 1977)
- No. 27 Integrated systems analysis at PIK: A brief epistemology
A. Bronstert, V. Brovkin, M. Krol, M. Lüdeke, G. Petschel-Held, Yu. Svirezhev, V. Wenzel (März 1997)
- No. 28 Implementing carbon mitigation measures in the forestry sector - A review
M. Lindner (Mai 1997)
- No. 29 Implementation of a Parallel Version of a Regional Climate Model
M. Kücken, U. Schättler (Oktober 1997)
- No. 30 Comparing global models of terrestrial net primary productivity (NPP): Overview and key results
W. Cramer, D. W. Kicklighter, A. Bondeau, B. Moore III, G. Churkina, A. Ruimy, A. Schloss, participants of "Potsdam '95" (Oktober 1997)
- No. 31 Comparing global models of terrestrial net primary productivity (NPP): Analysis of the seasonal behaviour of NPP, LAI, FPAR along climatic gradients across ecotones
A. Bondeau, J. Kaduk, D. W. Kicklighter, participants of "Potsdam '95" (Oktober 1997)
- No. 32 Evaluation of the physiologically-based forest growth model FORSANA
R. Grote, M. Erhard, F. Suckow (November 1997)
- No. 33 Modelling the Global Carbon Cycle for the Past and Future Evolution of the Earth System
S. Franck, K. Kossacki, Ch. Bounama (Dezember 1997)
- No. 34 Simulation of the global bio-geophysical interactions during the Last Glacial Maximum
C. Kubatzki, M. Claussen (Januar 1998)
- No. 35 CLIMBER-2: A climate system model of intermediate complexity. Part I: Model description and performance for present climate
V. Petoukhov, A. Ganopolski, V. Brovkin, M. Claussen, A. Eliseev, C. Kubatzki, S. Rahmstorf (Februar 1998)
- No. 36 Geocybernetics: Controlling a rather complex dynamical system under uncertainty
H.-J. Schellnhuber, J. Kropp (Februar 1998)
- No. 37 Untersuchung der Auswirkungen erhöhter atmosphärischer CO₂-Konzentrationen auf Weizenbestände des Free-Air Carbondioxid Enrichment (FACE) - Experimentes Maricopa (USA)
Th. Kartschall, S. Grossman, P. Michaelis, F. Wechsung, J. Gräfe, K. Waloszczyk, G. Wechsung, E. Blum, M. Blum (Februar 1998)
- No. 38 Die Berücksichtigung natürlicher Störungen in der Vegetationsdynamik verschiedener Klimagebiete
K. Thonicke (Februar 1998)
- No. 39 Decadal Variability of the Thermohaline Ocean Circulation
S. Rahmstorf (März 1998)
- No. 40 SANA-Project results and PIK contributions
K. Bellmann, M. Erhard, M. Flechsig, R. Grote, F. Suckow (März 1998)
- No. 41 Umwelt und Sicherheit: Die Rolle von Umweltschwellenwerten in der empirisch-quantitativen Modellierung
D. F. Sprinz (März 1998)
- No. 42 Reversing Course: Germany's Response to the Challenge of Transboundary Air Pollution
D. F. Sprinz, A. Wahl (März 1998)
- No. 43 Modellierung des Wasser- und Stofftransportes in großen Einzugsgebieten. Zusammenstellung der Beiträge des Workshops am 15. Dezember 1997 in Potsdam
A. Bronstert, V. Krysanova, A. Schröder, A. Becker, H.-R. Bork (eds.) (April 1998)
- No. 44 Capabilities and Limitations of Physically Based Hydrological Modelling on the Hillslope Scale
A. Bronstert (April 1998)
- No. 45 Sensitivity Analysis of a Forest Gap Model Concerning Current and Future Climate Variability
P. Lasch, F. Suckow, G. Bürger, M. Lindner (Juli 1998)
- No. 46 Wirkung von Klimaveränderungen in mitteleuropäischen Wirtschaftswäldern
M. Lindner (Juli 1998)
- No. 47 SPRINT-S: A Parallelization Tool for Experiments with Simulation Models
M. Flechsig (Juli 1998)

- No. 48 The Odra/Oder Flood in Summer 1997: Proceedings of the European Expert Meeting in Potsdam, 18 May 1998
A. Bronstert, A. Ghazi, J. Hladny, Z. Kundzewicz, L. Menzel (eds.) (September 1998)
- No. 49 Struktur, Aufbau und statistische Programmbibliothek der meteorologischen Datenbank am Potsdam-Institut für Klimafolgenforschung
H. Österle, J. Glauer, M. Denhard (Januar 1999)
- No. 50 The complete non-hierarchical cluster analysis
F.-W. Gerstengarbe, P. C. Werner (Januar 1999)
- No. 51 Struktur der Amplitudengleichung des Klimas
A. Hauschild (April 1999)
- No. 52 Measuring the Effectiveness of International Environmental Regimes
C. Helm, D. F. Sprinz (Mai 1999)
- No. 53 Untersuchung der Auswirkungen erhöhter atmosphärischer CO₂-Konzentrationen innerhalb des Free-Air Carbon Dioxide Enrichment-Experimentes: Ableitung allgemeiner Modelllösungen
Th. Kartschall, J. Gräfe, P. Michaelis, K. Waloszczyk, S. Grossman-Clarke (Juni 1999)
- No. 54 Flächenhafte Modellierung der Evapotranspiration mit TRAIN
L. Menzel (August 1999)
- No. 55 Dry atmosphere asymptotics
N. Botta, R. Klein, A. Almgren (September 1999)
- No. 56 Wachstum von Kiefern-Ökosystemen in Abhängigkeit von Klima und Stoffeintrag - Eine regionale Fallstudie auf Landschaftsebene
M. Erhard (Dezember 1999)
- No. 57 Response of a River Catchment to Climatic Change: Application of Expanded Downscaling to Northern Germany
D.-I. Müller-Wohlfel, G. Bürger, W. Lahmer (Januar 2000)
- No. 58 Der "Index of Sustainable Economic Welfare" und die Neuen Bundesländer in der Übergangsphase
V. Wenzel, N. Herrmann (Februar 2000)
- No. 59 Weather Impacts on Natural, Social and Economic Systems (WISE, ENV4-CT97-0448)
German report
M. Flechsig, K. Gerlinger, N. Herrmann, R. J. T. Klein, M. Schneider, H. Sterr, H.-J. Schellnhuber (Mai 2000)
- No. 60 The Need for De-Aliasing in a Chebyshev Pseudo-Spectral Method
M. Uhlmann (Juni 2000)
- No. 61 National and Regional Climate Change Impact Assessments in the Forestry Sector - Workshop Summary and Abstracts of Oral and Poster Presentations
M. Lindner (ed.) (Juli 2000)
- No. 62 Bewertung ausgewählter Waldfunktionen unter Klimaänderung in Brandenburg
A. Wenzel (August 2000)
- No. 63 Eine Methode zur Validierung von Klimamodellen für die Klimawirkungsforschung hinsichtlich der Wiedergabe extremer Ereignisse
U. Böhm (September 2000)
- No. 64 Die Wirkung von erhöhten atmosphärischen CO₂-Konzentrationen auf die Transpiration eines Weizenbestandes unter Berücksichtigung von Wasser- und Stickstofflimitierung
S. Grossman-Clarke (September 2000)
- No. 65 European Conference on Advances in Flood Research, Proceedings, (Vol. 1 - Vol. 2)
A. Bronstert, Ch. Bismuth, L. Menzel (eds.) (November 2000)
- No. 66 The Rising Tide of Green Unilateralism in World Trade Law - Options for Reconciling the Emerging North-South Conflict
F. Biermann (Dezember 2000)
- No. 67 Coupling Distributed Fortran Applications Using C++ Wrappers and the CORBA Sequence Type
Th. Slawig (Dezember 2000)
- No. 68 A Parallel Algorithm for the Discrete Orthogonal Wavelet Transform
M. Uhlmann (Dezember 2000)
- No. 69 SWIM (Soil and Water Integrated Model), User Manual
V. Krysanova, F. Wechsung, J. Arnold, R. Srinivasan, J. Williams (Dezember 2000)
- No. 70 Stakeholder Successes in Global Environmental Management, Report of Workshop, Potsdam, 8 December 2000
M. Welp (ed.) (April 2001)

- No. 71 GIS-gestützte Analyse globaler Muster anthropogener Waldschädigung - Eine sektorale Anwendung des Syndromkonzepts
M. Cassel-Gintz (Juni 2001)
- No. 72 Wavelets Based on Legendre Polynomials
J. Fröhlich, M. Uhlmann (Juli 2001)
- No. 73 Der Einfluß der Landnutzung auf Verdunstung und Grundwasserneubildung - Modellierungen und Folgerungen für das Einzugsgebiet des Glan
D. Reichert (Juli 2001)
- No. 74 Weltumweltpolitik - Global Change als Herausforderung für die deutsche Politikwissenschaft
F. Biermann, K. Dingwerth (Dezember 2001)
- No. 75 Angewandte Statistik - PIK-Weiterbildungsseminar 2000/2001
F.-W. Gerstengarbe (Hrsg.) (März 2002)
- No. 76 Zur Klimatologie der Station Jena
B. Orłowsky (September 2002)
- No. 77 Large-Scale Hydrological Modelling in the Semi-Arid North-East of Brazil
A. Güntner (September 2002)
- No. 78 Phenology in Germany in the 20th Century: Methods, Analyses and Models
J. Schaber (November 2002)
- No. 79 Modelling of Global Vegetation Diversity Pattern
I. Venevskaia, S. Venevsky (Dezember 2002)
- No. 80 Proceedings of the 2001 Berlin Conference on the Human Dimensions of Global Environmental Change "Global Environmental Change and the Nation State"
F. Biermann, R. Brohm, K. Dingwerth (eds.) (Dezember 2002)
- No. 81 POTSDAM - A Set of Atmosphere Statistical-Dynamical Models: Theoretical Background
V. Petoukhov, A. Ganopolski, M. Claussen (März 2003)
- No. 82 Simulation der Siedlungsflächenentwicklung als Teil des Globalen Wandels und ihr Einfluß auf den Wasserhaushalt im Großraum Berlin
B. Ströbl, V. Wenzel, B. Pfützner (April 2003)
- No. 83 Studie zur klimatischen Entwicklung im Land Brandenburg bis 2055 und deren Auswirkungen auf den Wasserhaushalt, die Forst- und Landwirtschaft sowie die Ableitung erster Perspektiven
F.-W. Gerstengarbe, F. Badeck, F. Hattermann, V. Krysanova, W. Lahmer, P. Lasch, M. Stock, F. Suckow, F. Wechsung, P. C. Werner (Juni 2003)
- No. 84 Well Balanced Finite Volume Methods for Nearly Hydrostatic Flows
N. Botta, R. Klein, S. Langenberg, S. Lützenkirchen (August 2003)
- No. 85 Orts- und zeitdiskrete Ermittlung der Sickerwassermenge im Land Brandenburg auf der Basis flächendeckender Wasserhaushaltsberechnungen
W. Lahmer, B. Pfützner (September 2003)
- No. 86 A Note on Domains of Discourse - Logical Know-How for Integrated Environmental Modelling, Version of October 15, 2003
C. C. Jaeger (Oktober 2003)
- No. 87 Hochwasserrisiko im mittleren Neckarraum - Charakterisierung unter Berücksichtigung regionaler Klimaszenarien sowie dessen Wahrnehmung durch befragte Anwohner
M. Wolff (Dezember 2003)
- No. 88 Abflußentwicklung in Teileinzugsgebieten des Rheins - Simulationen für den Ist-Zustand und für Klimaszenarien
D. Schwandt (April 2004)
- No. 89 Regionale Integrierte Modellierung der Auswirkungen von Klimaänderungen am Beispiel des semi-ariden Nordostens von Brasilien
A. Jaeger (April 2004)
- No. 90 Lebensstile und globaler Energieverbrauch - Analyse und Strategieansätze zu einer nachhaltigen Energiestruktur
F. Reusswig, K. Gerlinger, O. Edenhofer (Juli 2004)
- No. 91 Conceptual Frameworks of Adaptation to Climate Change and their Applicability to Human Health
H.-M. Füssel, R. J. T. Klein (August 2004)
- No. 92 Double Impact - The Climate Blockbuster 'The Day After Tomorrow' and its Impact on the German Cinema Public
F. Reusswig, J. Schwarzkopf, P. Polenz (Oktober 2004)
- No. 93 How Much Warming are we Committed to and How Much Can be Avoided?
B. Hare, M. Meinshausen (Oktober 2004)

No. 94 Urbanised Territories as a Specific Component of the Global Carbon Cycle
A. Svirejeva-Hopkins, H.-J. Schellnhuber (Januar 2005)